

# PROCEEDINGS OF THE 1996 ATB MODEL USERS' GROUP CONFERENCE

**DISTRIBUTION STATEMENT A**

Approved for public release;  
Distribution Unlimited



Sponsored by:  
U.S. Air Force Armstrong Laboratory  
and GESAC, Inc.

19960321 082

February 8th and 9th 1996  
Quality Inn South Mountain  
Phoenix, Arizona USA

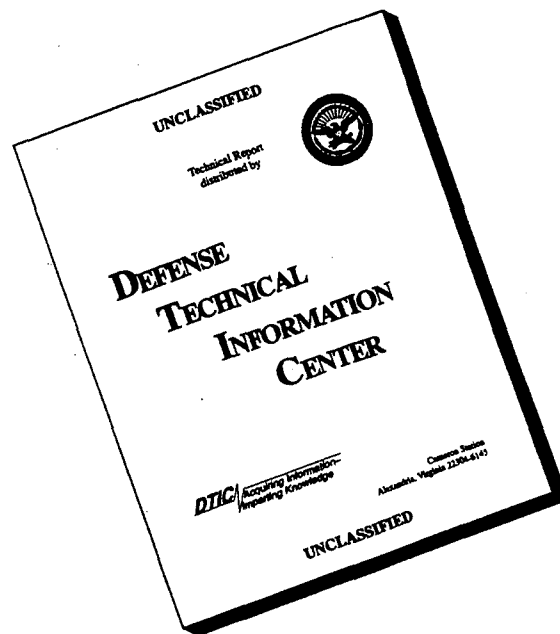
# REPORT DOCUMENTATION PAGE

Form Approved  
OMB No. 0704-0188

Public reporting burden for this collection of information is estimated to average 1 hour per response, including the time for reviewing instructions, searching existing data sources, gathering and maintaining the data needed, and completing and reviewing the collection of information. Send comments regarding this burden estimate or any other aspect of this collection of information, including suggestions for reducing this burden, to Washington Headquarters Services, Directorate for Information Operations and Reports, 1215 Jefferson Davis Highway, Suite 1204, Arlington, VA 22202-4302, and to the Office of Management and Budget, Paperwork Reduction Project (0704-0188), Washington, DC 20503.

<b>1. AGENCY USE ONLY (Leave blank)</b>		<b>2. REPORT DATE</b> February 1996	<b>3. REPORT TYPE AND DATES COVERED</b> Meeting Proceedings	
<b>4. TITLE AND SUBTITLE</b> Proceedings of the 1996 ATB Model Users' Group Conference			<b>5. FUNDING NUMBERS</b> PE 62202F PR 7184 TA 43 WU 01	
<b>6. AUTHOR(S)</b>				
<b>7. PERFORMING ORGANIZATION NAME(S) AND ADDRESS(ES)</b> North Dakota State University Fargo ND 58105			<b>8. PERFORMING ORGANIZATION REPORT NUMBER</b>	
<b>9. SPONSORING / MONITORING AGENCY NAME(S) AND ADDRESS(ES)</b> Armstrong Laboratory, Crew Systems Directorate Biodynamics and Biocommunications Division Human Systems Center Air Force Materiel Command Wright-Patterson AFB OH 45433-7901			<b>10. SPONSORING / MONITORING AGENCY REPORT NUMBER</b>	
<b>11. SUPPLEMENTARY NOTES</b>				
<b>12a. DISTRIBUTION / AVAILABILITY STATEMENT</b> Approved for public release; distribution is unlimited			<b>12b. DISTRIBUTION CODE</b>	
<b>13. ABSTRACT (Maximum 200 words)</b> The 1996 Articulated Total Body (ATB) Model Users' Group Conference was held at the Quality Inn South Mountain, Phoenix AZ on 8-9 February 1996. This Conference, sponsored by the Armstrong Laboratory (AL), US Department of the Air Force, and GESAC Inc, brought together over fifty users of the ATB model and its derivatives (CVS, Cal-3D, and DYNAMAN). The two day conference offered the opportunity to present and exchange the latest ATB modeling techniques and applications. Invited presentations, group discussions, and interactive exercises covered areas such as model features, harness belt modeling, vehicle and aircraft crashworthiness, design applications, and animation techniques. In addition, the newly-elected charter offices of the ATB Users' Group were introduced and committees formed to initiate group activities.				
<b>14. SUBJECT TERMS</b> Articulated Total Body Model, Computer Simulation, Rigid Body Dynamics, Anthropometry, Crash Safety			<b>15. NUMBER OF PAGES</b> 154	
			<b>16. PRICE CODE</b>	
<b>17. SECURITY CLASSIFICATION OF REPORT</b> UNCLASSIFIED	<b>18. SECURITY CLASSIFICATION OF THIS PAGE</b> UNCLASSIFIED	<b>19. SECURITY CLASSIFICATION OF ABSTRACT</b> UNCLASSIFIED	<b>20. LIMITATION OF ABSTRACT</b> UL	

# DISCLAIMER NOTICE



**THIS DOCUMENT IS BEST QUALITY AVAILABLE. THE COPY FURNISHED TO DTIC CONTAINED A SIGNIFICANT NUMBER OF PAGES WHICH DO NOT REPRODUCE LEGIBLY.**

## PREFACE

The 1996 ATB Model Users' Group Conference was held in Phoenix, Arizona, on February 8 and 9, 1996. This was the second meeting of scientists, engineers, accident investigators, designers, occupant safety advocates, and others who use the Articulated Total Body model and its derivatives (CVS, CAL-3D, and DYNAMAN) in their professional endeavors. More than fifty users attended the two-day conference, which offered them the opportunity to present and exchange information on the latest ATB modeling techniques and applications.

The program included an introduction to ATB for new users, eight presentations by users, and group workshops discussing various modeling topics. In addition, the newly-elected charter officers of the ATB Users' Group were introduced, and committees were formed to initiate the various activities of the group. These include planning regular meetings, starting an on-line computer bulletin board for the group to exchange information, forming an ATB training program, and formalizing the membership requirements.

As this conference was designed to be an informal meeting, please do not reference the presentations appearing in these proceedings in the open literature.

This conference was sponsored by the U.S. Air Force Armstrong Laboratory. GESAC, Inc provided the first day's luncheon. Major support was also provided by Systems Research Laboratories and Simula, Inc. Particular thanks go to Laura Liptai, University of California - Davis, Gina Bertocci, University of Pittsburgh, and Louise Obergefell, Armstrong Laboratory, for recruiting the speakers; Wesley Grimes, Collision Engineering Associates, Dr. Obergefell, and Ms. Bertocci for organizing the workshops; Lindley Bark, Simula, for organizing a tour of Simula's facilities; Al Karl, Systems Research Laboratories, for handling the registration fees; and Dave Furey and Carla Wells, Simula, for administrative support. Much appreciation is also extended to the speakers for investing the resources needed to prepare the presentations contained in these proceedings.

Ms. Annette Rizer  
*Systems Research Laboratories*  
*Conference Organizer*

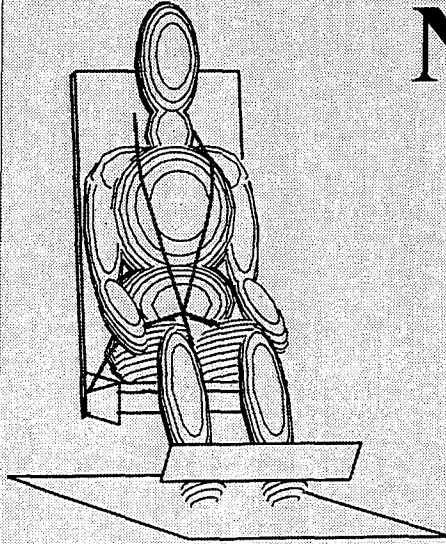
Dr. Mariusz Ziejewski  
*North Dakota State University*  
*Proceedings Editor*



## Table of Contents

TITLE <i>Author(s)</i>	Page
<b>PREFACE</b> .....	i
<b>ABC's of ATB for New Users</b> <i>Louise Obergefell - Armstrong Laboratory</i> .....	1
<b>Advanced Dummy Neck Design Using DYNAMAN</b> <i>Narayan Yoganandan, Joseph Cheng, Frank Pintar - Department of Neurosurgery, Medical College of Wisconsin and Department of Veterans Affairs Medical Center Tariq Shams, Nagarajan Rangarajan - GESAC Inc.</i> .....	28
<b>DYNTASK: Program for Ergonomic Analysis of Human Tasks</b> <i>Tariq Shams, Nagarajan Rangarajan - GESAC Inc. Richard McMahon - U.S. Army Research Laboratory, HRED</i> .....	34
<b>A New Harness Algorithm for Simulating Belt Slippage During Occupant Impact Motion</b> <i>Yih-Chang Deng - General Motors R &amp; D Center</i> .....	43
<b>Aircraft Seat Development with DYNAMAN</b> <i>Anne Curzon - Failure Analysis Associates, Inc.</i> .....	87
<b>Application of Ellipses, Ellipsoids, and Hyperellipsoids in Computer Modeling of the Human Body and Interior Surfaces</b> <i>Mariusz Ziejewski, Xiaofeng Pan - North Dakota State University</i> .....	91
<b>Three Dimensional Computer Animation Generated from ATB Output</b> <i>Mariusz Ziejewski, Beth Anderson - North Dakota State University David Grangaard - Insim, Inc.</i> .....	97
<b>List Of Attendees</b> .....	Appendix

# ABCs of ATB for New Users



*Louise Obergefell*  
*8 February 1996*

## ATB Model

---

*Predicts Dynamics During Ejection, Aircraft & Automobile Crashes, & Other Hazardous Events*

- ▶ **3-D Coupled Rigid Body Dynamics**
- ▶ **Angular & Linear Joints**
- ▶ **Applied Forces**
  - *Internal Joint Resistive Torques*
  - *External Contact Forces*
  - *Belt Forces*
  - *Aerodynamic Forces*
- ▶ **Ellipsoid, Hyperellipsoid, & Plane Surfaces**

# Applications

---

- ▶ **Automobile Crashes**
    - *Frontal*
    - *Side*
    - *Rollover*
  - ▶ **Aircraft Crashes**
  - ▶ **Aircraft Ejection**
  - ▶ **Helicopter Crashes**
  - ▶ **Aircraft Extraction**
  - ▶ **Emergency Escape Through Chute**
  - ▶ **Parachute Opening**
  - ▶ **Falls & Landing**
- 

# History

---

- ▶ **CVS developed by Calspan Corp in early 1970s for NHTSA & MVMA**
  - ▶ **Modified Air Force version named ATB in 1975**
  - ▶ **VIEW program developed in 1978**
  - ▶ **CVS & ATB codes integrated in 1981 (version 20)**
  - ▶ **GEBOD program developed in 1983**
  - ▶ **GESAC developed PC version with pre- & post processors in 1989**
  - ▶ **Current Air Force version is ATB-IV.4**
-



# Programs

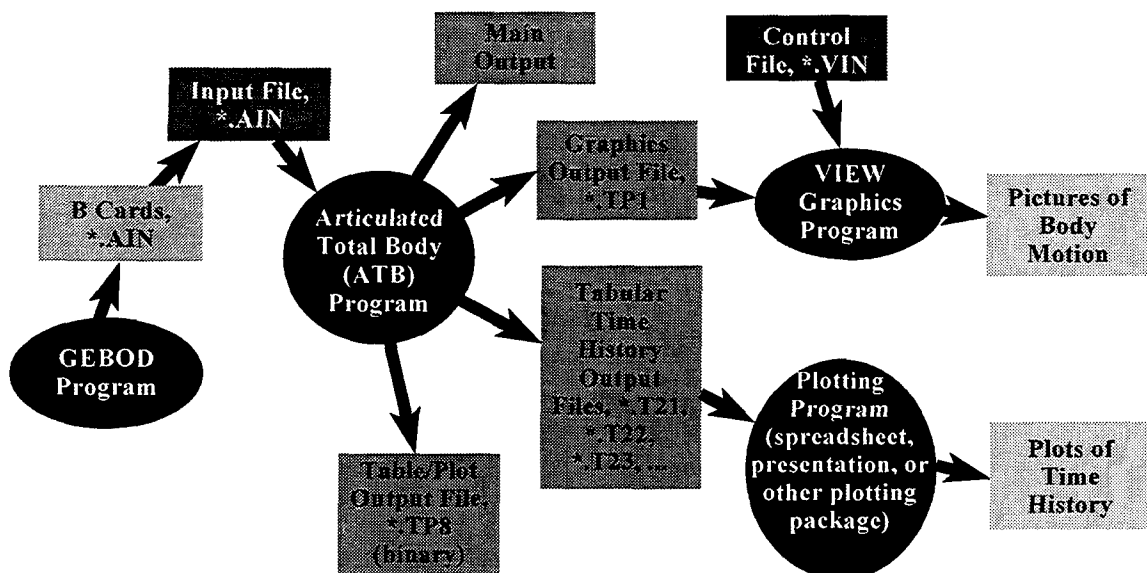
---

- ▶ **Articulated Total Body (ATB) Model**
    - *Crash Victim Simulator (CVS) & CAL3D*
  - ▶ **DYNAMAN**
    - *GESAC Inc.*
    - *Preprocessor & Postprocessor*
  - ▶ **GEBOD**
    - *Generates Body Data Sets*
  - ▶ **VIEW**
    - *Depicts Body Motion*
  - ▶ **IMAGE**
    - *Silicon Graphics Solid Model Graphics*
- 

# ATB Program Files

---

## *File & Program Interconnectivity*



# GEBOD

---

## *Generator of Body Data Sets*

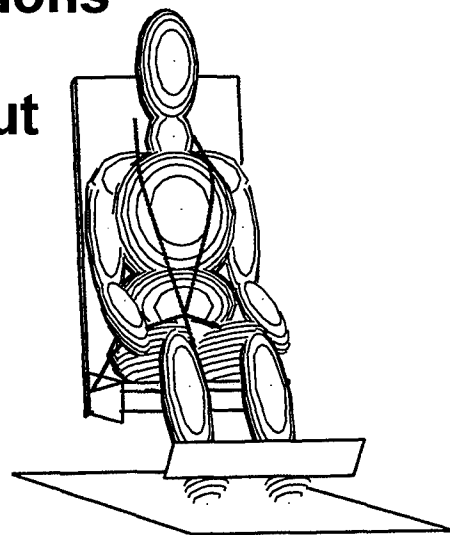
- ▶ **Adult Human Male**
    - *Height and/or Weight*
  - ▶ **Adult Human Female**
    - *Height and/or Weight*
  - ▶ **Human Child**
    - *Age, Height and/or Weight*
  - ▶ **User Defined Human**
    - *32 Body Dimensions*
  - ▶ **Hybrid II Dummy (Part 572)**
  - ▶ **Hybrid III Dummy**
- 

# VIEW

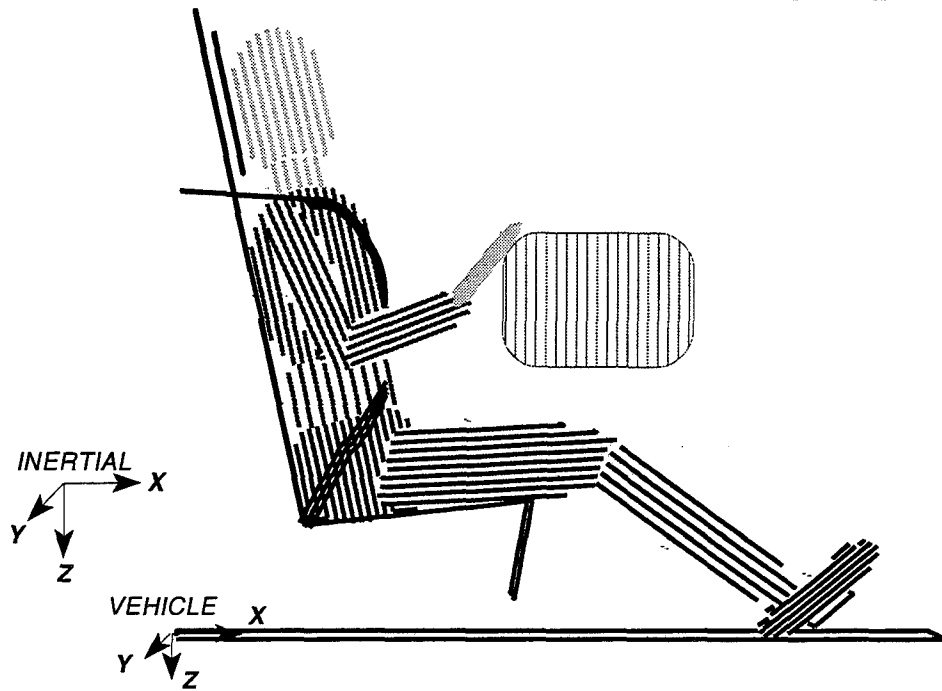
---

## *Depicts Body Motion*

- ▶ **Variable Viewing Positions**
- ▶ **Hidden Line Drawings**
- ▶ **Uses ATB Model Output**
- ▶ **Computers**
  - *DOS Based PCs*
  - *Silicon Graphics*
  - *FORTRAN With:*
    - *Calcomp Plotter Drivers*
    - *DEC FORTRAN Graphics Library*
    - *GL Library*
    - *Other Calcomp Interpreters*



# Simulation Setup



# Input Data

	DYNAMAN	ATB
Body Data - Segments & Joints	SEGMENT	B Cards
Prescribed Motions	MOTION	C Cards
Environment Definitions		
Contact Plane Geometry	EVRNMNT/Planes	D.2 Cards
Additional (Hyper)Ellipsoids	EVRNMNT/Ellipses	D.5 Cards
Simple Belt Geometry	EVRNMNT/Std Belts	D.3 Cards
Harness Belt Geometry	EVRNMNT/Harness	F.8 Cards
Airbag Geometry	EVRNMNT/Airbags	D.4 Cards
Spring/Dampers	EVRNMNT/Spring-Dampers	D.8 Cards
Applied Forces & Torques	EVRNMNT/Forces	D.9 Cards
Wind Forces	CONTACT/Wind-Segment	F.7 Cards
Functions	FUNCTN	E Cards
Contacts	CONTACT	F Cards
Initial Conditions	SETUP	G Cards
Time Steps	RUNINFO/Integration Info	A.4 Card
Units of Measurement	RUNINFO/Units Info	A.3 Card
Output		
Time Histories	RUNINFO/Output/Plot-Tables	H Cards
Pictures	RUNINFO/Output/Picture	A.5 Card

# Units of Measurement

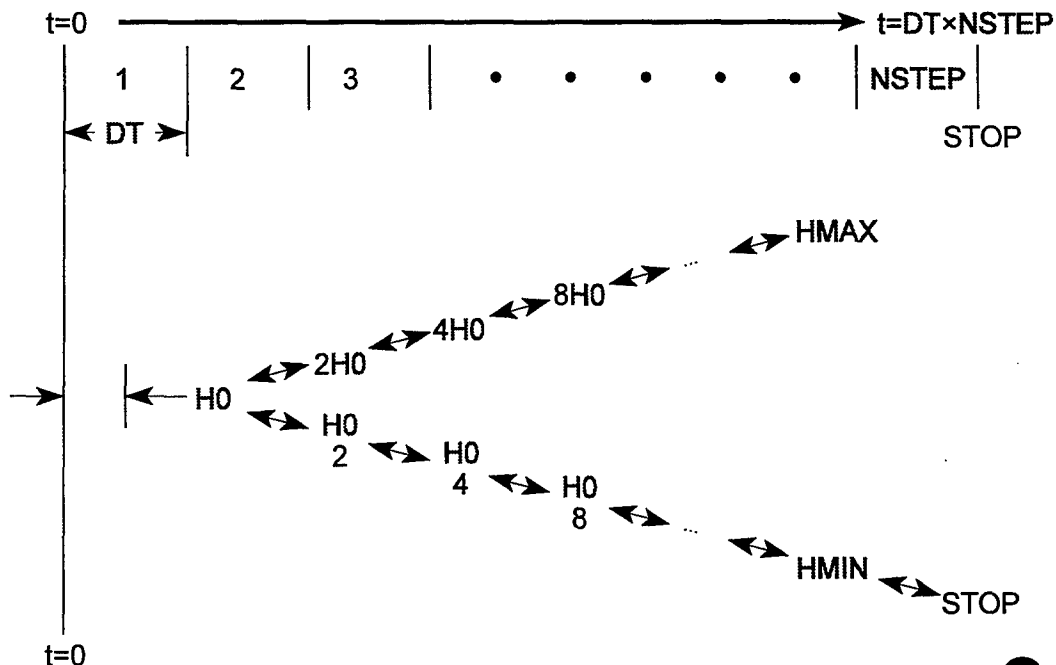
---

- ▶ **Specify Length, Force, & Time Units**
- ▶ **English - Inches, Pounds, Seconds**
  - *Most commonly used*
  - *Field width problems may occur with other units*
- ▶ **Metric - Meters, Newtons, Seconds**

---

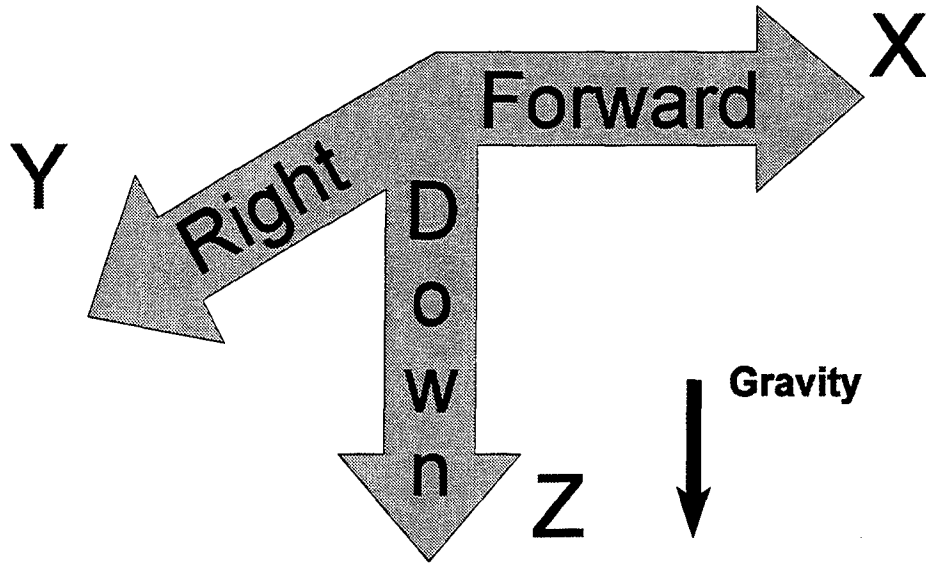
## Time Step Definitions

---



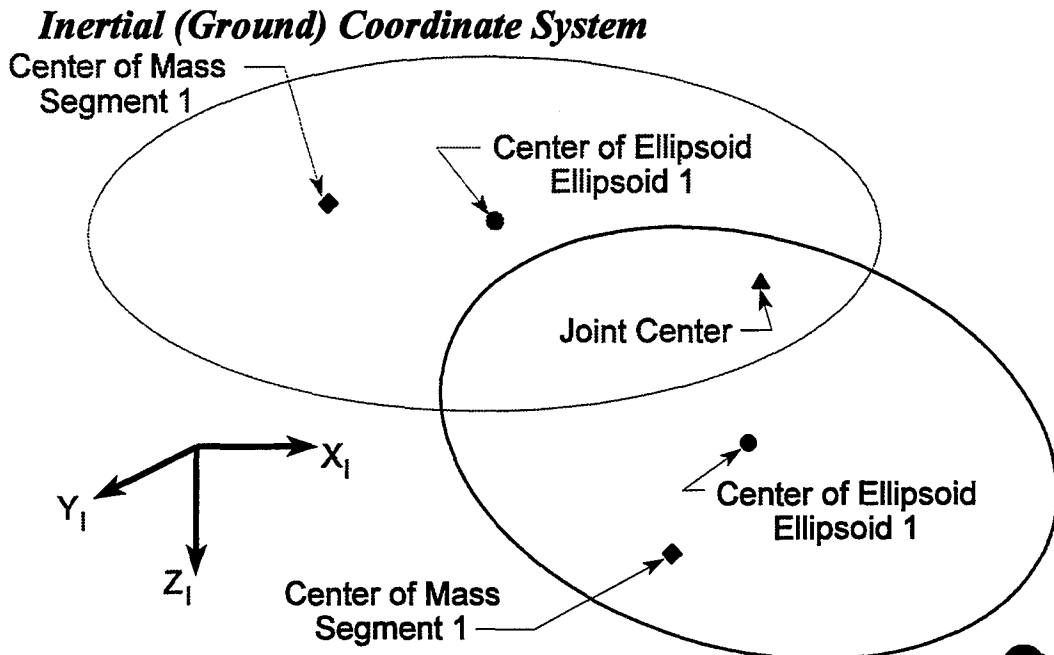
# General Coordinate System Convention

---



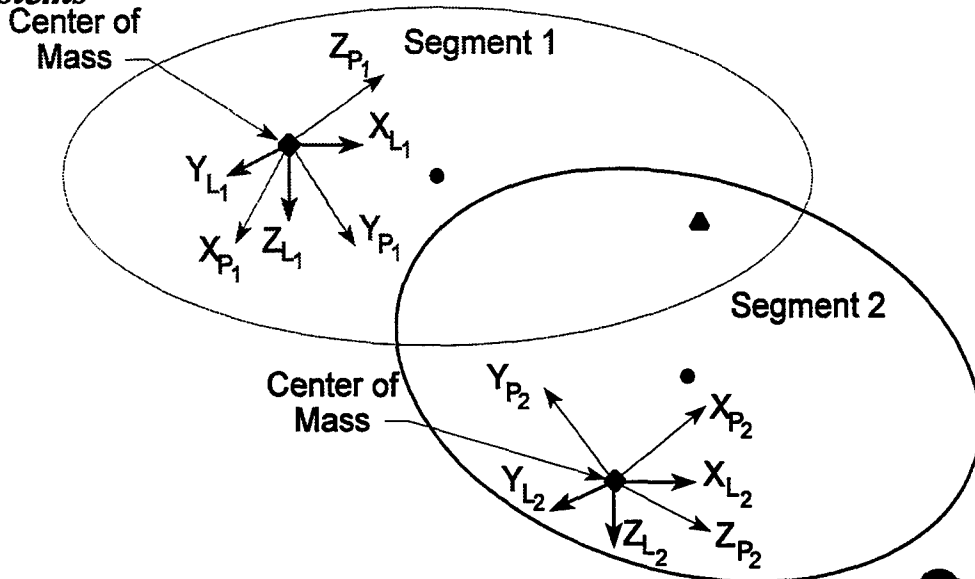
## Coordinate Systems

---



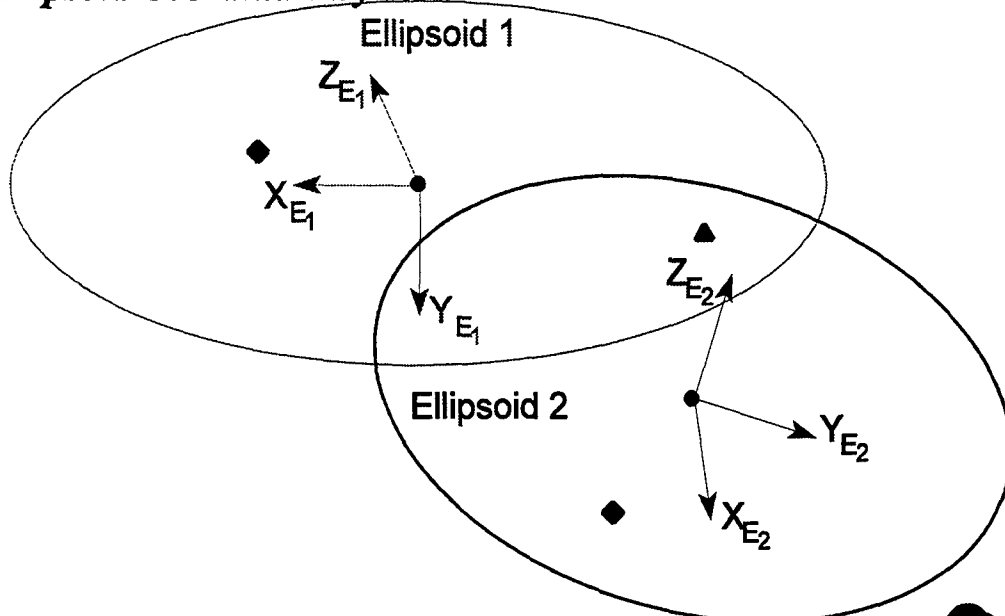
# Coordinate Systems

## *Segment Local & Principal Moment of Inertia Coordinate Systems*



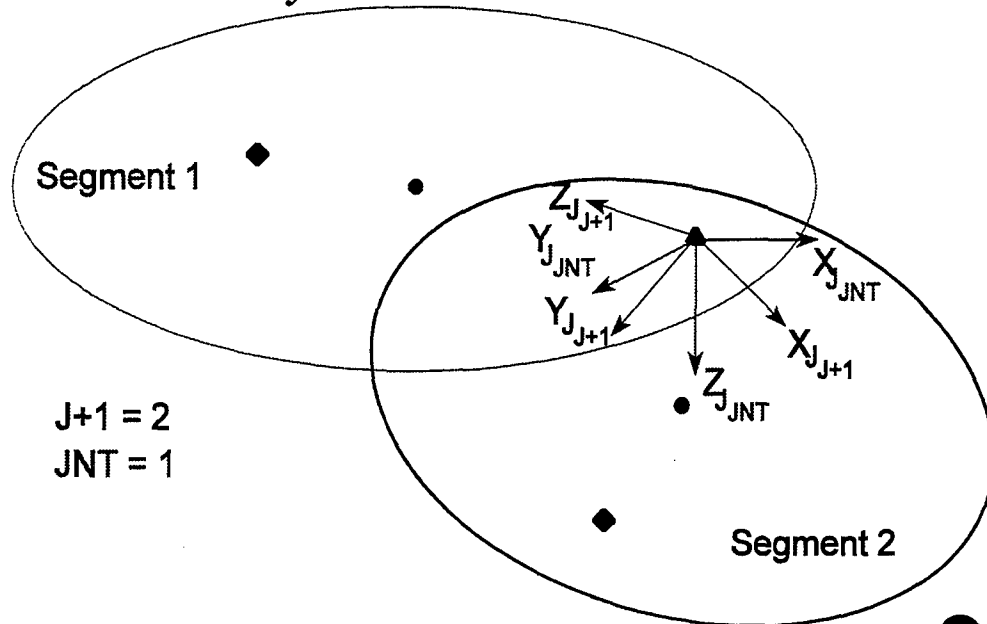
# Coordinate Systems

## *Ellipsoid Coordinate Systems*

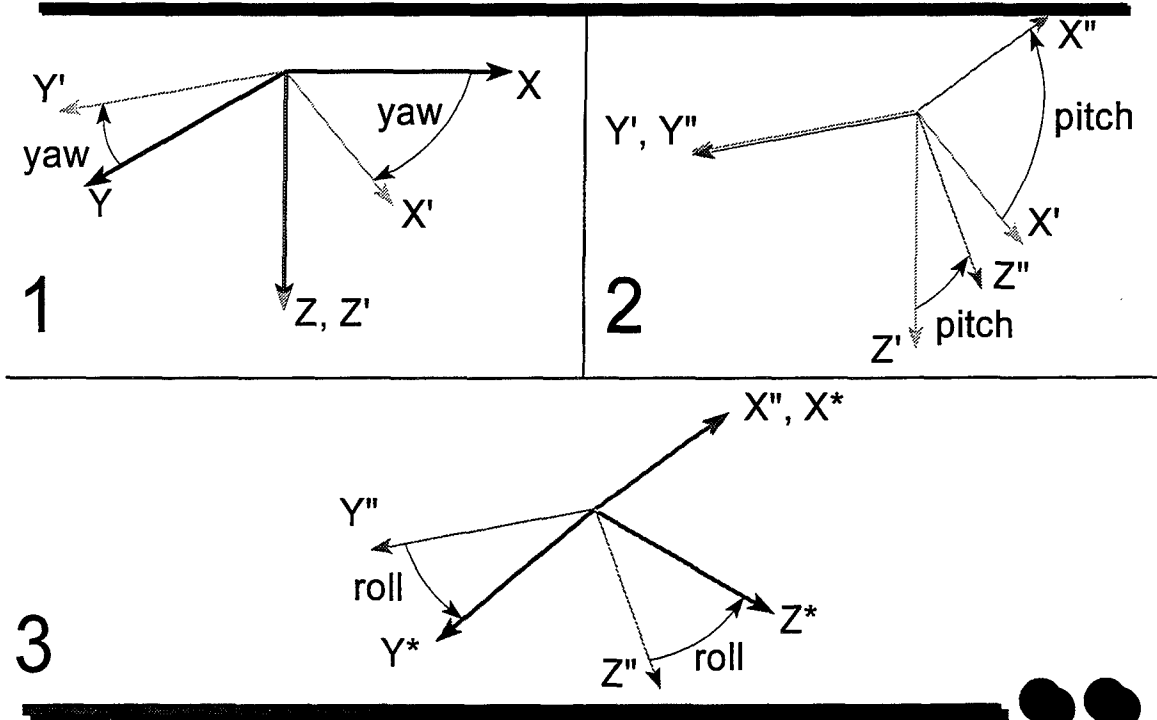


# Coordinate Systems

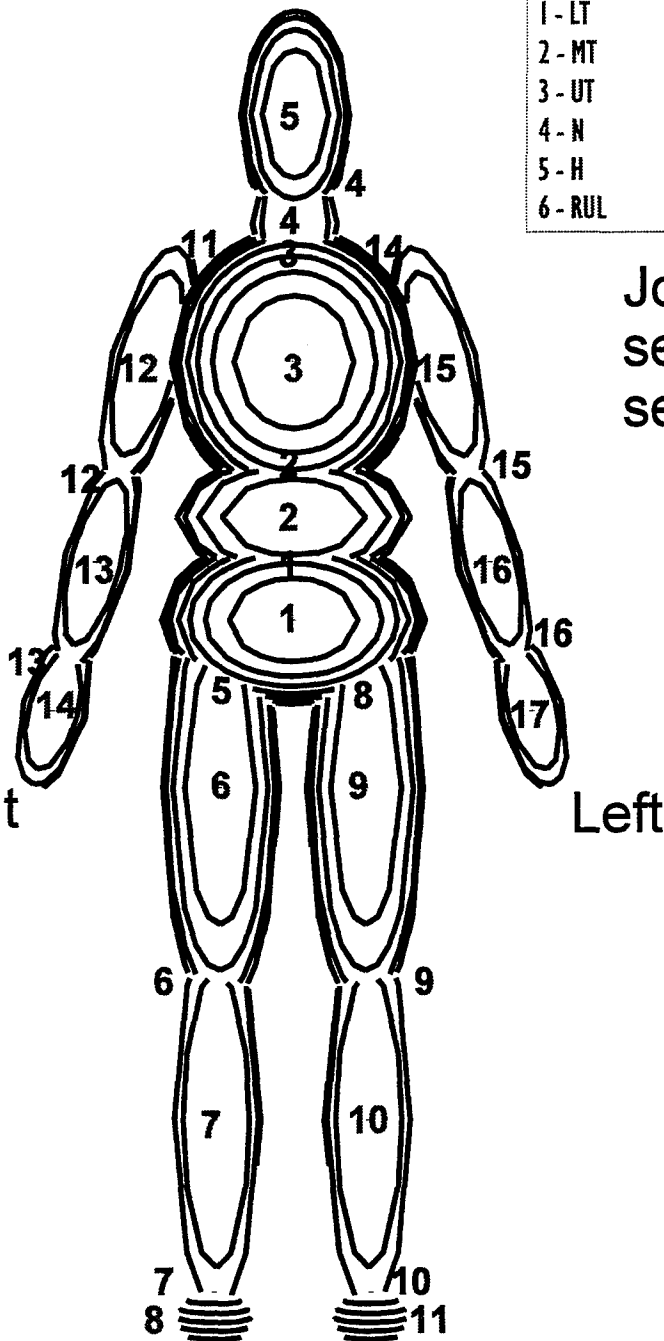
## Joint Coordinate Systems



## Yaw, Pitch, & Roll



# Standard Body Setup



Segments		
1 - LT	7 - RLL	13 - RLA
2 - MT	8 - RF	14 - RH
3 - UT	9 - LUL	15 - LUA
4 - N	10 - LLL	16 - LLA
5 - H	11 - LF	17 - LH
6 - RUL	12 - RUA	

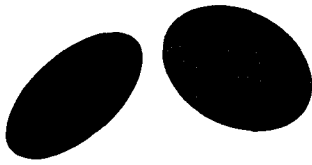
Joint J connects segment J+1 to segment JNT.

JOINT	JNT
1 - P	1
2 - W	2
3 - NP	3
4 - HP	4
5 - RH	1
6 - RK	6
7 - RA	7
8 - LH	1
9 - LK	9
10 - LA	10
11 - RS	3
12 - RE	12
13 - RW	13
14 - LS	3
15 - LE	15
16 - LW	16

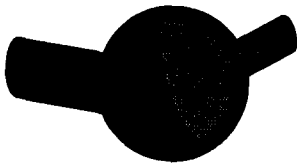


# JOINT TYPES

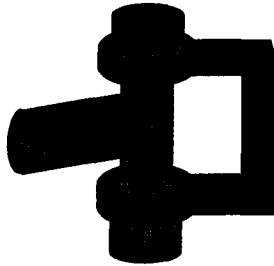
Null



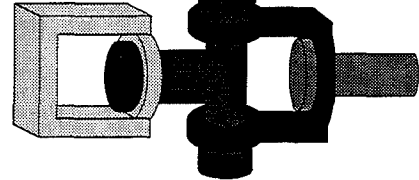
Ball & Socket or Free



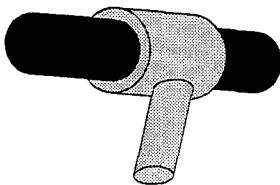
Pin (Hinge)



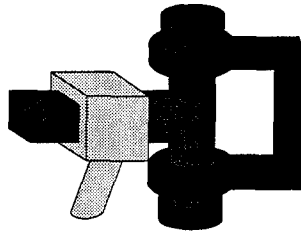
Euler



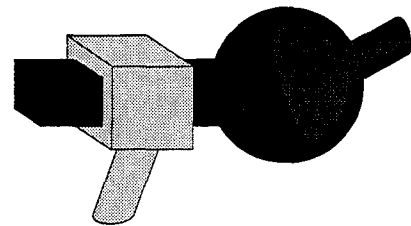
Slip With Rotation  
About Z Axis



Slip With Rotation  
About Y Axis

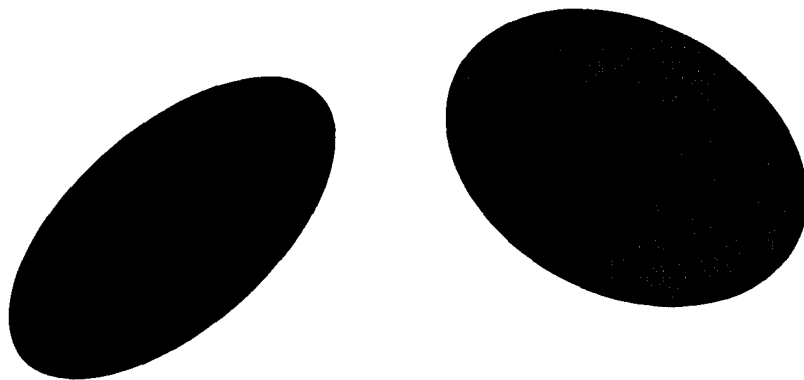


Slip With Complete  
Angular Freedom



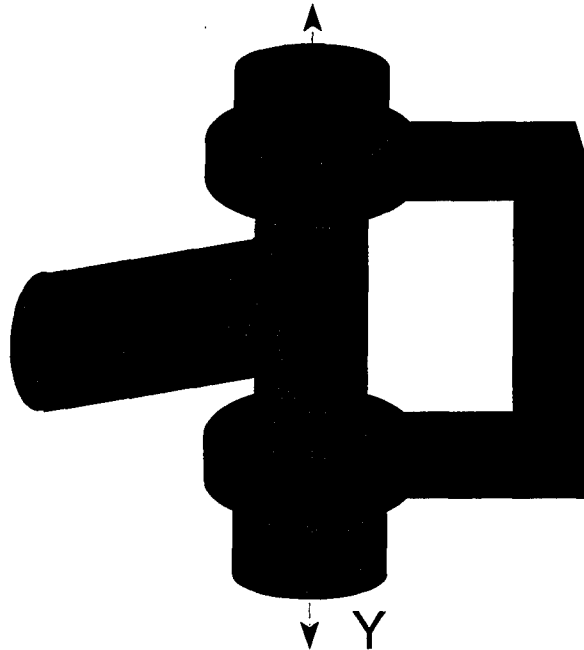
## Null Joint

---



# Pin (Hinge) Joint

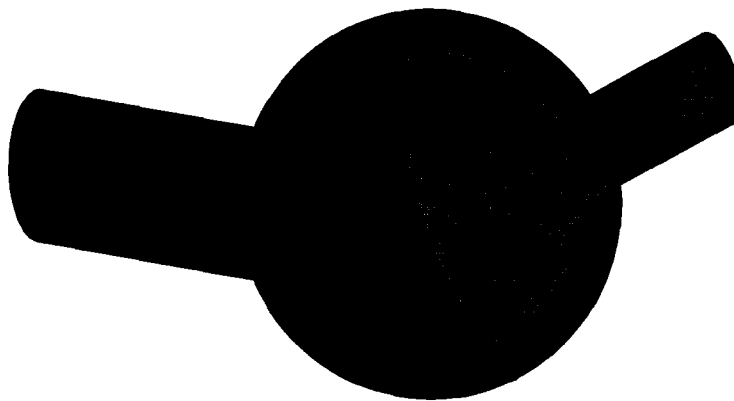
---



# Ball & Socket Joint

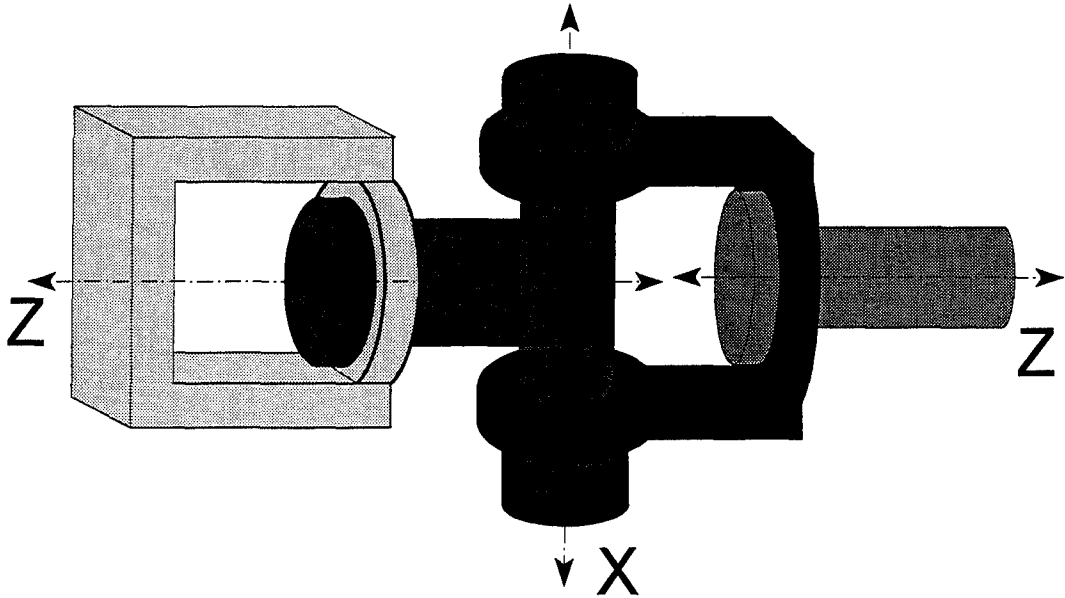
---

*Free Joint*



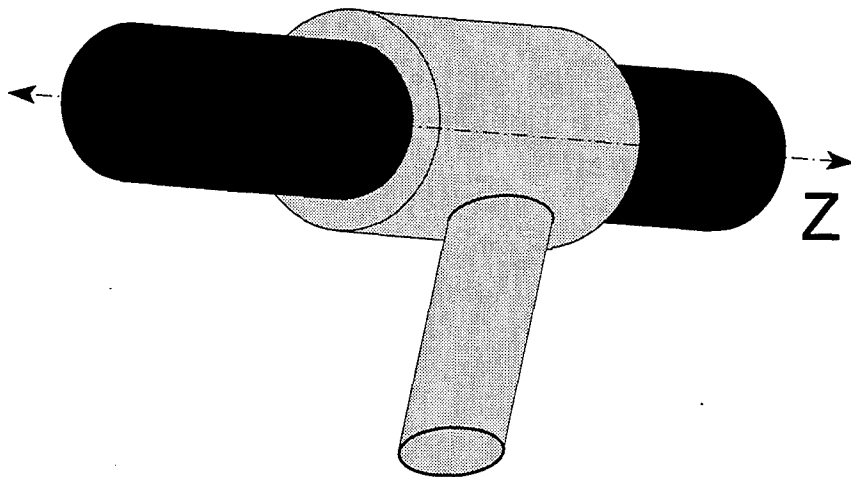
# Euler Joint

---



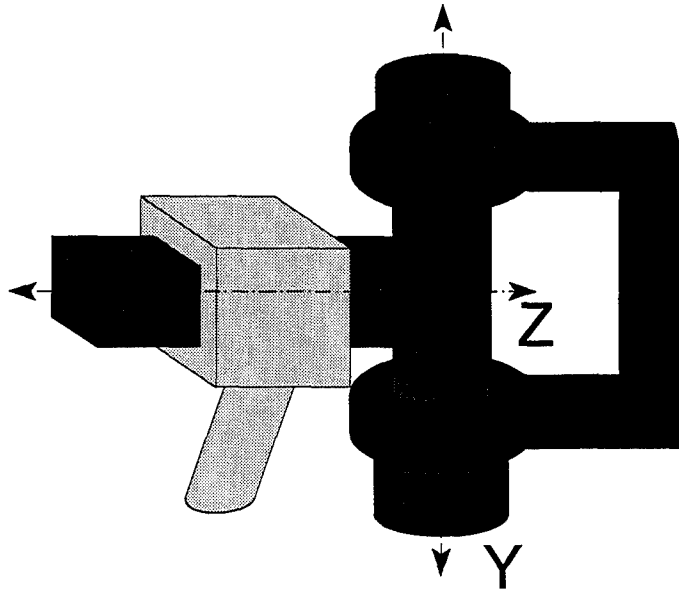
# Slip Joint With Rotation About Z Axis

---



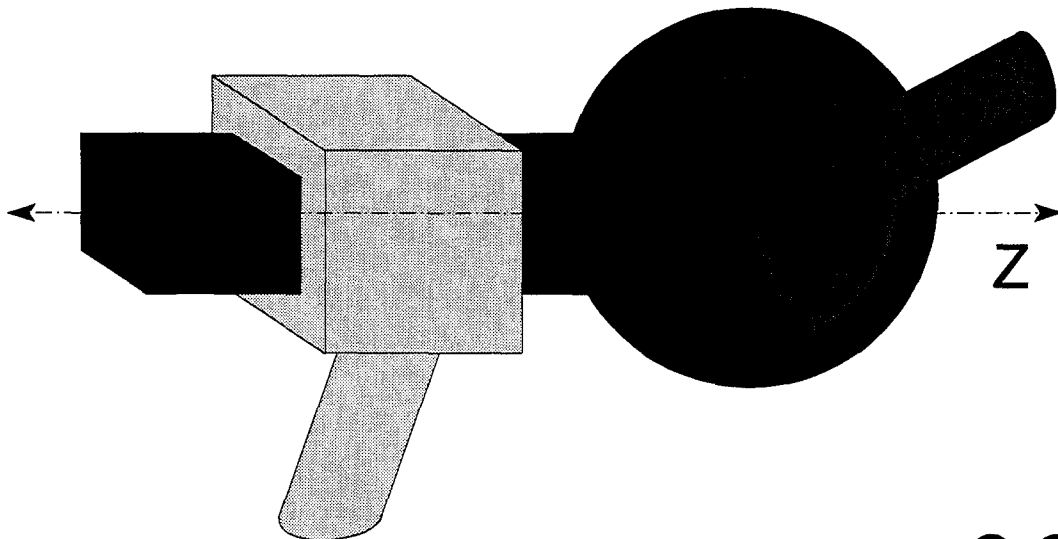
## Slip Joint With Rotation About Y Axis

---

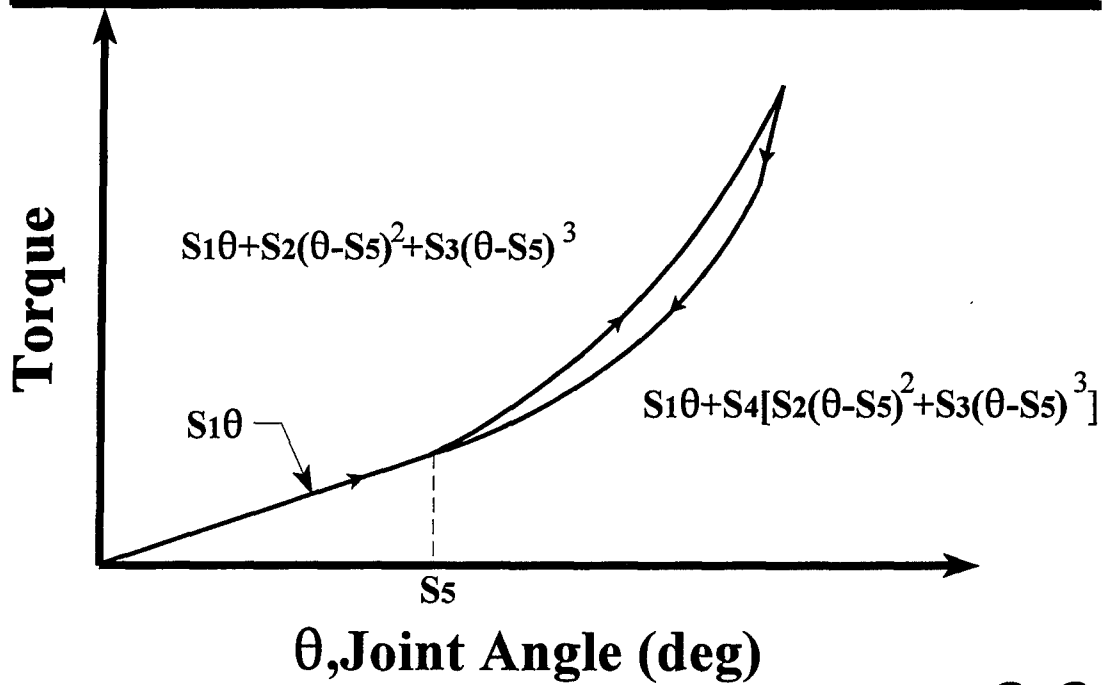


## Slip Joint With Complete Angular Freedom

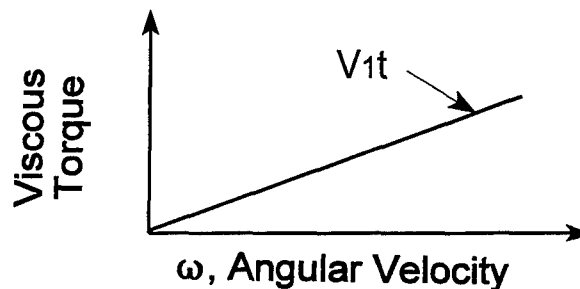
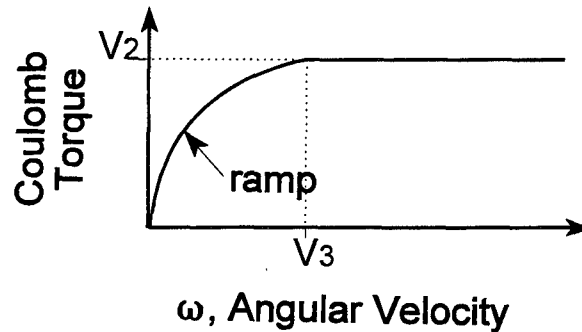
---



# Joint Spring Torque



# Joint Torques

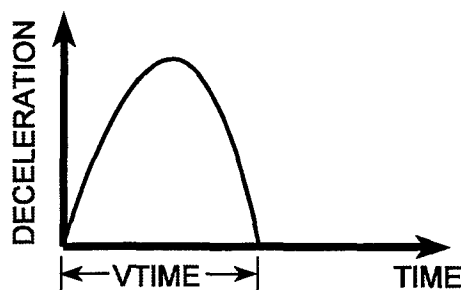


# Prescribed Motion Options

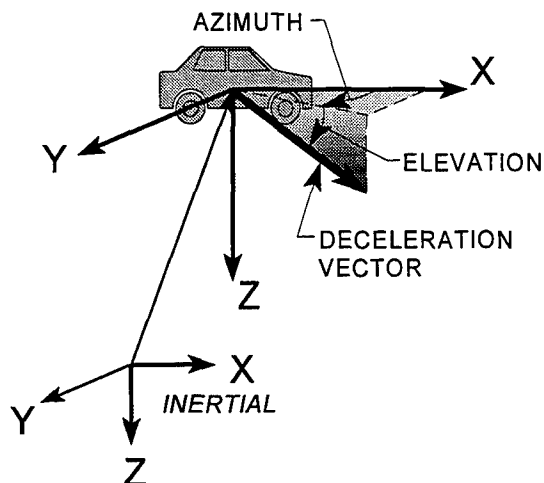
- ▶ **Option 1**
  - *Half Sine Wave Deceleration Pulse*
- ▶ **Option 2**
  - *Tabular Unidirectional Deceleration*
- ▶ **Option 3**
  - *Six Degree of Freedom Deceleration*
- ▶ **Option 4**
  - *Spline Fit Position, Velocity, or Deceleration*

## Option 1

### *Half Sine Wave Deceleration Pulse*

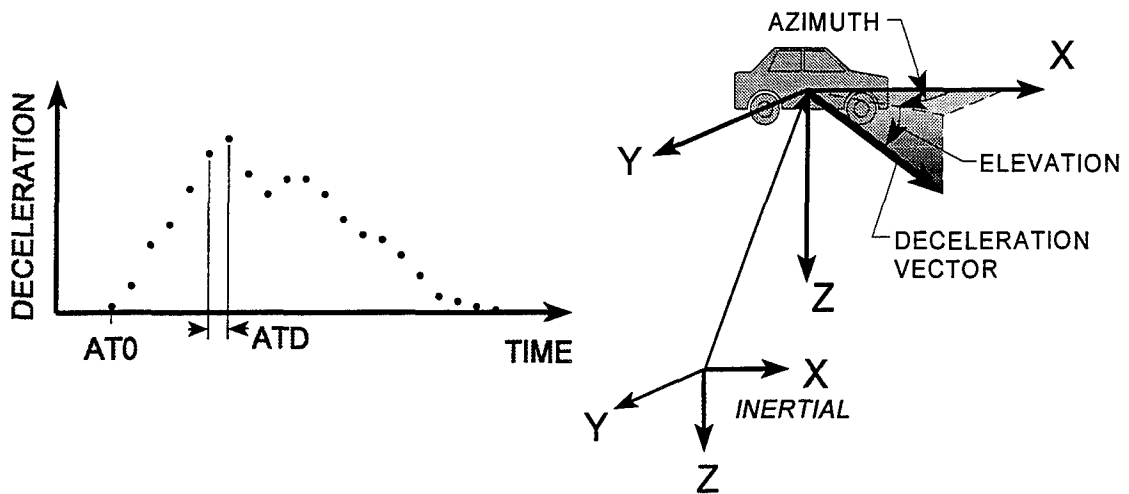


Note: The user inputs the initial speed (VIPS). The amplitude of the deceleration is calculated so that the speed after VTIME is zero. Alternatively, if the initial speed is specified as negative, the vehicle will accelerate from zero velocity to a final speed of -VIPS.

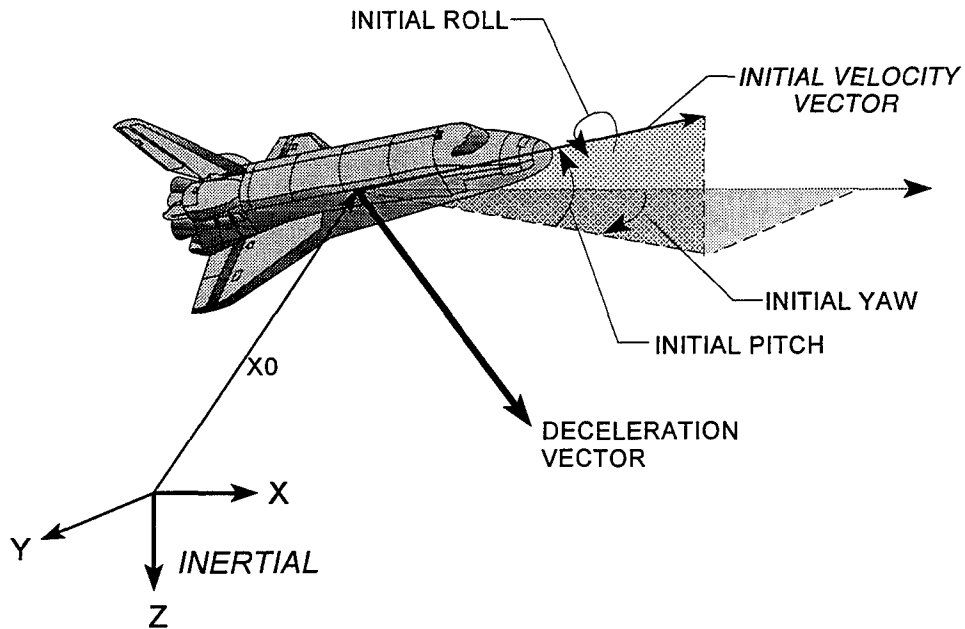


# Option 2

## *Tabular Unidirectional Deceleration*

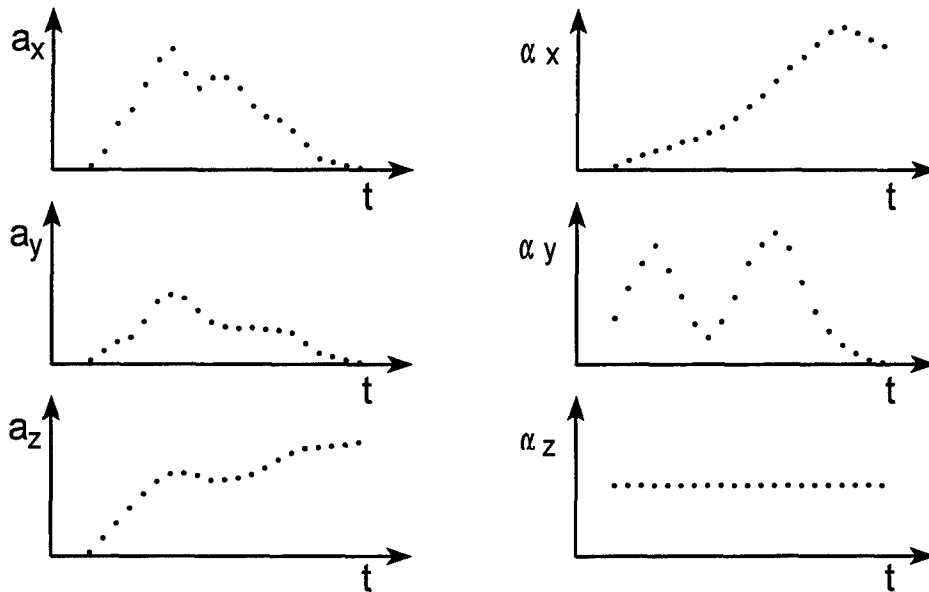


# Option 3

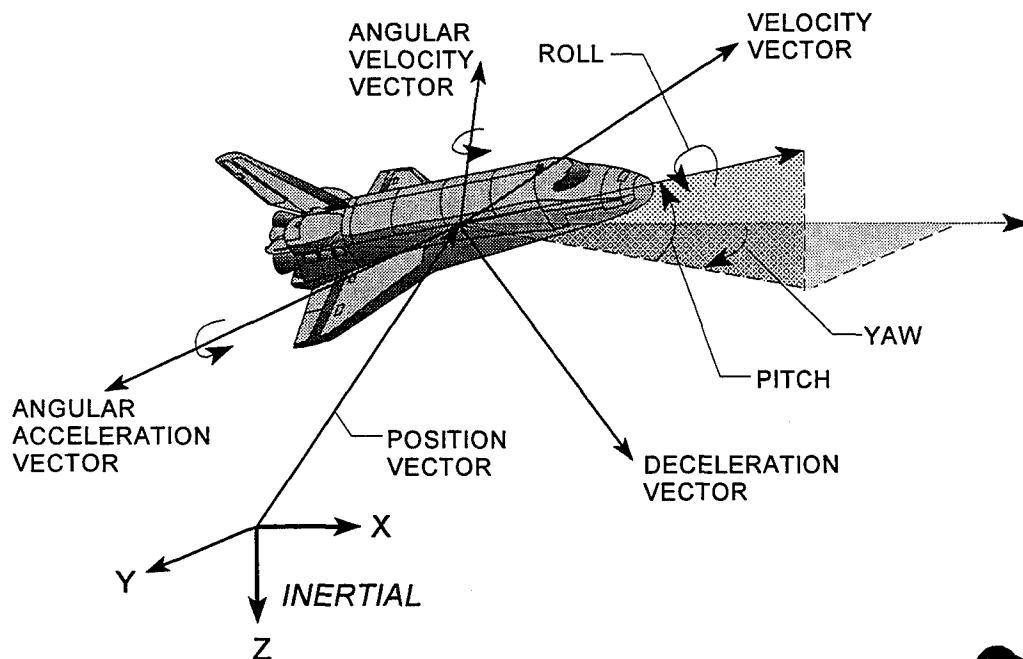


# Option 3

## Six Degree of Freedom Deceleration



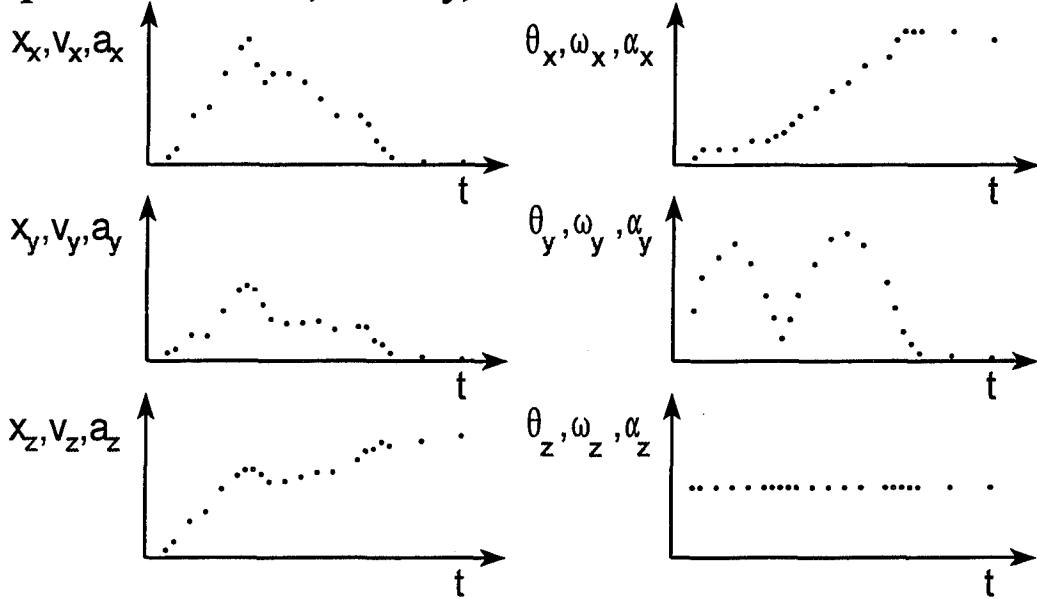
# Option 4





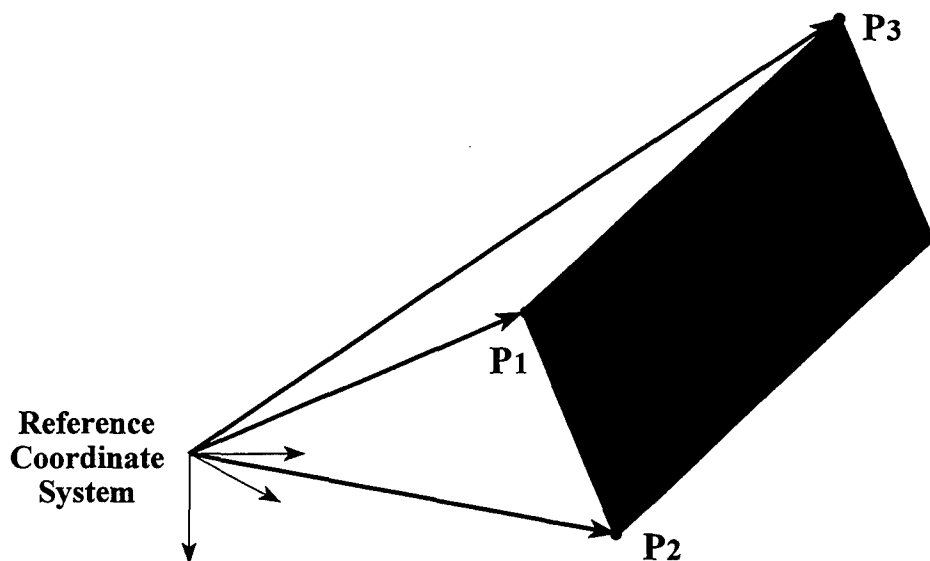
# Option 4

## *Spline Fit Position, Velocity, or Deceleration*



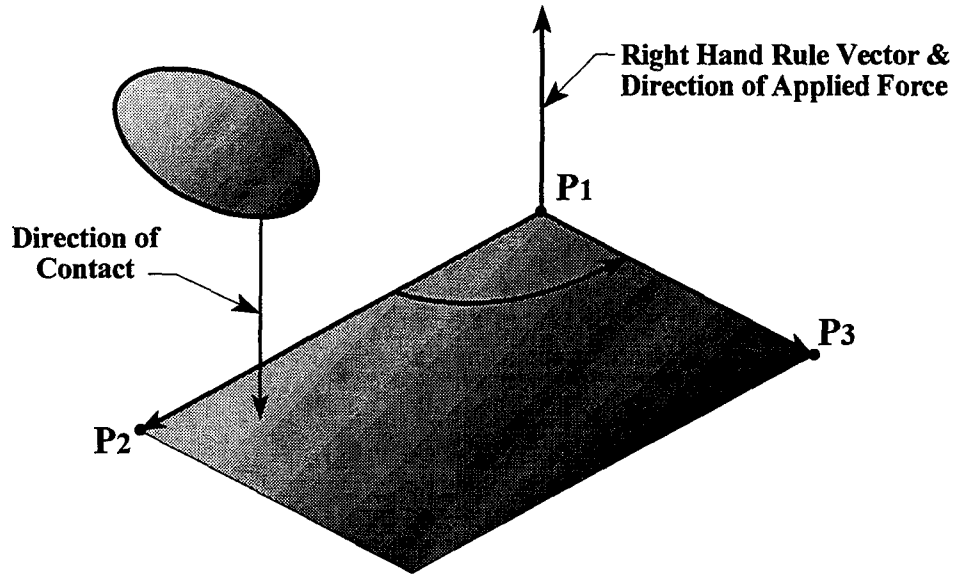
# Plane Definition

## *Three Corner Points*



# Positive Side of Plane

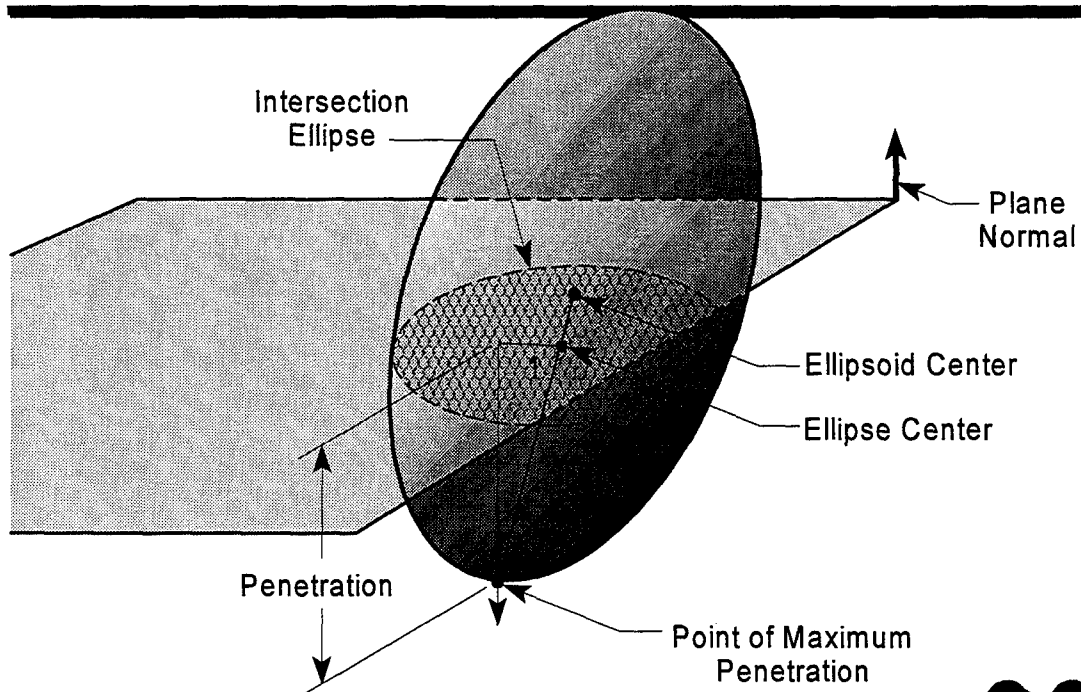
---



---

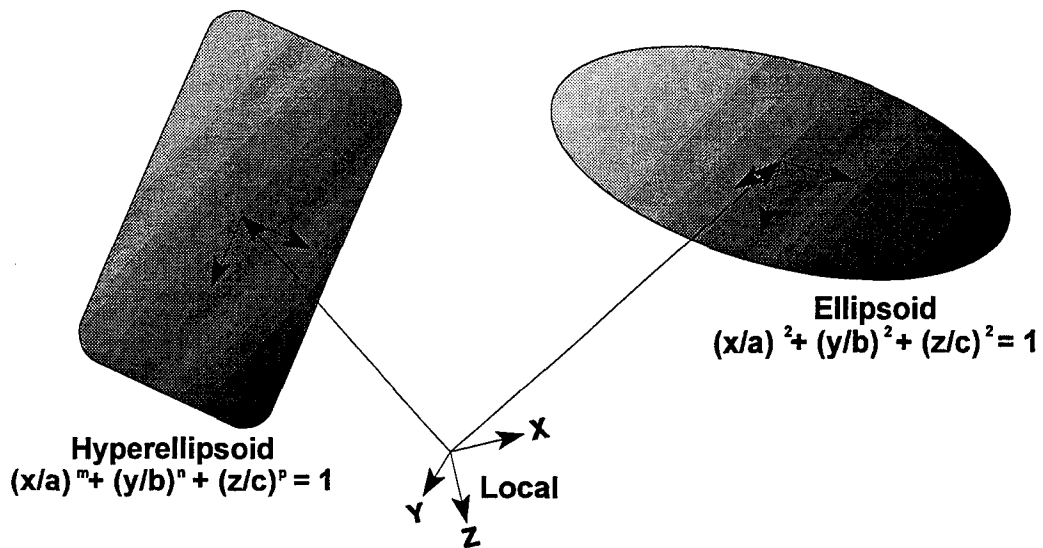
# Plane-Segment Contact

---



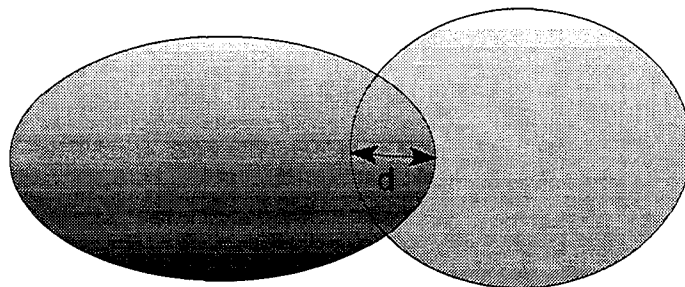
# Additional (Hyper)Ellipsoids

---



## Ellipsoid-Ellipsoid Contact

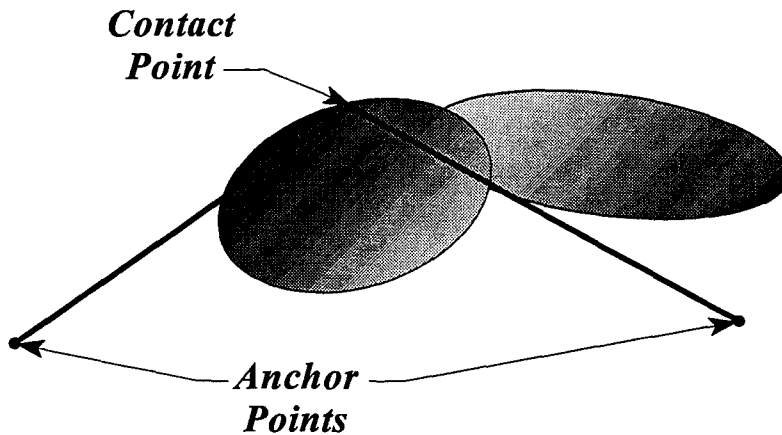
---



# Simple Belt

---

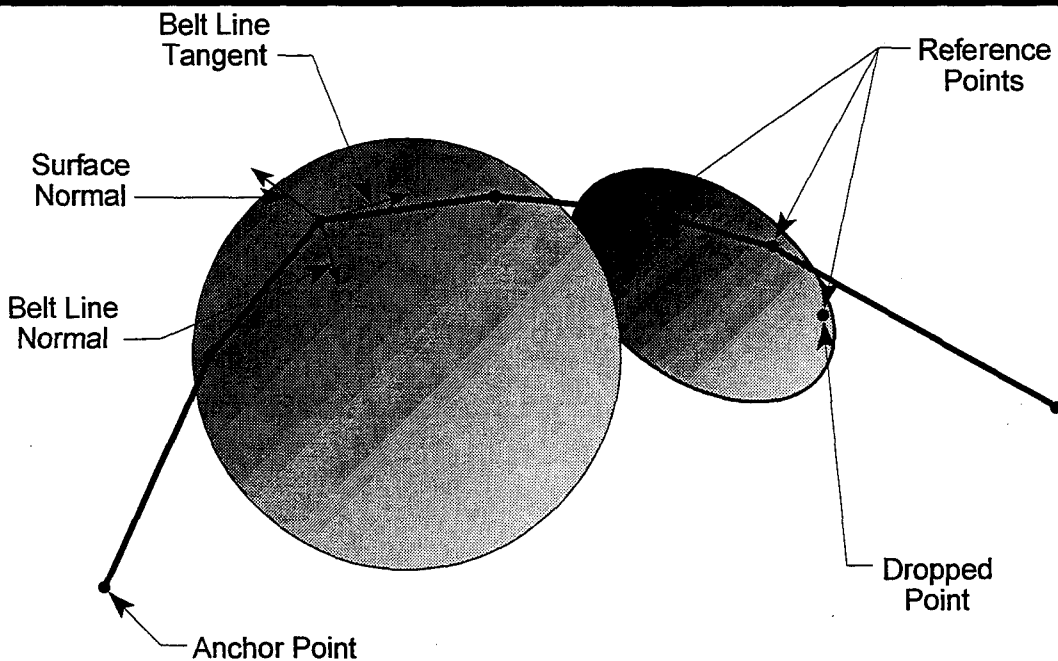
- ▶ Two Anchor Points
- ▶ One Body Contact Point



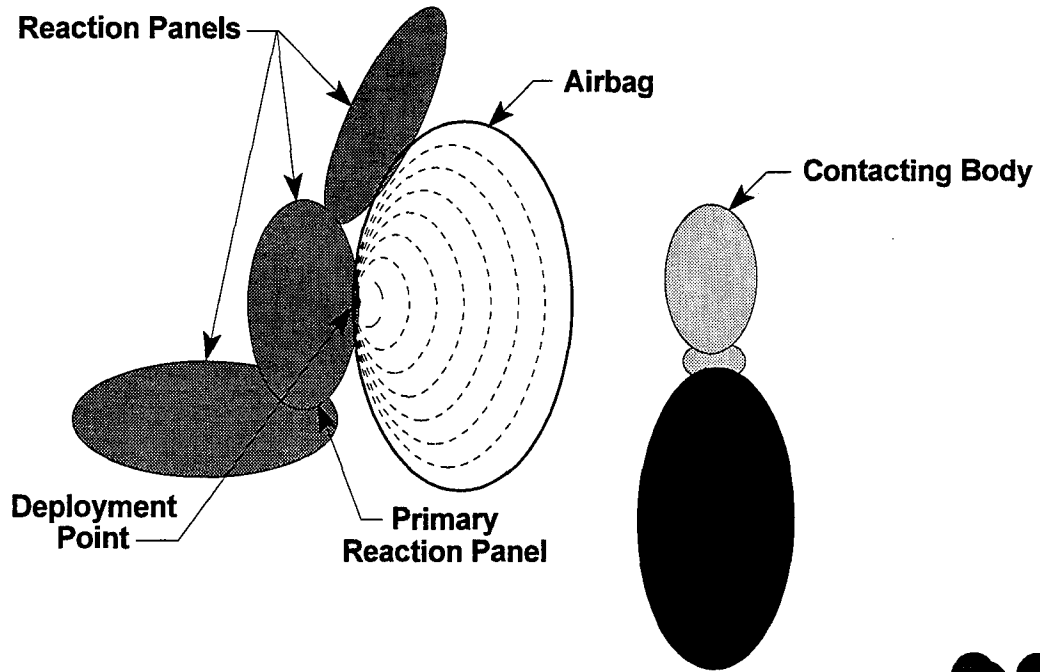
---

# Harness Belt

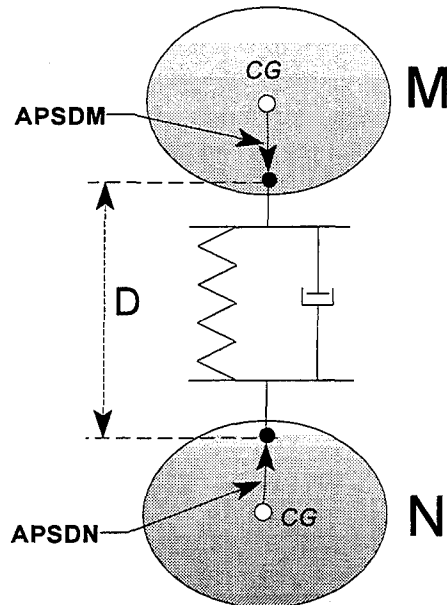
---



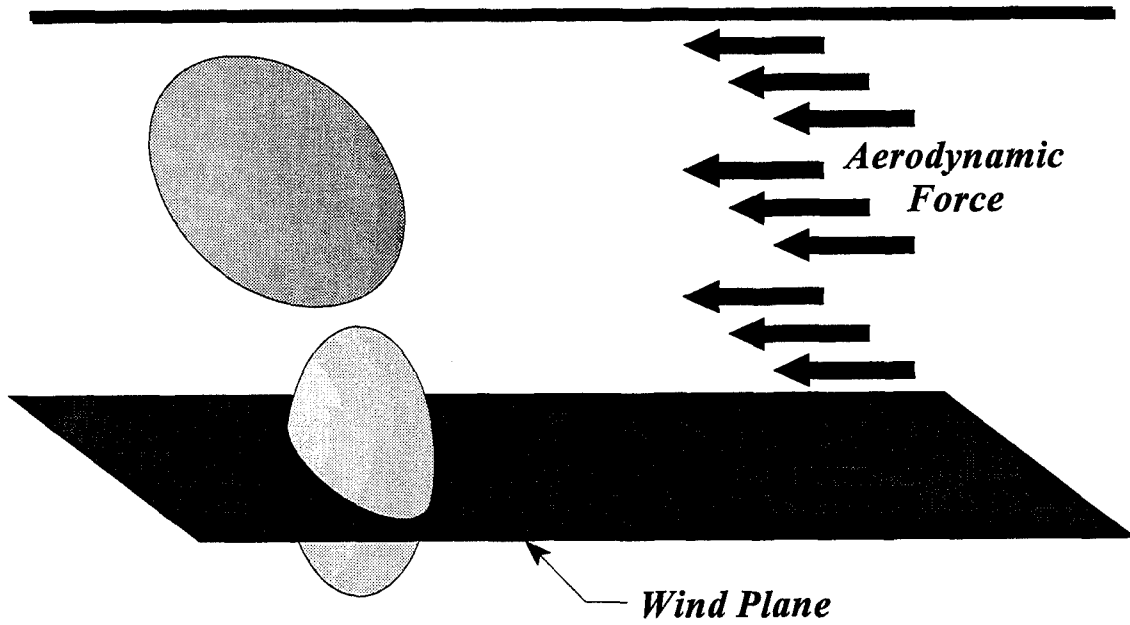
# Airbags



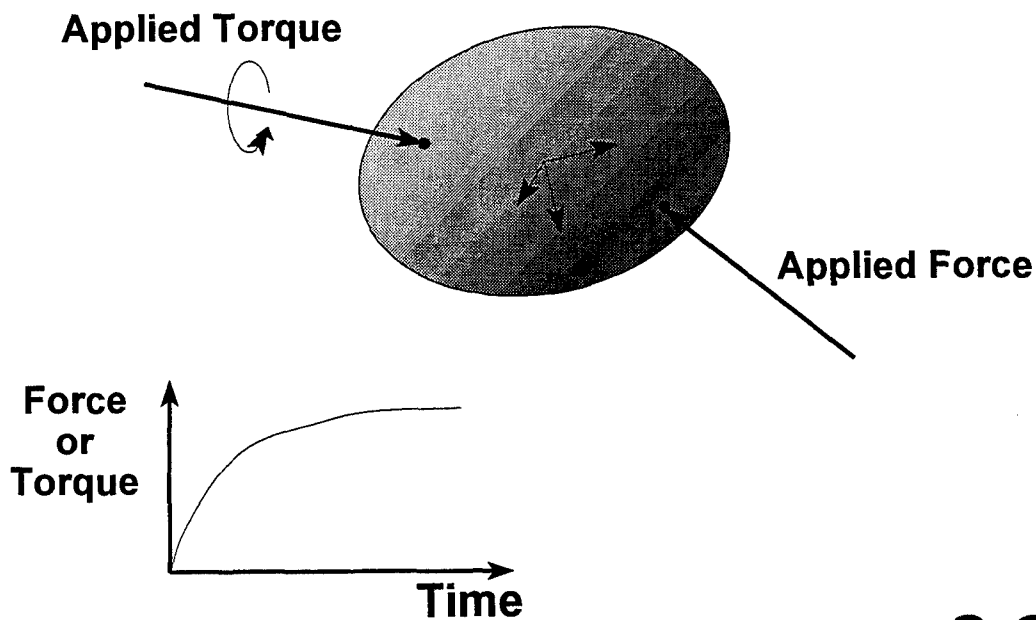
# Spring-Dampers



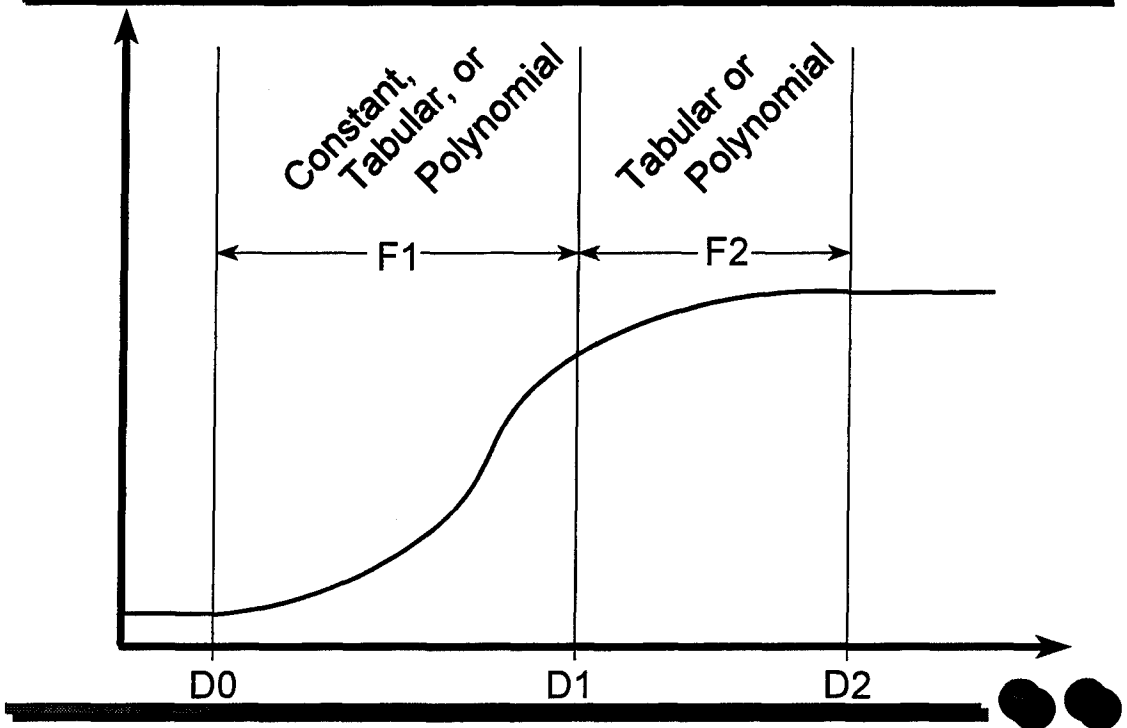
# Wind Forces



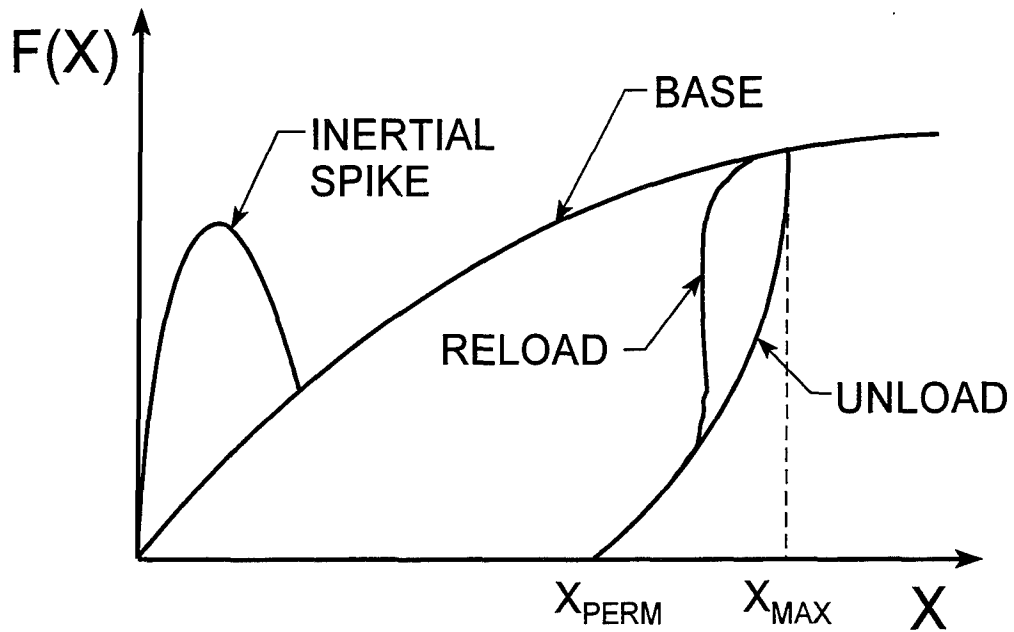
# Applied Forces



# Function Subdivisions

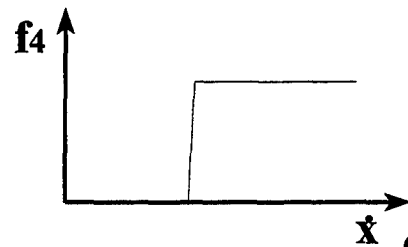
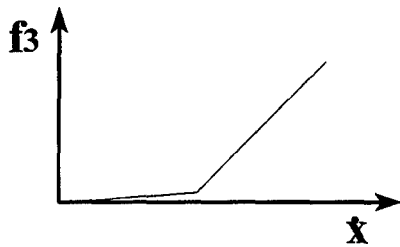
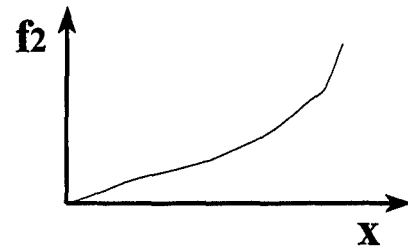
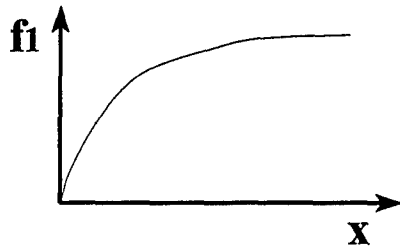


# Functions

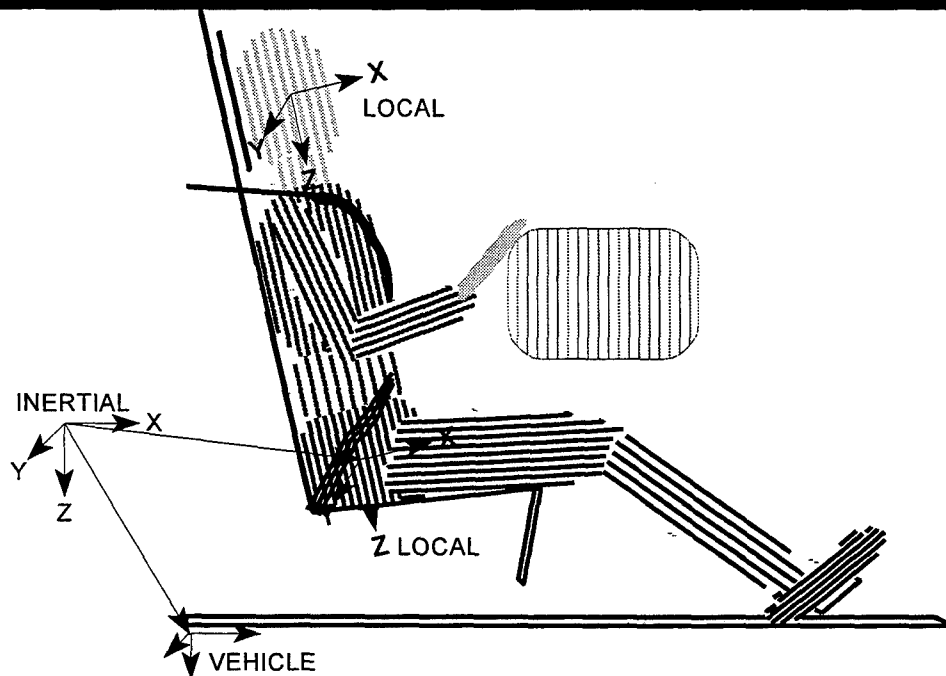


# Rate Dependent Functions

$$F = f_1(x) + f_2(\dot{x})f_3(x) + f_4(\dot{x})$$



# Initial Conditions





# Balancing

---

## *Suggested Procedure for Seating Body*

- ▶ **Start Position**
    - *Torso Segments Parallel with Seat Back*
    - *Legs Rotated Above Floor & Pedals*
  - ▶ **Adjust Lower Torso Position to Balance More than Half Body Weight**
    - *Rotate Torso Segments to Contact Seat Back*
  - ▶ **Rotate Upper Legs Down to Balance Most Weight**
    - *Check Horizontal Forces*
  - ▶ **Rotate Lower Legs to Fully Balance Weight with Foot/Floor Contact**
- 

# Time Histories

---

- |  |  |
|--|--|
| <ul style="list-style-type: none"><li>▶ <b>Specified</b><ul style="list-style-type: none"><li>- <i>Point Linear</i><ul style="list-style-type: none"><li>• <i>Accelerations,</i></li><li>• <i>Velocities, &amp;</i></li><li>• <i>Positions</i></li></ul></li><li>- <i>Segment Angular</i><ul style="list-style-type: none"><li>• <i>Accelerations,</i></li><li>• <i>Velocities, &amp;</i></li><li>• <i>Positions</i></li></ul></li><li>- <i>Joint Parameters</i></li><li>- <i>Segment Wind Forces</i></li><li>- <i>Joint Forces &amp; Torques</i></li><li>- <i>Total Body Properties</i></li></ul></li></ul> | <ul style="list-style-type: none"><li>▶ <b>Default</b><ul style="list-style-type: none"><li>- <i>Plane/Segment Contacts</i></li><li>- <i>Belt Contacts</i></li><li>- <i>Harness Belt Contacts</i></li><li>- <i>Spring-Damper Forces</i></li><li>- <i>Ellipsoid/Ellipsoid Contacts</i></li><li>- <i>Airbag Contacts</i></li></ul></li></ul> |
|--|--|
-

## ADVANCED DUMMY NECK DESIGN USING DYNAMAN

Narayan Yoganandan, Ph.D., \*Tariq Shams, Ph.D.,  
Joseph Cheng, M.D., \*Nagarajan Rangarajan, Ph.D., Frank Pintar, Ph.D.

Department of Neurosurgery, Medical College of Wisconsin  
and Department of Veterans Affairs Medical Center

Milwaukee, Wisconsin

\* GESAC Inc., Kearneysville, WV

### PURPOSE

The objective of the present study was to develop a methodology to advance the design of a prototype physical model of the human head-neck structure with particular emphasis to the neck. This was accomplished using a combination of the DYNAMAN software to guide the design of controlled laboratory experimentation. The research procedures are divided into the following phases: a) Design and modeling methodology, b) Neck modeling using DYNAMAN, and c) Necessary experimental protocol for the testing phase of the project.

### MATERIALS AND METHODS

#### A: Design And Modeling Methodology

##### Requirements of the advanced neck:

Ideally, the advanced neck has to meet appropriate design performance requirements. These include anthropometric, kinematic, dynamic axial compressive and torsional stiffness requirements. The anthropometric requirements ensure the proper length, mass and shape, and correct occipital condyle locations in the neck model. The kinematics requirements, in this

study, were based on human volunteers tests conducted at the Naval Biodynamics Research Laboratory, New Orleans, Louisiana (NBDL). These data define the specifications regarding the time varying response of the head and neck (rotation) under frontal and lateral modes of loading. Some limited extension data were also available from tests conducted by the Japanese Automobile Research Institute (JARI). These low velocity data, described in terms of the torque versus angle corridors, were used for the development of the advanced dummy neck model. The axial stiffness in the compression mode was obtained from tests conducted by researchers at the Medical College of Wisconsin, Milwaukee, WI, and the torsion stiffness data were obtained from test conducted at Duke University.

Initial design review: The advanced neck was derived from a prototype developed by the Vehicle Research Test Center (VRTC). This neck consists of five layers of aluminum and butyl rubber disks. A pair of cables, with inferiorly attached extension springs, connect the head to the base of the neck along the anterior and posterior directions. Dynamic tests conducted by VRTC

using the acceleration pulses used in the NBDL tests, indicated a reasonable agreement with the response of this neck with the human volunteer data. Additional information on the bending stiffness of the neck was obtained using the quasi-static tests conducted at the Armstrong Research Laboratories of the Wright Patterson Air Force Base.

#### Modeling of the advance neck design:

The design goals for the advanced neck were to maintain the biofidelity achieved with the VRTC neck and properly interface the neck with the thoracic spine and the head. In addition, the neck should also meet the limited requirements under the extension load vector. A final goal was to allow the user to set the initial angle of the head with respect to the neck prior to a planned test. The principal design parameters to be derived from the output of the DYNAMAN modeling were:

- i. Stiffness of compliant disks
- ii. Stiffness of springs
- iii. Size of compliant disks
- iv. Spring and cable attachment locations for the location of the stop mechanism

The stop mechanism served a two-fold purpose. One stop was designed to produce an appropriate contact between the neck and the head at the end of the motion. A second set of stops were designed to control the stiffness of the neck during extension.

#### **B: DYNAMAN Modeling**

The aluminum disks were modeled as rigid segments. Each intermediate compliant disk was modeled with a pair of spring-dampers. A pin joint was defined between adjacent segments. The

cables were modeled using the harness belt option. The connection with the springs were defined as slip joints, The head/neck stop was modeled using hyperellipsoids to preserve the rectangular geometry. Additional stop at the bottom of the neck were modeled using ordinary ellipsoids and planes. The model was validated using the dynamic tests conducted by VRTC and the quasi-static tests performed by the Armstrong Laboratories. A series of simulations was conducted to determine the optimum design parameters which offered the best agreement with the kinematic specifications.

#### Design and manufacture of the advanced

neck: Once the design parameters were selected, part and assembly drawings of the neck were obtained. The disk stiffness was used to specify the appropriate material for this component. The disks were built from urethane (neck 3) and rubber (neck1 and neck2). The stiffness data were used to specify a nominal durometer and a compression specification. Additional disks were manufactured with durometer values which were two points less than the nominal target value. The appropriate spring and the associated dampers were selected. The design also included the friction joint at the occipital condyles, the head/neck stop, and the extension stop. Photographs of the prototype neck are shown in Figure 1.

#### **C: Experimental Methodology**

Inertial (dynamic) loading procedures were developed to allow for multi-axis (flexion, extension, lateral bending or any orientation in the sagittal or coronal plane) and multiple acceleration/deceleration testing at varying velocity levels with varying wave forms (G-time

histories). The methodology permitted a complete documentation of the dynamic temporal kinetics and kinematics of the head-neck prototype.

Testing Assembly: A mini-sled pendulum equipment was developed at the Medical College of Wisconsin Neuroscience Laboratories to house the computer designed head-neck and the loading assembly. The mini-sled consisted of two precision ground rails which were rigidly attached to a steel frame. Four precision rolled ball bearings formed the interface between the cart assembly and the precision rails. A six-axis load cell was included in the cart assembly. In addition, the cart assembly allowed for a vertical axis of rotation of the head-neck structure under test to permit different loading modalities. A flat surface was attached to the cart assembly to accept the impact from the pendulum. The hollow pendulum impactor assembly was cylindrical in shape. It was designed such that varying mass (up to 100 kg) could be added at its center thereby adjusting initial momentum input. A load cell was attached at the leading face of the impactor with capabilities to attach energy absorbing materials such as padded surfaces.

Instrumentation: A uniaxial accelerometer (Entran, Model EGA-7231, Morgantown, CA) was attached rigidly to the rear face of the pendulum for measuring the input accelerations. A uniaxial load cell (Interface, Model 1210A0, Scottsdale, AZ) was attached to the leading face of the impactor to record the input longitudinal forces. A triaxial accelerometer and a triaxial angular velocity sensor (ATA Sensors Inc., Albuquerque, NM) were attached to the head to measure the linear and angular components of the acceleration and velocity, respectively. A six-axis load cell

(Denton Inc., Rochester Hills, MI) was attached to the head-neck junction to measure the generalized force (and moment) time histories. In addition, an accelerometer placed at the inferior (base) level recorded the acceleration along the slider direction. Another six-axis load cell (Denton Inc., Rochester Hills, MI) was placed at the base to gather the output generalized force histories. A total of 21 channels of information were collected. All information were gathered using a digital data acquisition system (ODAS, DSP Technology, San Francisco, CA) according to the SAE J211b specifications at a sampling rate of 12,500 Hz. A high-speed video camera (Kodak, Model 4050, Rochester, NY) operating at 2250 full frames per second captured the impact event.

Specimen Mounting and Loading: The head-neck assembly was rigidly fixed at the inferior end. The superior end, i.e., the head was unconstrained. Retroreflective targets were placed on the head, as well as on every level of the neck according to standard procedures. The head-neck assembly was and inserted into the fixation on the mini-sled. The initial mounting orientation determined whether the loading was flexion (anterior region facing the impactor), extension (posterior region facing the impactor), or, lateral bending (lateral aspect facing the impactor). By rotating the head-neck assembly in the fixture housed in the mini-sled through 180 degrees, the orientation was changed from flexion to extension or, vice-versa. Like wise, a 90 degree rotation resulted in left or right lateral bending orientation. The head-neck assembly was subjected to non contact type inertial loading by impacting at the inferior end, i.e., the base, with the pendulum impactor. Three velocities were chosen to induce

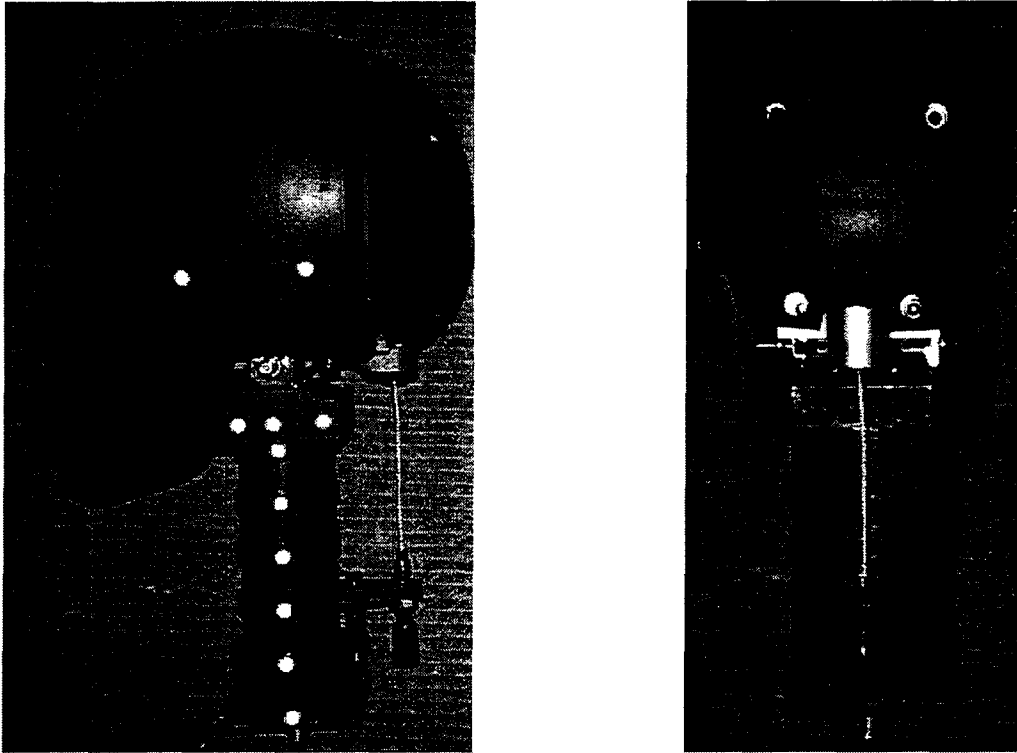


**Figure 1:** Photograph of the dummy neck designed using DYNAMAN software. Left side photo shows the side view; right side photo shows the back view.

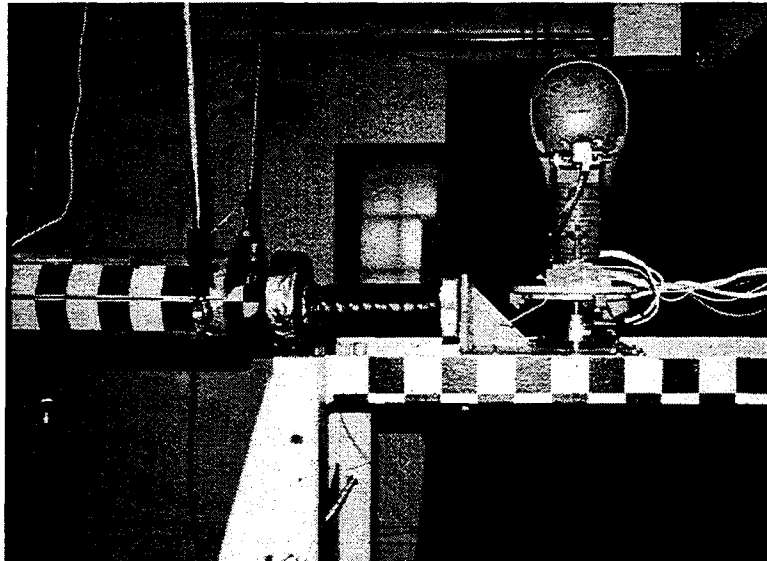


**Figure 2:** Experimental test set-up illustrating the mini-sled pendulum used to apply dynamic loading to the head-neck assembly. Refer to text for details.

the inertial insult. Figure 2 is a photograph of the test set-up for a lateral bending test.

## RESULTS AND DISCUSSION

Three prototypes were evaluated in the present study; neck1, neck2 and neck3. While neck1 and neck2 were identical except for the durometer of the rubber (78 and 76, respectively), neck3 was made out of urethane. Flexion, extension, and lateral bending tests were conducted at 5, 7.5 and 10 mph velocities for all the three necks. The generalized forces from the inferiorly placed six-axis load cell was not gathered for the first two prototypes. In contrast, all channels of data were gathered for the neck 3 prototype. The right-handed Cartesian frame of reference was consistently used in the present study; the positive x, y, and z-axis referred to the anatomical posterior to anterior, right to left, and inferior to superior directions, respectively.

Under the flexion mode of external loading, the generalized force-time histories recorded by the six-axis load cell placed at the head-neck junction demonstrated bending moment (flexion/extension) and shear (anterior/posterior) forces to be predominant during the loading phase without any significant off-axis forces (lateral shear or axial load) or moments (torsion or lateral-flexion). This suggests that the head-neck structure is primarily subjected to a planar type of dynamic force input. This phenomenon was observed for the three velocities of impact under these testing modalities. As apart of further analysis of test data, the positions of the retroreflective targets were digitized from the high speed video at equal intervals. Head and neck rotation angles, head lag angle, and head center of gravity displacement

were computed. In order to compare the prediction from the simulation with the tests, a set of new simulations were conducted using the actual experimental environment. The stiffness data for the disks were also updated using the compression test results of the manufactured disks.

The preliminary analysis indicate good agreement between the DYNAMAN simulation and the experimental test results. Figure 3 shows the comparison for the head-rotation angle, figure 4 shows the head lag angle with respect to the neck and Figure 5 includes the head displacement at its center of gravity for the 10 mph velocity test (this produced a peak acceleration of approx. 7.5 G). These data indicate that the head and neck angles and the lag motions are well predicted by the DYNAMAN simulation. Individual results will be discussed during the presentation.

In the present study, we have developed a methodology to further the advancement of a new dummy neck design. Principles of computer modeling combined with dynamic experimental techniques were adopted. Initial designs based on the simulations led to the selection of three prototypes designs minimizing the testing of a wide variety of alternatives. Initial experiments on the selected designs provided the necessary confidence in the hybrid approach. Testing in the other modalities are necessary for full evaluation. Our results serve as a first step towards the development of neck with enhanced biofidelity.

## ACKNOWLEDGMENT:

This study was supported in part by PHS CDC Grant R49 CCR 507370, and the Department of Veterans Affairs Medical Research Service.

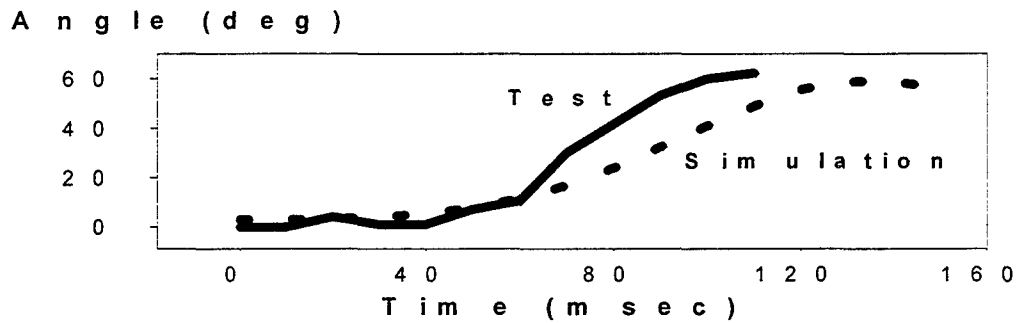


Figure 3: Head rotation angle for a 10 mph velocity input under flexion mode. Note a good comparison between the experimental results from the prototype and the DYNAMAN simulation results.

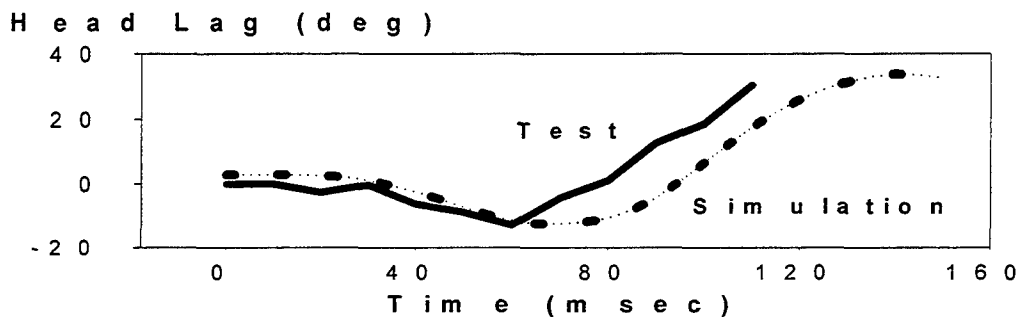


Figure 4: Head lag angle for a 10 mph velocity input under flexion mode. Note a good comparison between the experimental results from the prototype and the DYNAMAN simulation results.

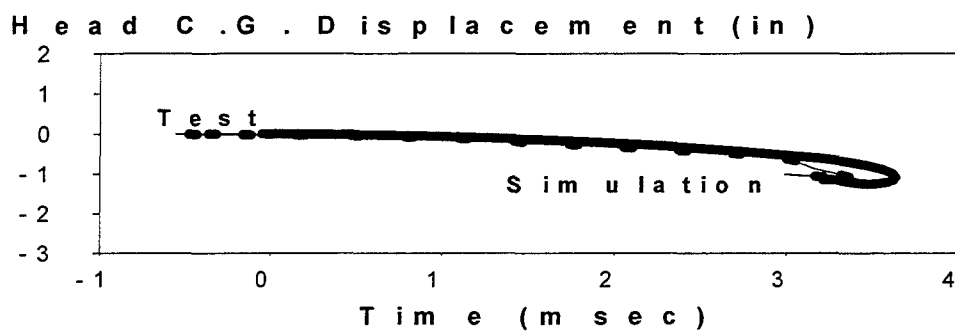


Figure 5: Head center of gravity displacement for a 10 mph velocity input under flexion mode. Note a good comparison between the experimental results from the prototype and the DYNAMAN simulation results.

## **DYNTASK: PROGRAM FOR ERGONOMIC ANALYSIS OF HUMAN TASKS**

T. Shams, GESAC  
R. McMahon, U.S. ARL, HRED  
N. Rangarajan, GESAC

### **INTRODUCTION**

DYNTASK is a software program that has been developed to analyze an individual performing a series of tasks. The software was developed to meet the requirements of the Human Research and Engineering Directorate of the U.S. Army Research Laboratory at Aberdeen. The aim of the software was to allow one to easily analyze design limits for lifting tasks.

Traditionally, MIL-STD-1472D is the reference for establishing design weight lift limits. This method had several shortcomings, principally:

- It was a paper and pencil based analysis and was difficult to visualize the lifting task.
- One could not determine the role of variables like posture in the analysis of the limits. Typically the limit would depend on the geometrical horizontal and vertical distance from the feet and not directly on posture.
- Loads and moments acting at the joints were not calculated in this scheme, and likelihood of exceeding joint strength limits could not be analyzed.
- The procedure was applicable to only lifting tasks.

Thus, there was a need for a PC-based model to supplement MIL-STD-1472D. The basic requirements of such a program were that it would use the NIOSH Lifting Equation [1] to determine the weight limits for a lifting task. It should be applicable to a variety of lifting tasks from different postures and would include an analyses of joint forces and moments. It was also required to provide a graphical display of the human subject with the load at different positions during the task, specially at the beginning and end of the lifting motion. DYNTASK was developed to address the above shortcomings.

### **GENERAL DESCRIPTION OF PROGRAM**

DYNTASK consists of several steps in the analysis of a task and in the manipulation of the data required for defining one or more tasks.

The first step is the selection of a human model. Male and female models can be defined with different weights and heights.



The size of the human model is used as the basis for calculating the joint load limits.

The second step is defining the various tasks. One or more tasks can be defined. The normal type of task is a lifting task, but the program also includes a provision for defining pushing or pulling tasks, though the limits for these types of tasks have not been as well defined as for the lifting types.

NIOSH Lifting Equation: The procedure for defining lifting tasks are based on the guidelines published by the U.S. Department of Health and Human Services in the document: "Applications Manual for the Revised NIOSH Lifting Equation". The equation is used to estimate the maximum load a healthy person can lift according to a set of parameters. Each parameter is defined within a range of values. Outside the range, lifting of any weight is not considered feasible. E.g., there is a coefficient that is used to determine the effect of the horizontal distance of the load being lifted from the center of the feet. This distance is defined only between the range of 10 inches and 25 inches. It is assumed that an average sized individual cannot bring a load, such as a box, closer to the feet than 10 inches in the horizontal direction or hold it further than 25 inches. Similar ranges are defined for other parameters. For a value of a parameter within a feasible range, a multiplier is defined, which is used in calculating the final load limit that is allowed. Figure 1 shows the screen used for defining a specific lifting task.

Task # 1: Task 1					
Avg.Weight	20.00	Max.Weight	20.00		
Length	10.00	Width	10.00	Height	10.00
Task Type	Lift	Frequency	1	(Lifts per 15 minutes)	
Work Duration (hour)	D <=1	Coupling	Good		
Origin	H (in)	10.00	V (in)	20.00	A (deg) 0.000
Destination	H (in)	10.00	V (in)	40.00	A (deg) 0.000
Significant Control	Yes				
					OK

Figure 1. Data Screen for Defining Lift Tasks

Once the tasks are defined, the program can be used to calculate the maximum load according to the NIOSH Lifting

Equation. The maximum load calculated depends on the following factors:

- Load weight
- Horizontal and vertical location of the origin of the lift
- Horizontal and vertical location of the destination of the lift
- Asymmetry of the posture at either the origin or destination. The asymmetry represents the twisting of the body about the vertical axis.
- Frequency of the lifts
- Duration of the work before resting
- Coupling of the hands to the load
- Level of control required at the destination of the lift

Figure 2 shows an example of the calculation done for estimating the maximum load limit for a given task.

JOB ANALYSIS WORKSHEET	
Task 1	
	$RML = LC \times HM \times UM \times DM \times AM \times FM \times CM$
ORIGIN:	$RML = 51 \times 1.00 \times .925 \times .918 \times 1.00 \times 1.00 \times 1.00 = 42.9 \text{ lbs}$
ORIGIN:	$LIFTING \text{ INDEX} = \text{Weight} / RML = 20.8 / 42.9 = .466$

Figure 2. Single Job Analysis Sheet

The program allows one to define any reasonable posture for the human subject carrying the load. Four default postures are defined to bring the body automatically to the closest posture that the user is interested. These are standing, bending, kneeling and squatting. The user can then modify any one of these postures to any specific posture that the user wants by rotating the individual segments.

Figure 3 shows an example of the posture display for a task. As the user scrolls through the list of tasks, the display will

be automatically updated with the corresponding posture for the new task.

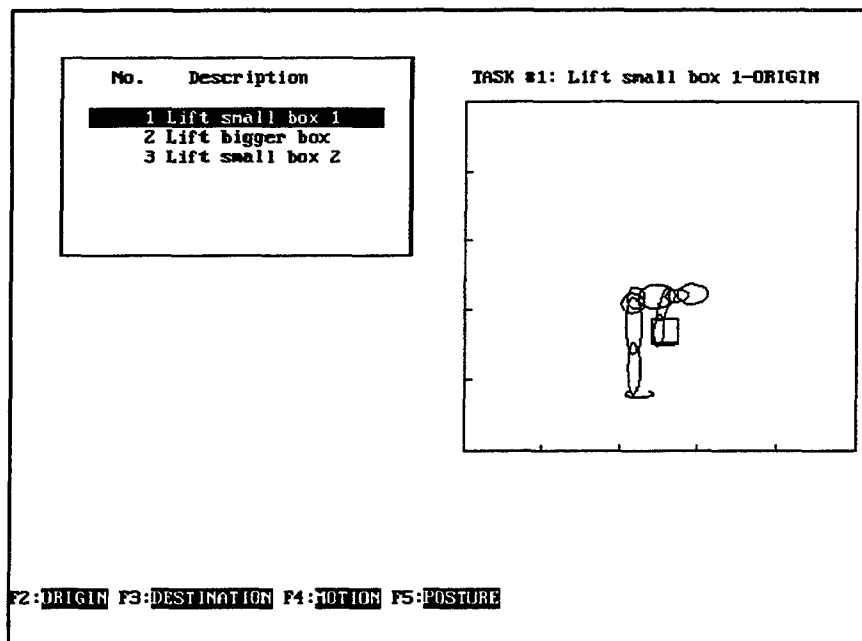


Figure 3. Screen Showing Postures for Different Tasks

Joint Load Analyses: In addition to the basic lifting calculation, a second type of analysis is also available. This second feature of the program can be used to perform a two-dimensional analysis of the task. This analysis provides estimates of the forces and moments that will be generated at the principal joints during a particular task. This analysis can also be used to do simple time dependent calculations.

The forces and torques required to maintain equilibrium at several joints are calculated. These are the wrist, elbow, shoulder, pelvis, hip, knee, and ankle. The analysis, at the present time, is two-dimensional, and it is assumed that the joint loads are symmetrically distributed between the left and right sides. Normally, the joint loads and moments are calculated for the origin and for the destination of the lifting task. These loads are compared with the biomechanically derived maximum values that can be borne at each joint by an average sized male or female [2]. A table is displayed which shows the forces and moments at each of the joint along with maximum allowed values for the specified load and posture conditions. The joint motions are also controlled by range of motion data for average males and females.

Figure 4 shows the display of a table listing the joint forces and moments along with the maximum allowed limits at each of the selected joints.

No.	Description
1	Lift small box 1
2	Lift bigger box
3	Lift small box 2

TASK #1: Lift small box 1-ORIGIN

Joint	Frc-X	Frc-Z	Moment	Trq Max	Lnk Ang
Ankle	0.000	-88.00	567.9	-1226.	90.00
Knee	0.000	-80.10	555.1	813.2	180.0
Hip	0.000	-60.41	577.8	1943.	126.0
Pelvis	0.000	-98.93	667.1	-1727.	94.00
Shoulder	216.4	55.09	-557.8	742.9	73.00
Elbow	215.5	40.82	1650.	557.7	171.0
Wrist	213.8	30.50	-174.4	0.000	94.00

F2: ORIGIN F3: DESTINATION F4: MOTION

### Screen for Joint Force/Torque

For the purpose of analyzing load limits for typical military personnel, provision has been made in the program to define a backpack which can be attached to the back of the individual. The additional force and moment produced by the pack are added to that produced by the load in the final calculations.

In addition to defining the task at the origin and destination, the program allows one to define simple motions. The trajectory is defined to be a straight line connecting the origin to the destination. Intermediate positions are calculated on the basis of two kinds of motion. The load can be translated with constant velocity, or an initial constant acceleration can be applied at the beginning to move the load from rest to a constant velocity. If significant control is required at the end of the trajectory, a similar deceleration is applied to bring the moving load to a stop. The joint angles required at the intermediate positions are determined from an interpolation function connecting the initial and final postures. Figure 5 shows the display of the model at a specific intermediate position.

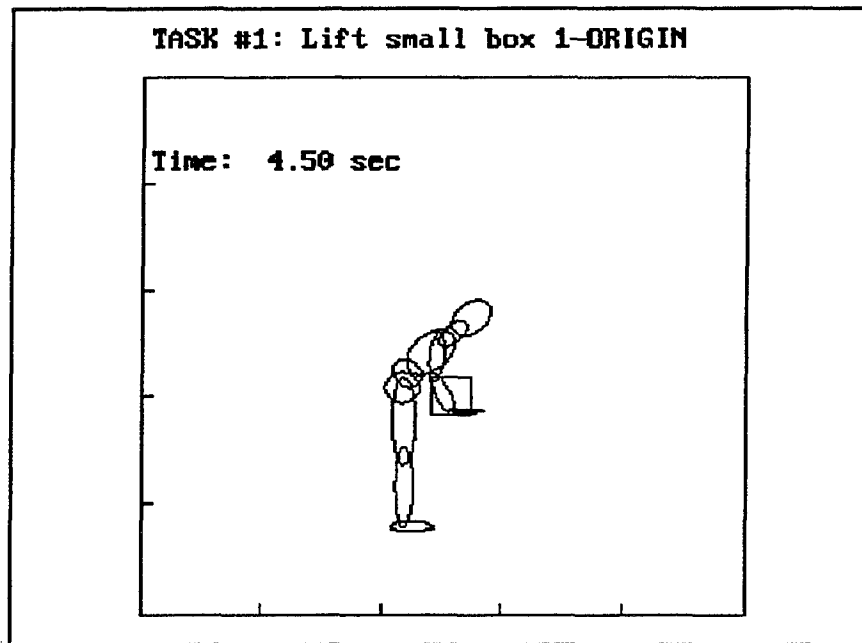


**Figure 5. Display of posture during motion**

Graphical Display: The viewing features of DYNAMAN have been utilized to display the human subject in a three-dimensional view. Thus the view can be rotated, panned and zoomed. The load is displayed as a rectangular parallelepiped, and if a backpack is defined, it is shown as an ellipsoid. The user is able to rotate each segment, though, because of the two-dimensional nature of the analyses, segments with left and right sides are moved symmetrically. The load is displayed as a rectangular parallelepiped and can be translated so that the hands can be attached at different locations on the load (e.g. under it or at the sides). Figure 6 shows the screen that is displayed when the user is in the main PICTURE menu. The various function keys allow access to the different kinds of graphical manipulation.

When a motion has been defined, the user can step through and view the intermediate positions. For any position, the user can view the table for the joint forces and moments. Additional preview features are available which allow the user to quickly view each task that has been defined. Similarly, the four default postures can be viewed before actually applying them to a task. When a motion is defined over time, the time history of the predicted joint forces and moments can also be viewed as plots. Figure 7 shows an example of a plot generated from such a motion.

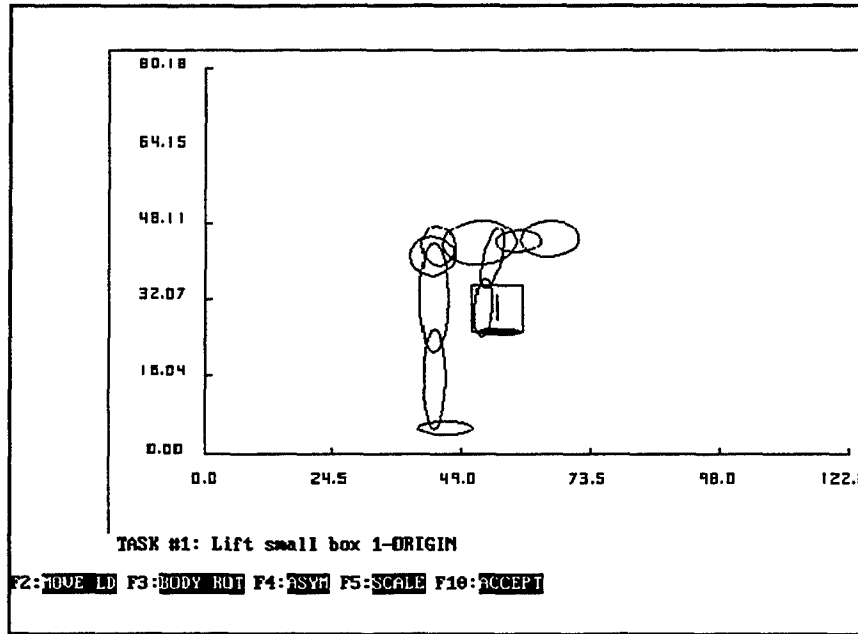


Figure 6. Screen Showing Menu for Modifying Subject and Load Positions

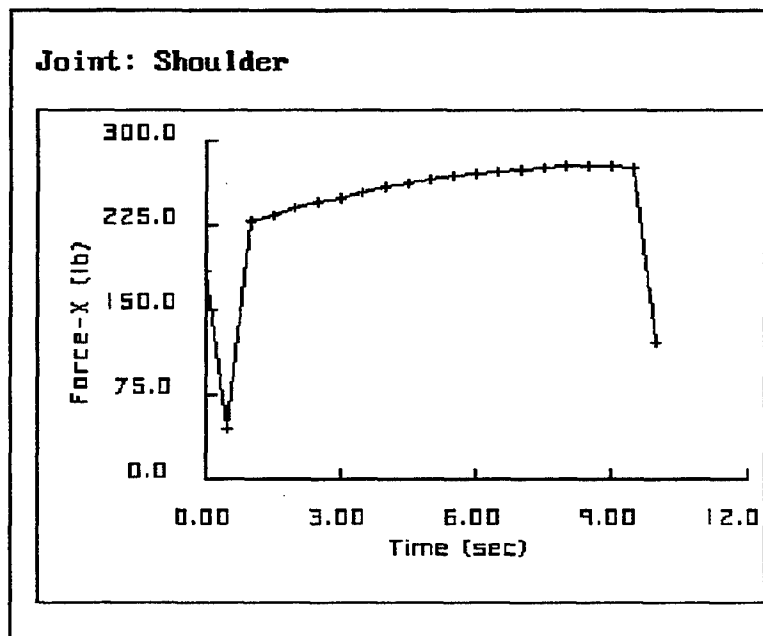


Figure 7. Display of Plots for Joint Data

## **DYNAMAN MODIFICATIONS USED IN PROGRAM**

The process of software development for DYNTASK was made considerably simpler by the use of several important modules from DYNAMAN. These were:

- The human model was based on the ATB/DYNAMAN model of linked segments. The actual inertial and geometric data generated for a model is based on the BODGEN/GEBOB program. Much of BODGEN has been fully integrated into the program, though DYNTASK only allows for adult male and female subjects and the 17 segment model with hands are automatically generated. In addition, the program generates the correct initial segment angles for a standing model.
- The joint model in DYNAMAN has been modified to allow for calculation of joint forces and torques for either static equilibrium (for a bilaterally symmetric case) or when a constant acceleration is applied.
- Most of the graphical features of DYNAMAN were retained. These included the viewing options, options for rotating the individual segments, and translating segments. In addition, the basic drawing module was used to provide for the additional previewing features.
- The plotting features of the DYNAMAN post-processor were utilized to view plots of the joint forces and moments, when motion data were defined.

## **FUTURE ENHANCEMENTS**

A number of enhancements are being contemplated to improve the software. These include:

- Extending the joint force/moment analysis to three dimensions.
- Enhanced analysis for biomechanical limits at the lower back, wrist and shoulder. This would include an improved model of grasping by the hand include application of twist.
- Extending the analysis to other types of tasks, apart from lifting, which includes improving the current crude models for pushing and pulling.
- Porting the software to the Microsoft Windows environment.

## REFERENCES

1. Waters, Thomas, Putz-Anderson, Vern, and Garg, Arun, "Applications Manual for the Revised NIOSH Lifting Equation," U.S. Department of Health and Human Services, January, 1994.
2. Chaffin, Don, and Andersson, Gunnar, "Occupational Biomechanics," Second Edition, John Wiley and Sons, 1991.



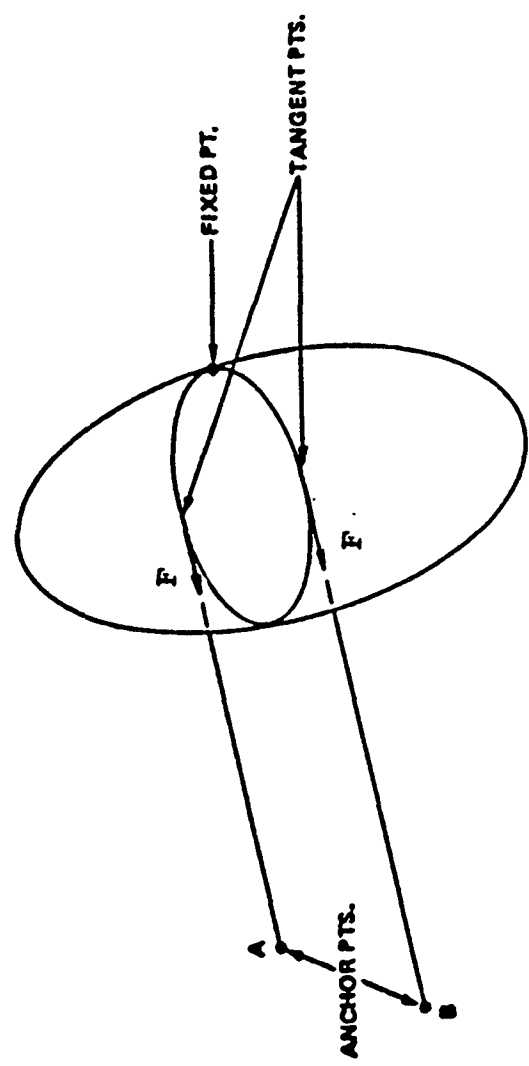
# **A New Harness Algorithm for Simulating Belt Slippage During Occupant Impact Motion**

**Yih-Chang Deng  
GM R & D Center**

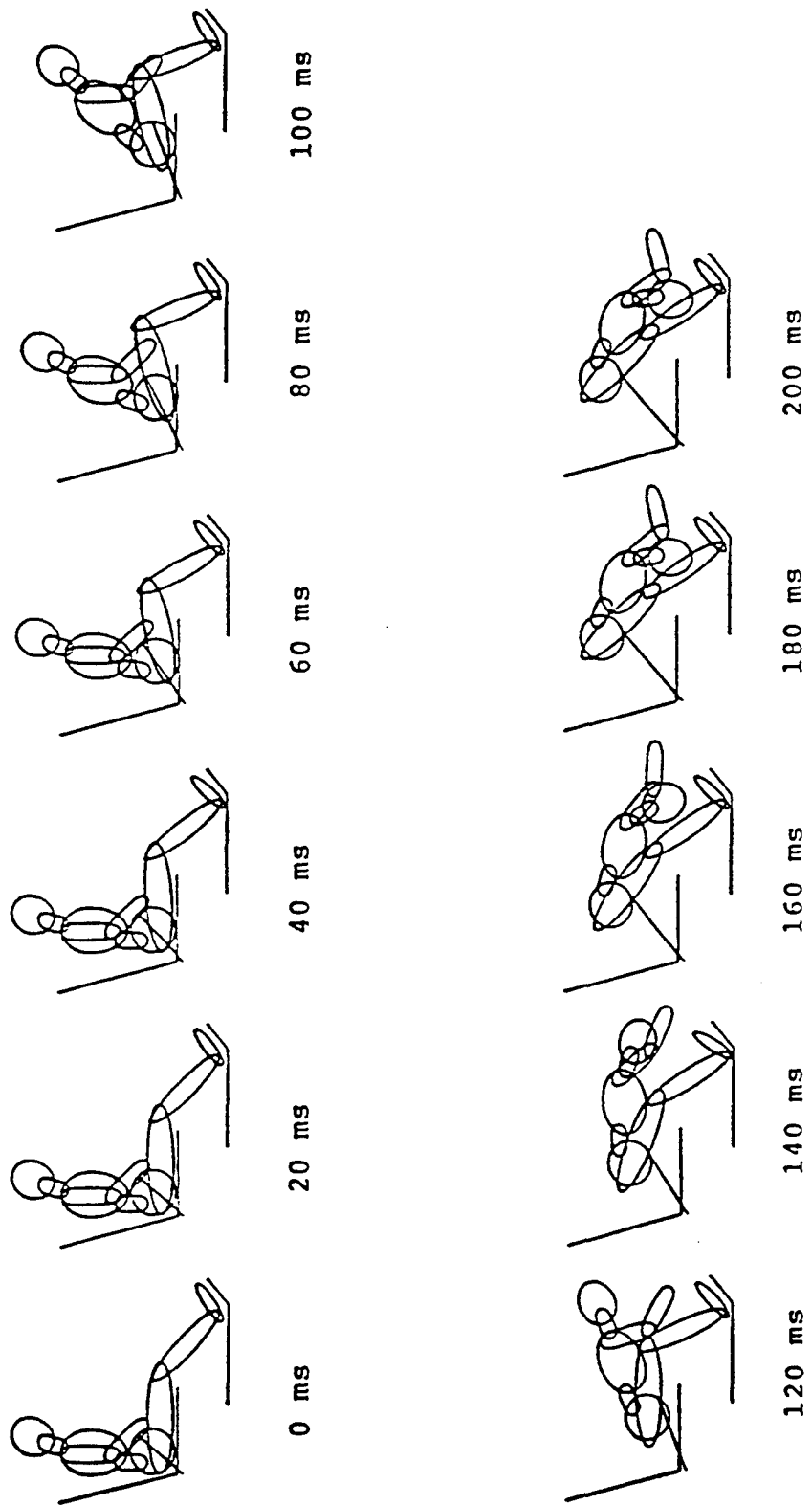
# **Options for Modeling the Belt Restraint System in the CAL3D Program**

- **3-Point Belt Model**
- **Harness Model**

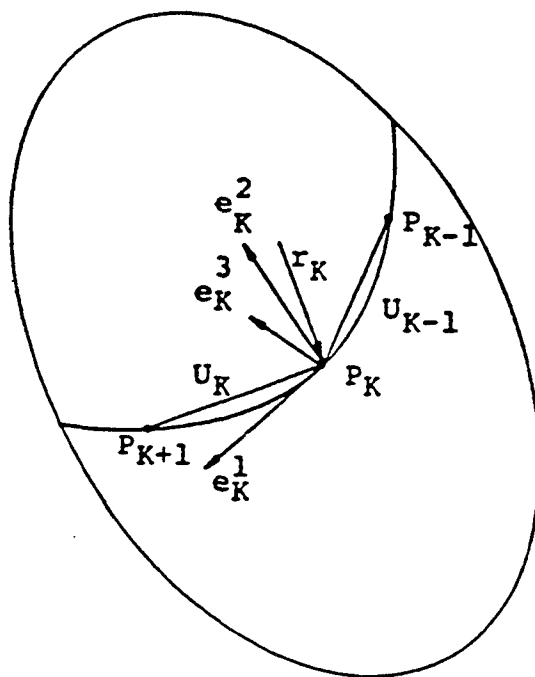
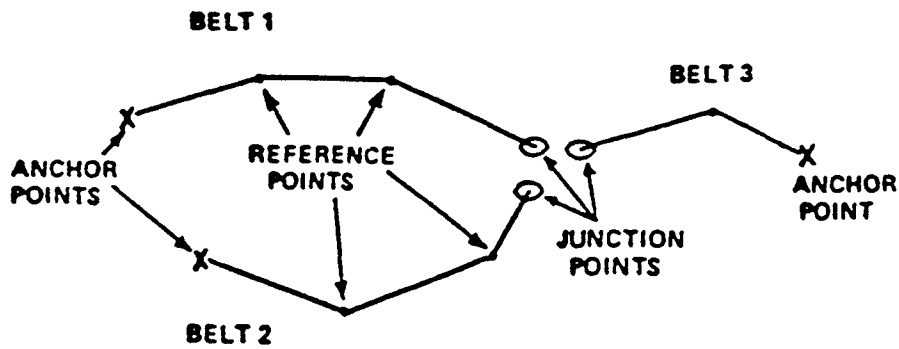
# The 3-Point Belt Model



# Simulation of a Lap Belt Restrained Occupant Using the 3-point Belt Model



# The Harness Model in CAL3D



- $P_K$  : Reference Point
- $U_K$  : Belt Segment
- $r_K$  : Position Vector
- $e_K^1$  : Belt Line
- $e_K^2$  : Perpendicular
- $e_K^3$  : Normal

$$|F_1| < \nu_1 |F_3|$$

$$|F_2| < \nu_2 |F_3|$$

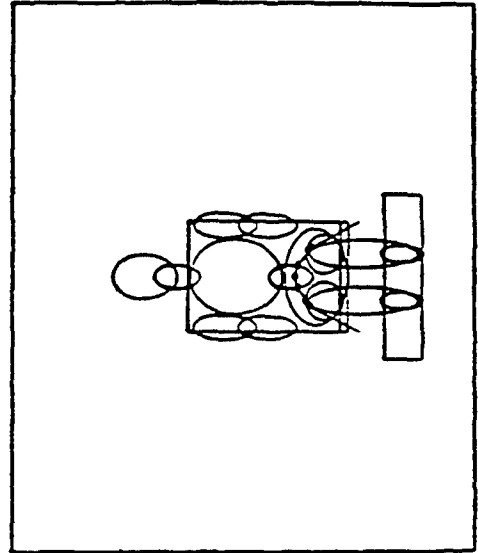
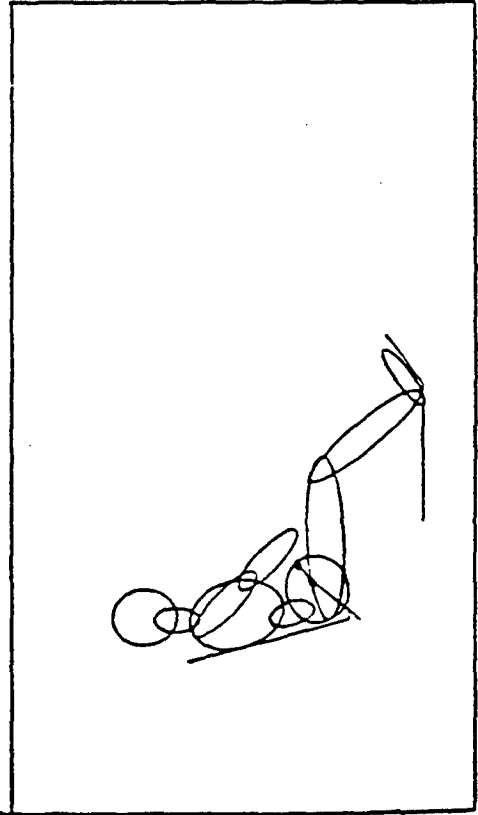
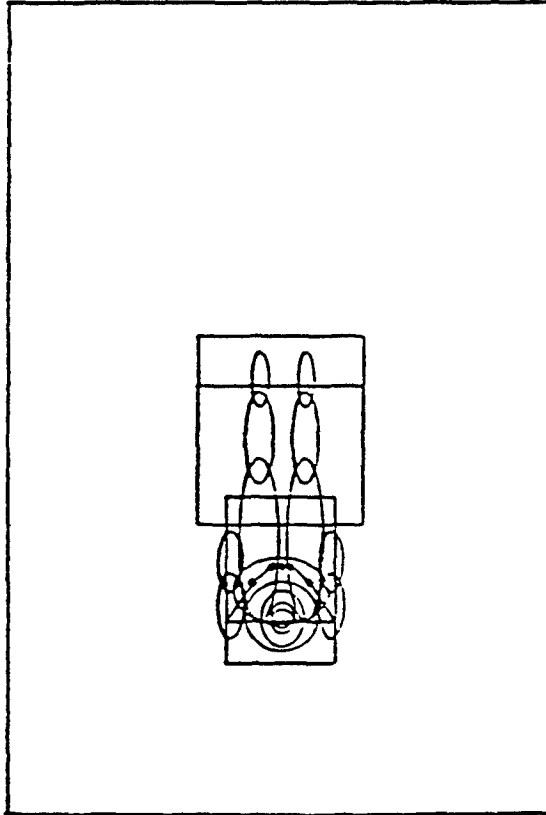
$$f_K(\rho_k) = |F_3|$$

By a perturbation scheme

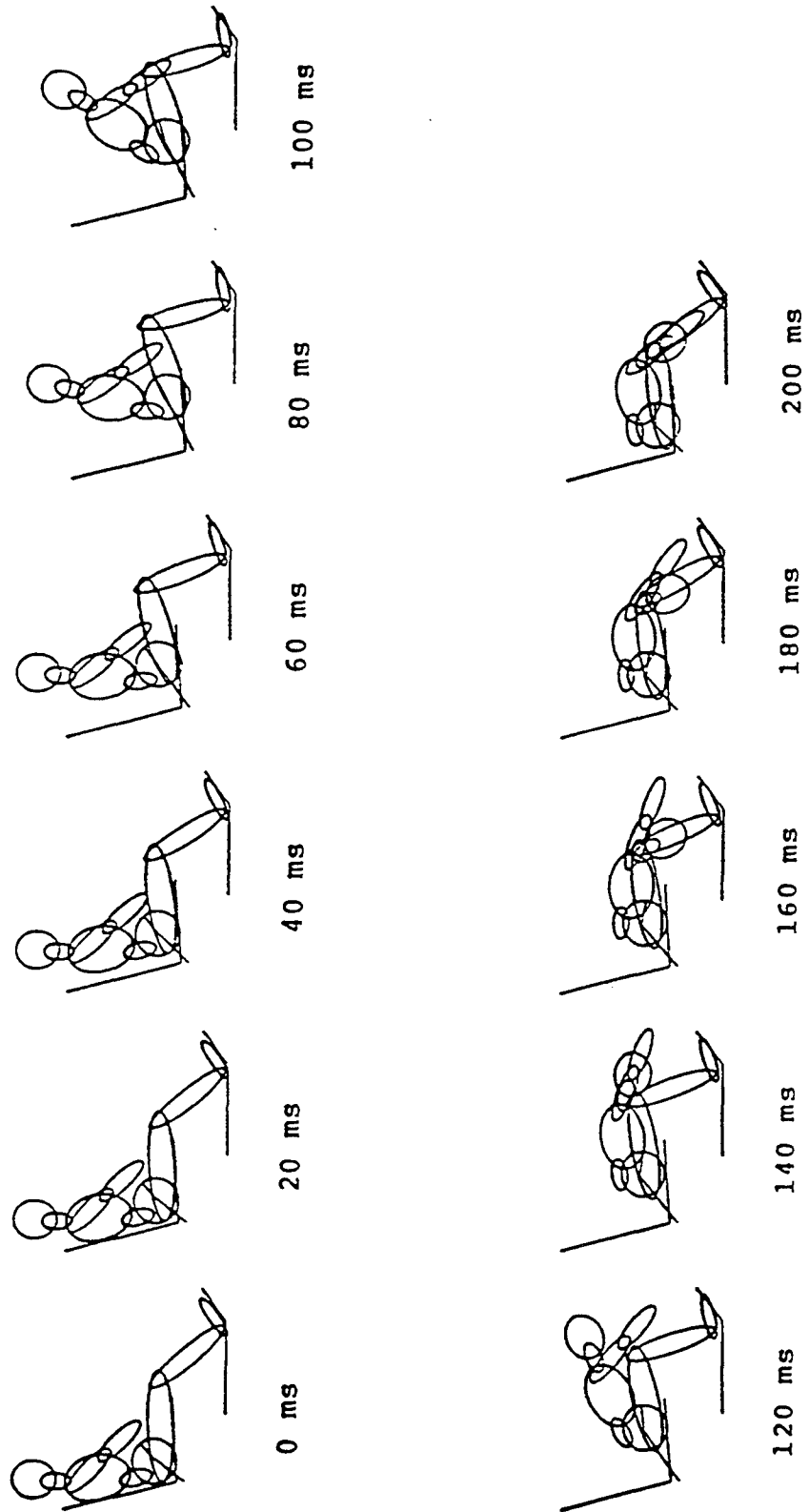
# Simulation of a Lap Belt Restrained Occupant Using the Harness Model

Lap Belt Restraint  
Hybrid III Dummy

Time = 0



# Simulation of a Lap Belt Restrained Occupant Using the Harness Model



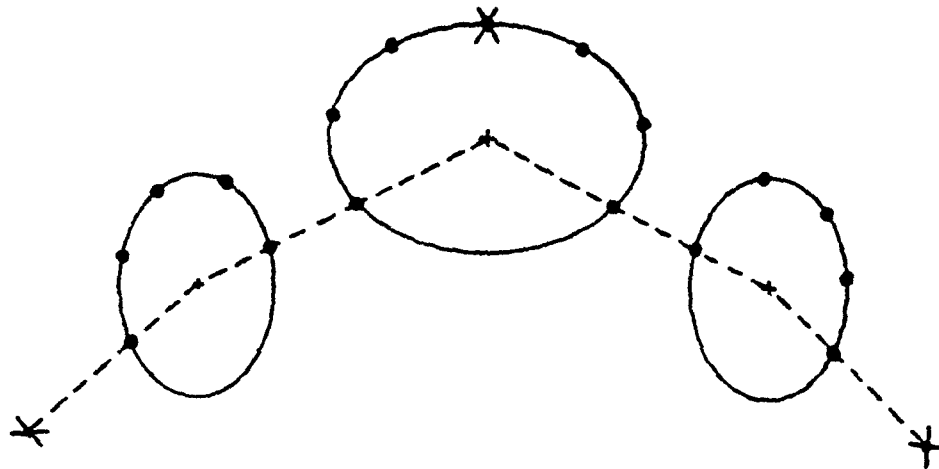
## **Assessment of the Harness Algorithm**

- **Reference point approach provides a useful feature for describing the occupant/belt interaction**
- **Specifying reference points on the occupant contact ellipsoid surface along the belt routing is difficult and time-consuming**
- **Slip algorithm does not work - the perturbation scheme does not converge**



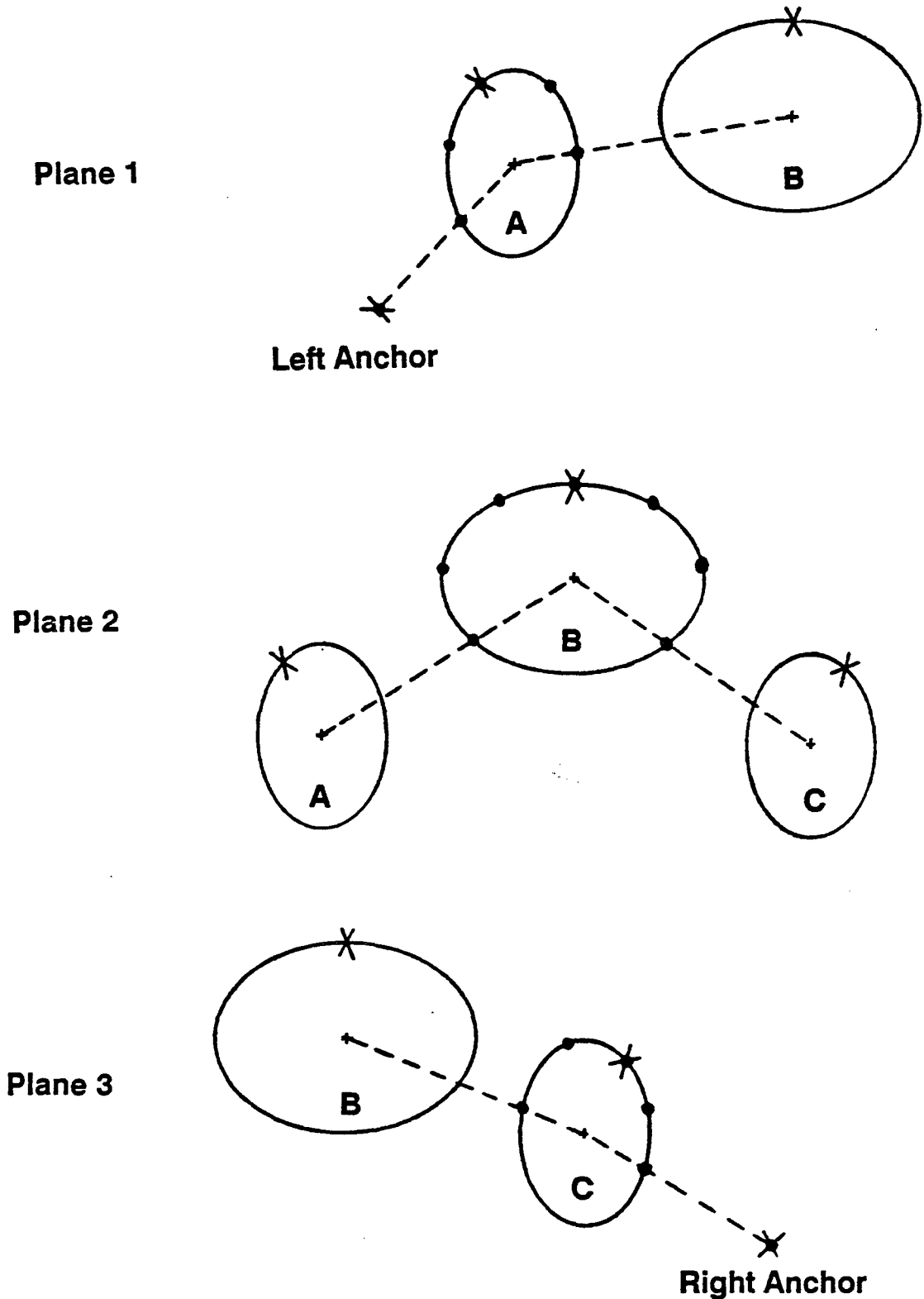
# **Automatic Reference Point Generation**

## Reference Points for A Planer Belt



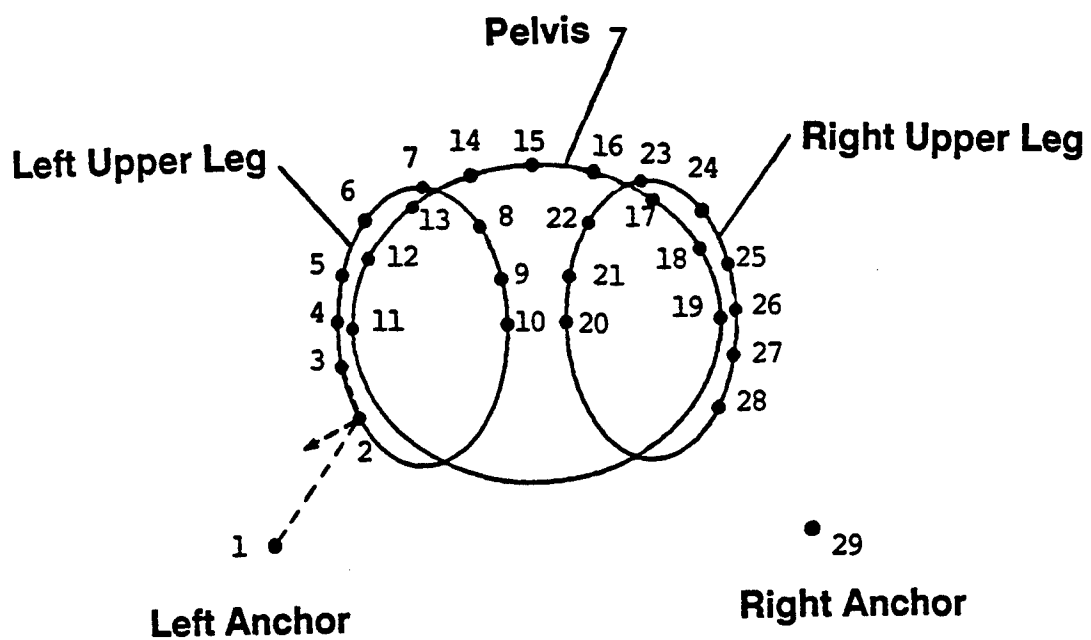
**X - Specified Points**

# Reference Points for A Non-planer Belt



**X - Specified Points**

## Reference Points for A Lap Belt



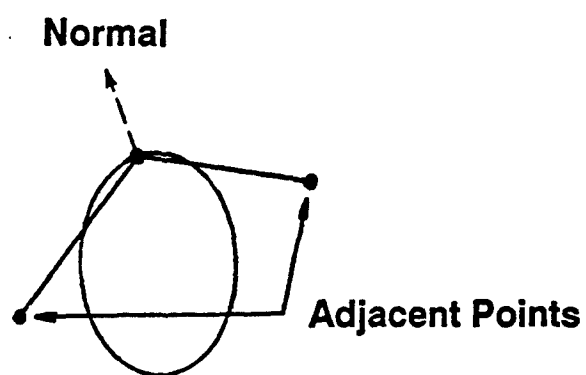
**Reference Points Selection Criteria:**

**(1). User-Specified Points are Included**

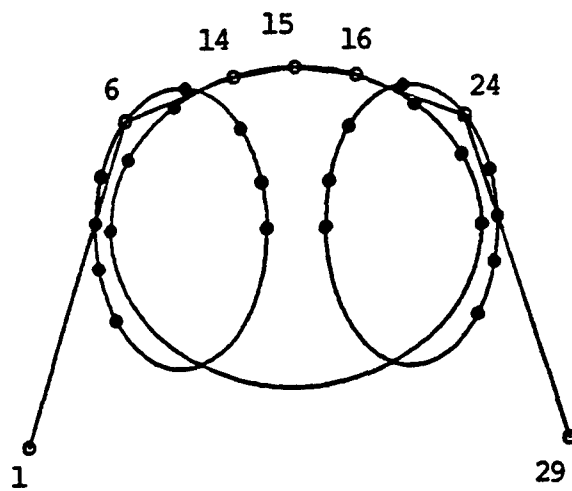
**(2). Points Inside Another Ellipse are Rejected**

**(3). Must Satisfy Convexity Test**

## Convexity Considerations

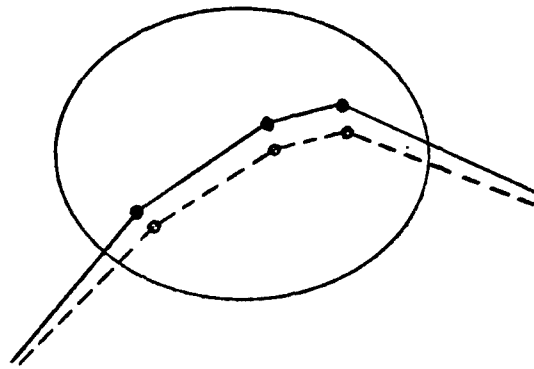


## The Final Lap Belt Configuration



# Difficulty of the Perturbation Scheme

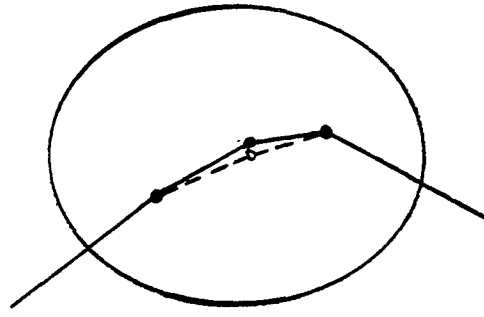
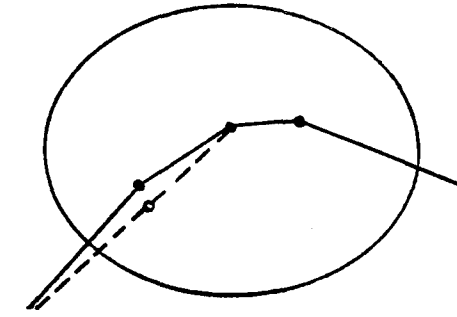
**Perturb all the reference points simultaneously**



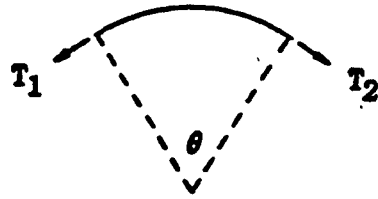


# A New Slip Algorithm

- **Successive Relaxation - Slip begins from the point with the maximum force imbalance**



- **Webbing Slip along the belt-line direction**
- **Reference Point Slip along the perpendicular direction**



$$T_1 = T_2 \cdot e^{\mu\theta}$$

Fig. 4a. Force relationship around a pulley

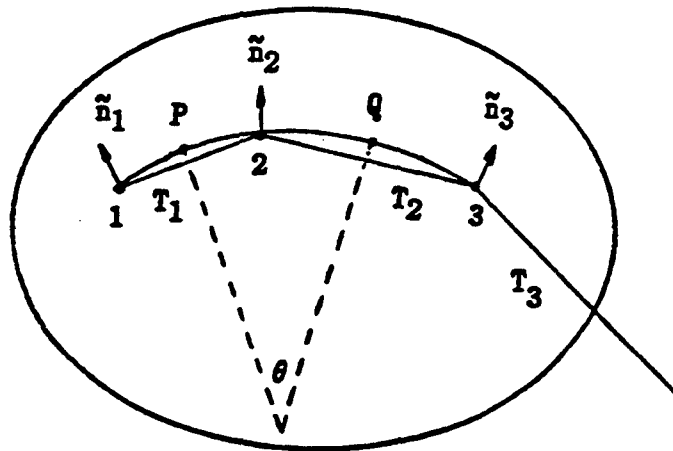
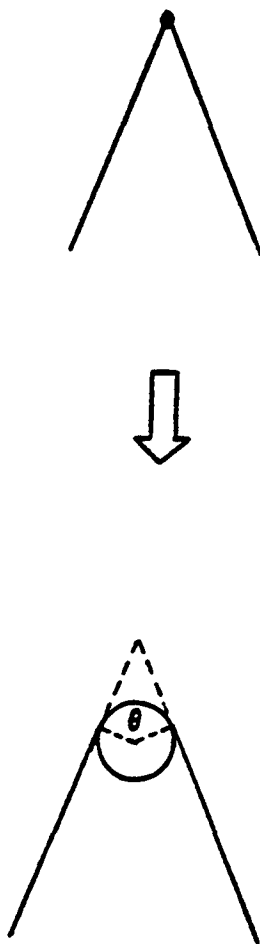
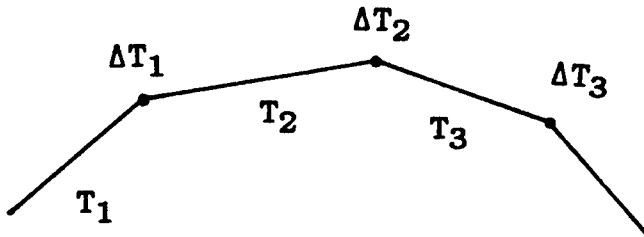


Fig. 4b. Angle computation on an ellipsoid



**Fig. 5. Angle at a guide loop**



$$\Delta T_i = T_i - T_{i+1} \cdot e^{\mu\theta}$$

$\Delta T_i > T_{\max}$  : Webbing Slip

Recompute  $T_i$ 's and  $\Delta T_i$ 's Affected by Slip

Iterate until all  $\Delta T_i < T_{\max}$

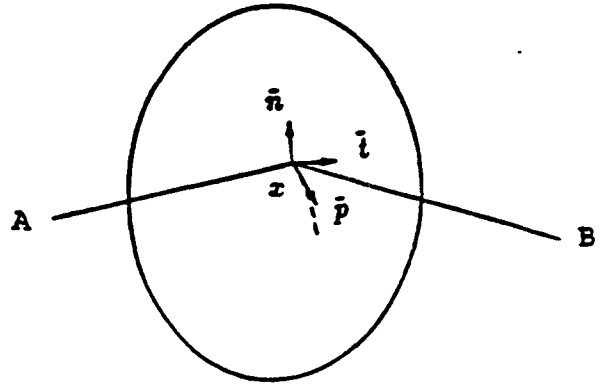
## Belt force of the two adjacent belt segments

$$\vec{t}_a = (t_a^n) \vec{n} + (t_a^p) \vec{p} + (t_a^t) \vec{t}$$

$$\vec{t}_b = (t_b^n) \vec{n} + (t_b^p) \vec{p} + (t_b^t) \vec{t}$$

## Friction force

$$f_p = |(t_a^n + t_b^n)| \cdot \sigma_p$$



## Compute force imbalance in the p-direction

$$\Delta P = 0, \quad \text{if } |t_a^p + t_b^p| < f_p$$

$$\Delta P = |t_a^p + t_b^p| - f_p, \quad \text{if } |t_a^p + t_b^p| > f_p$$

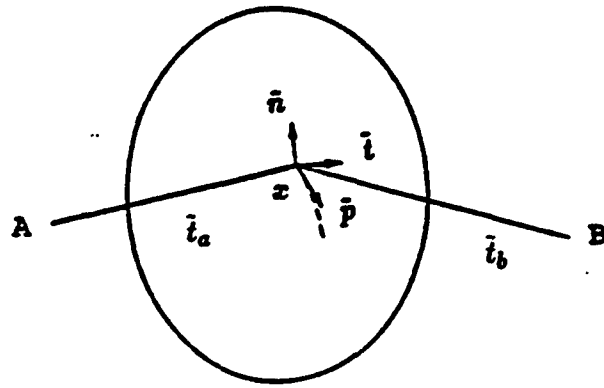
Threshold = 490 N

Use gradient method to iterate such that

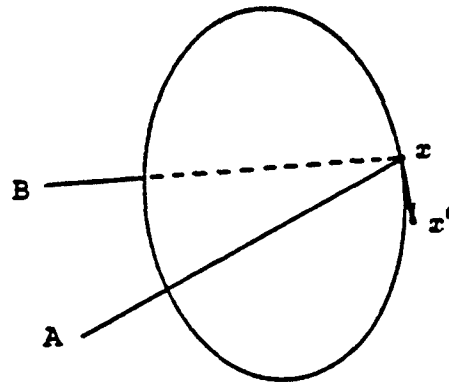
$$UB > \Delta P > LB$$

UB = 196 N    LB = 98 N

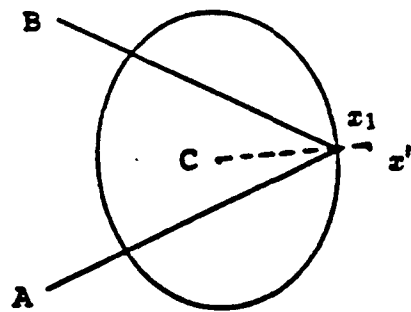
Can regard the remaining  $\Delta P$  as the inertia effect



(a)



(b)



(c)

Fig. 6. Reference point slips on an ellipsoid surface

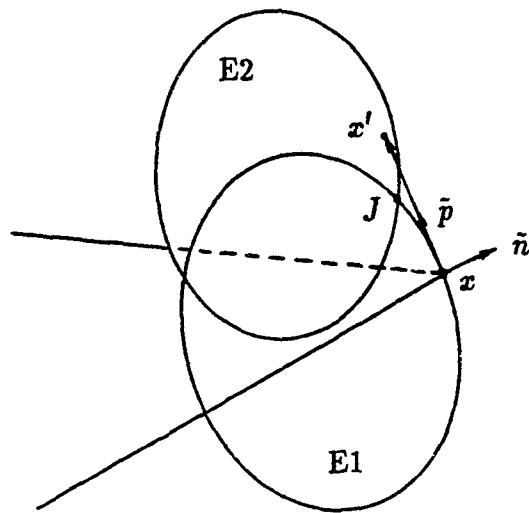


**Fig. 3 Point slips across ellipsoids**

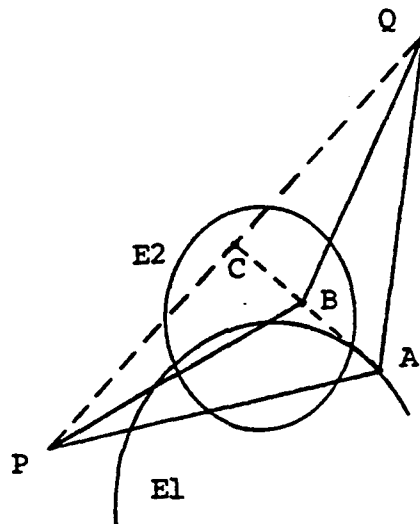


**Fig. 7 Transition of reference points between ellipsoids**



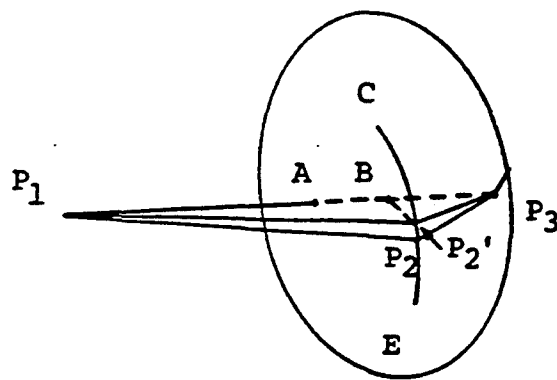
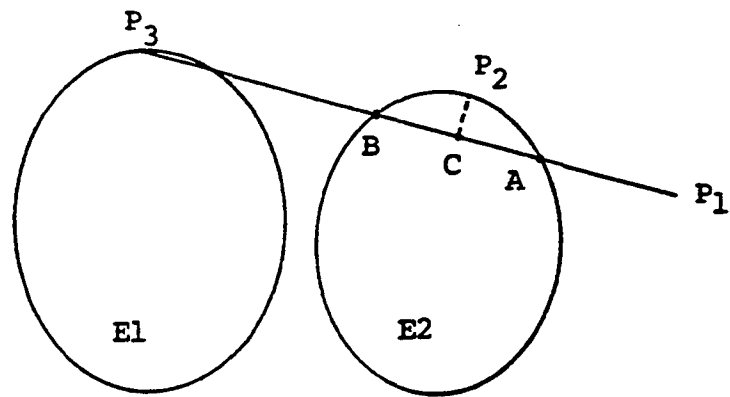
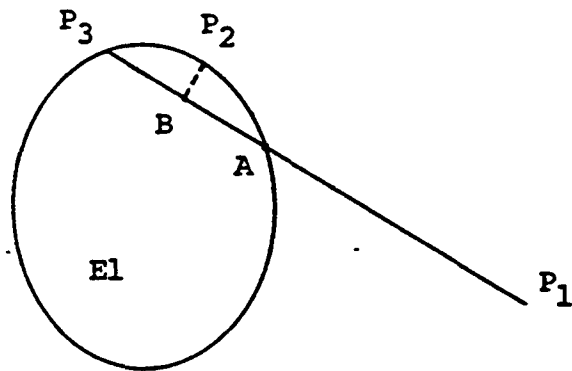


Fig. 4 Location change for a boundary point

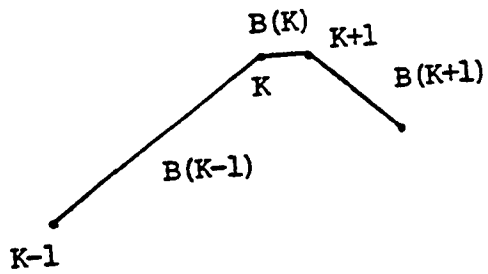


(a)

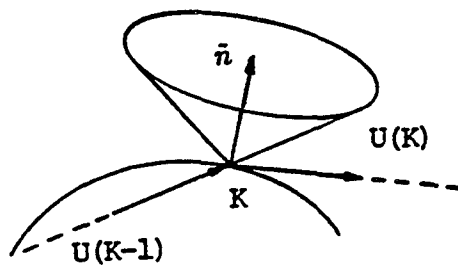


(b)

**Fig. 5 Generation of new reference points**



(a)



(b)

Fig. 6 Elimination of reference points

# **Modeling the Anchor Deformation**

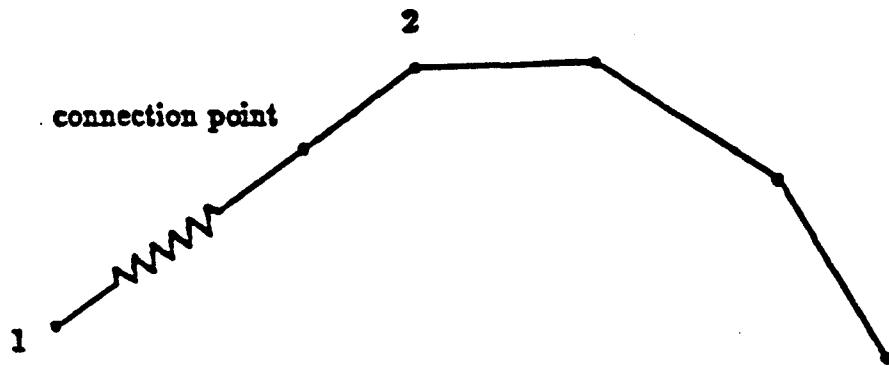


Fig. 7a. Schematic of type 1 anchor spring

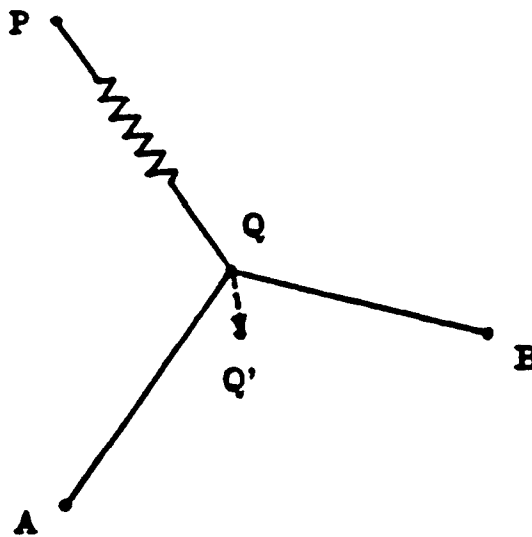
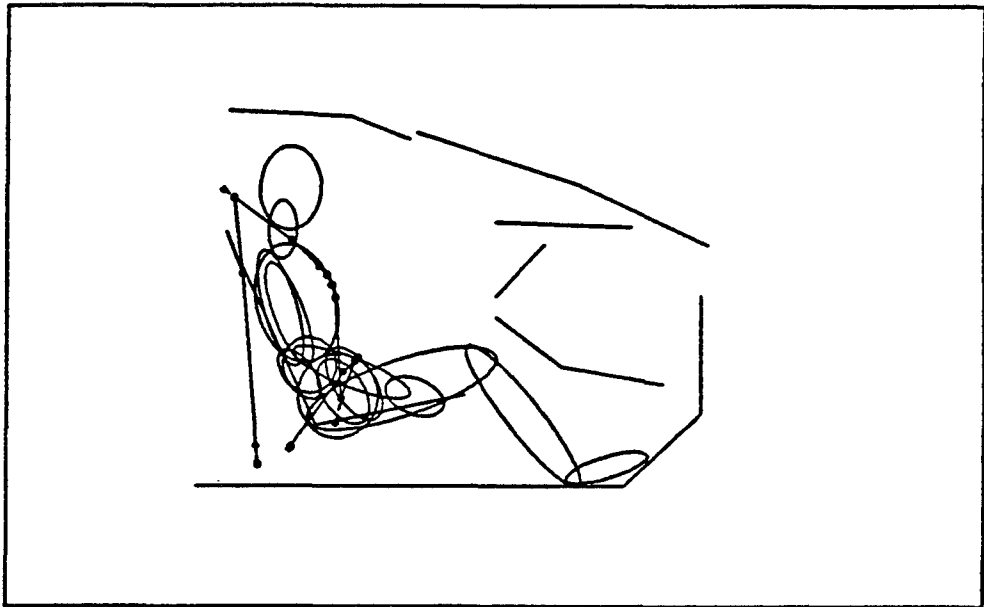


Fig. 7b. Schematic of type 2 anchor spring

# Applications



## **FMVSS 208 (30 mph) and NCAP (35 mph) Considerations**

- **Hybrid III Dummy**
- **HIC**
- **Neck Load**
- **Chest G and D**
- **Femur Load**
- **Submarining**

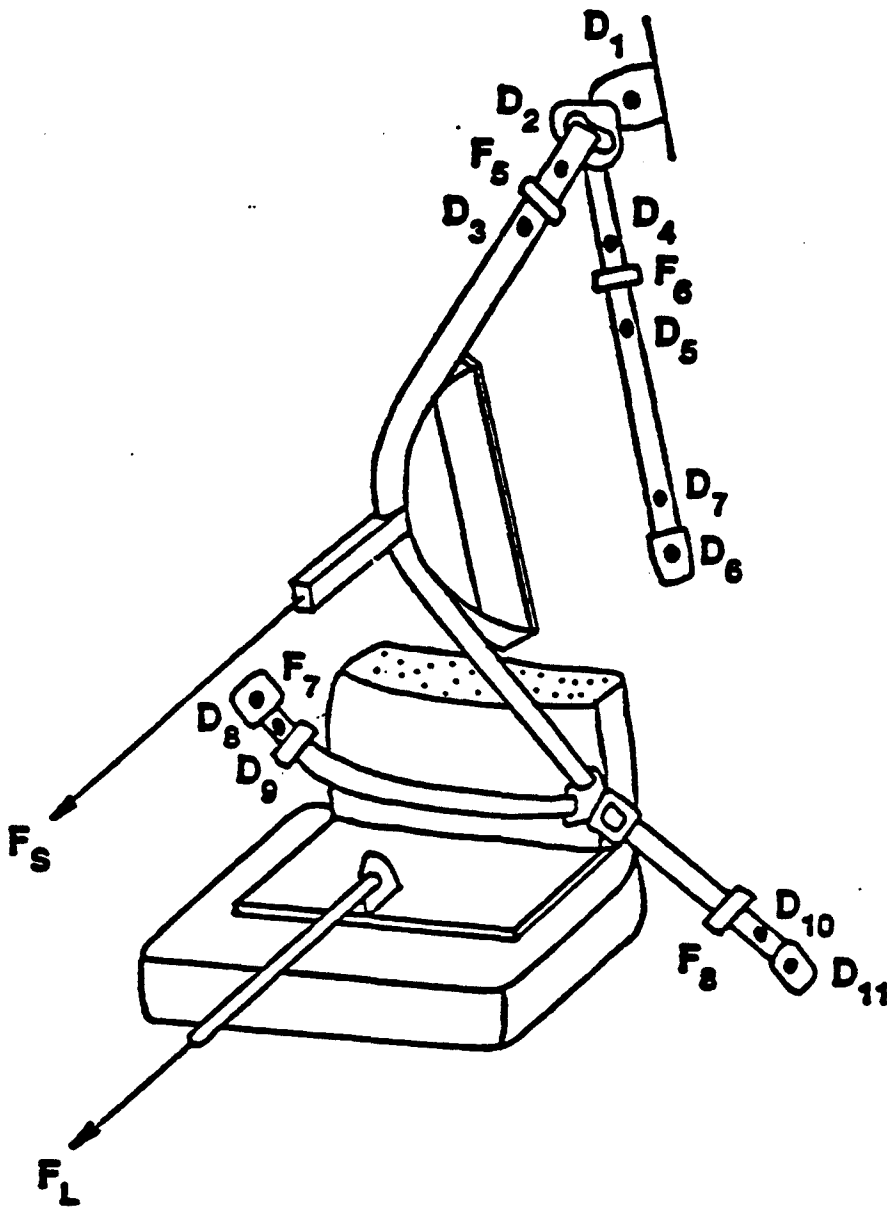
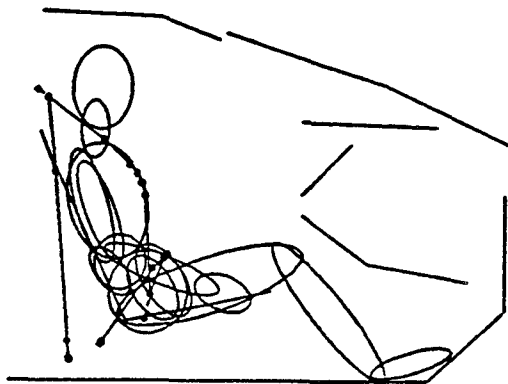


Fig. 8. Instrumentation on the MVSS 210 test for measuring anchor force-deflection



## **Occupant Model**

- **Hybrid 3 Dummy Representation**
- **Rigid Segments with Joints**
- **Contact Ellipsoids with F-D**
- **Springs and Dampers**



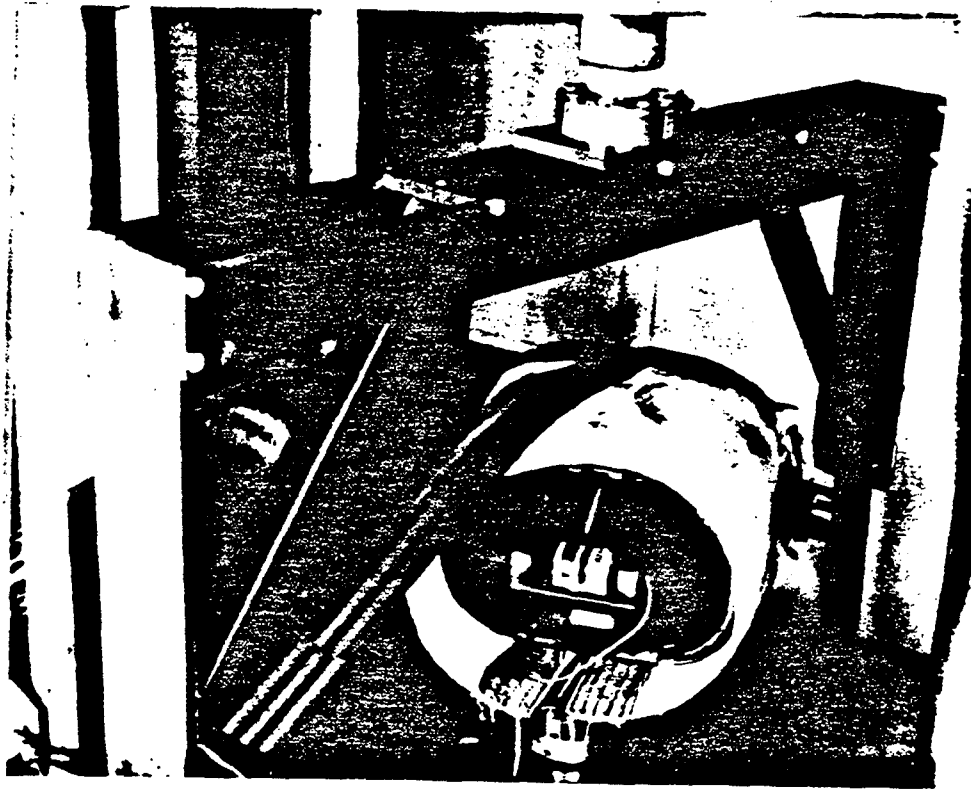


**Fig. 9. Hybrid III dummy thorax response to static belt loading**

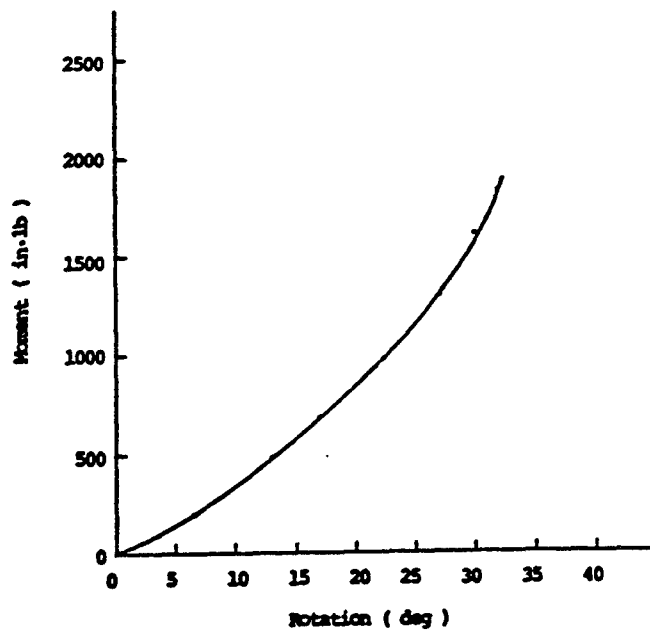
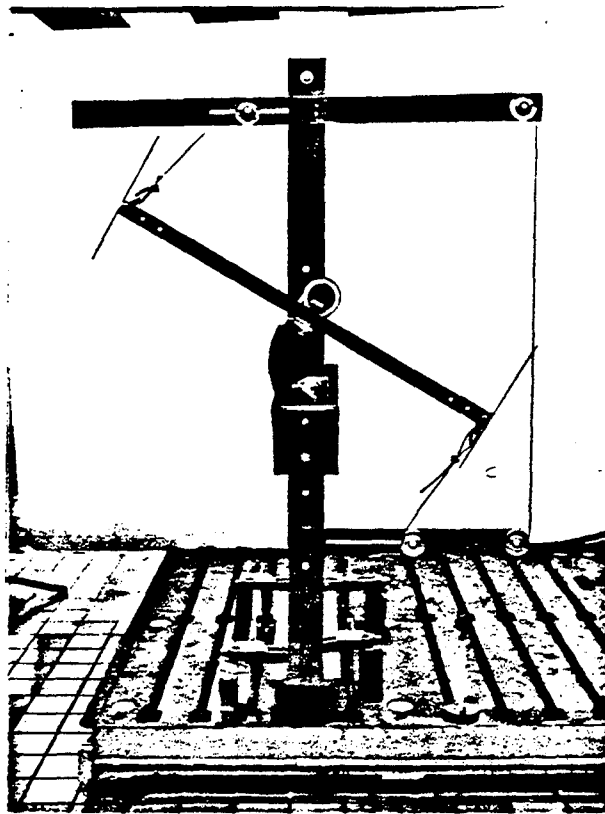
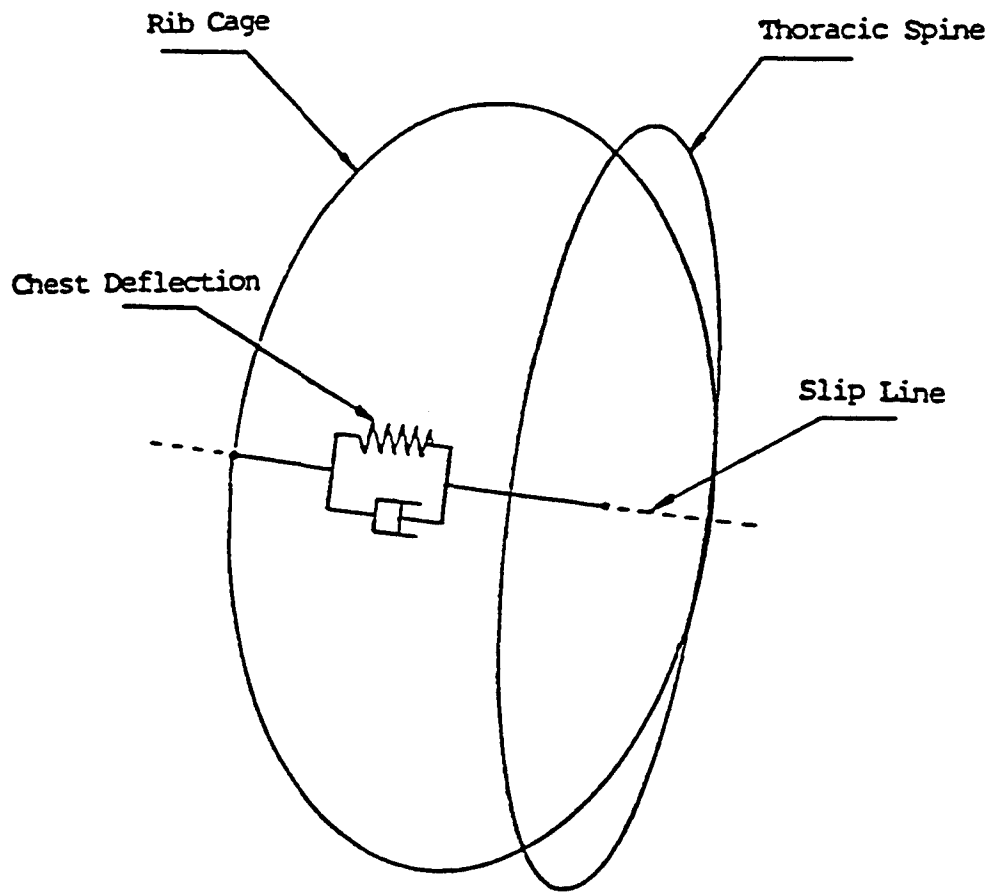


Fig. 12. Hybrid III dummy lumbar characterization



**Fig. 10. Hybrid III dummy thorax model**

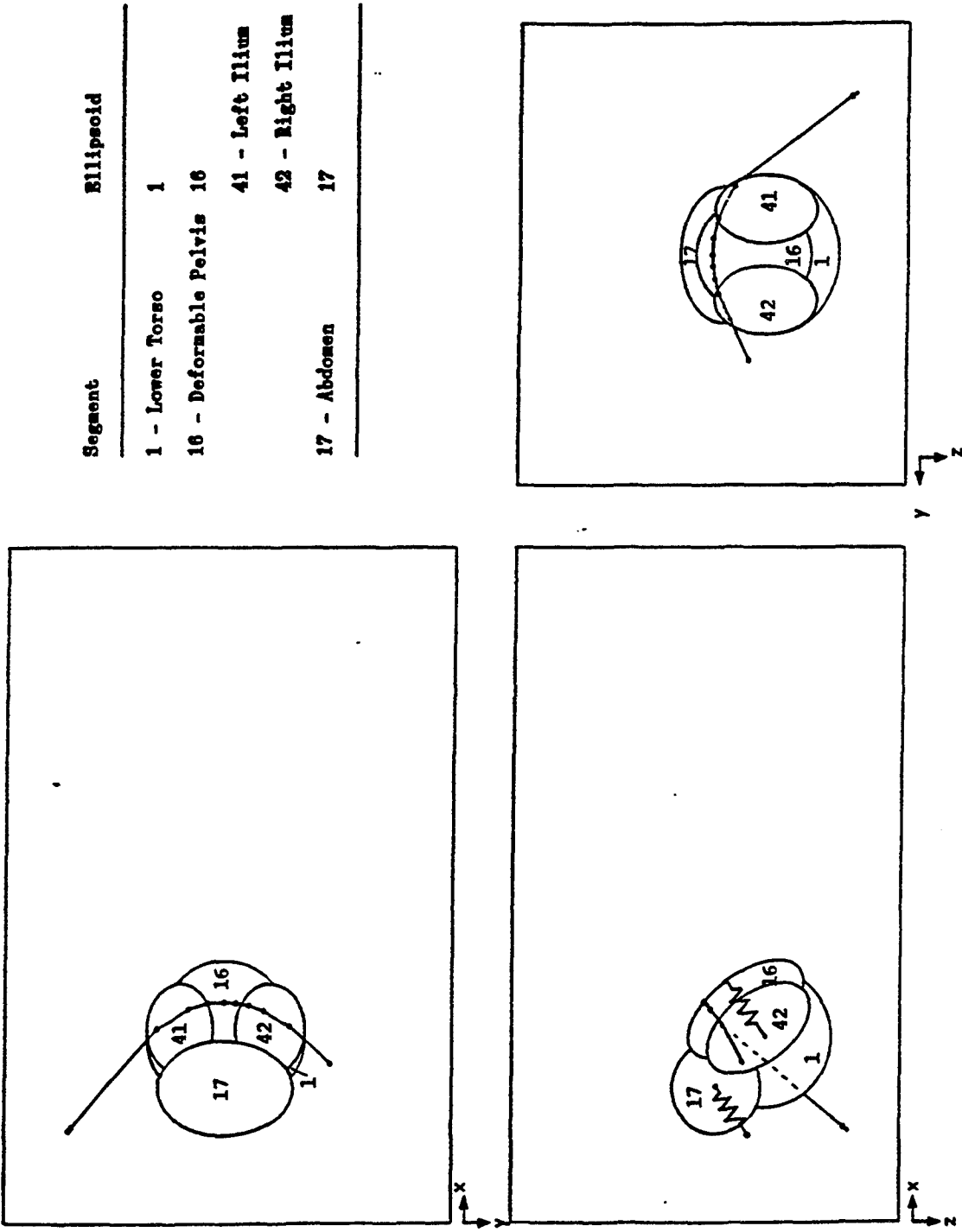
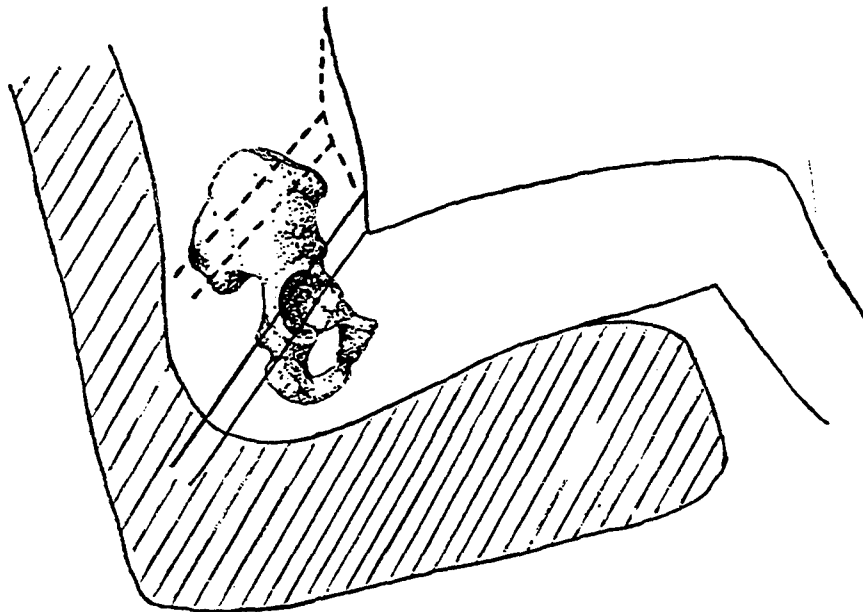


Fig. 11. Hybrid III dummy lower torso model

# Occupant Submarining

**Submarining : Lap belt slips over illiac crest to abdominal area causing injury**



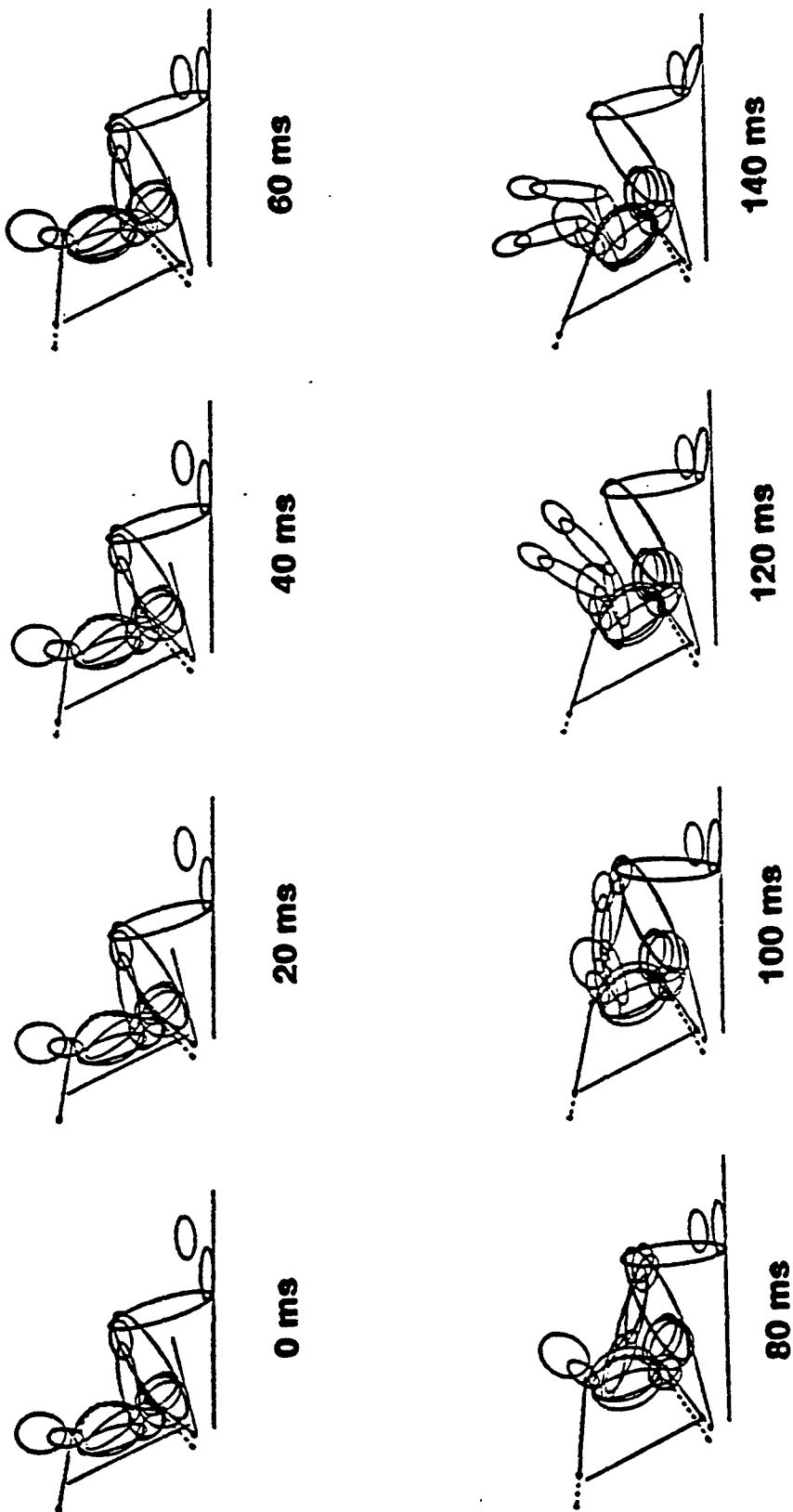
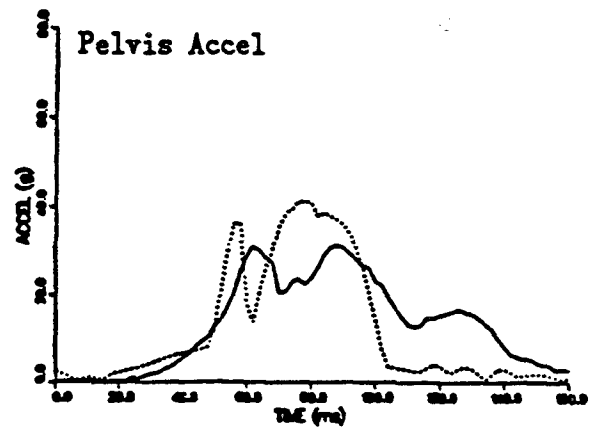
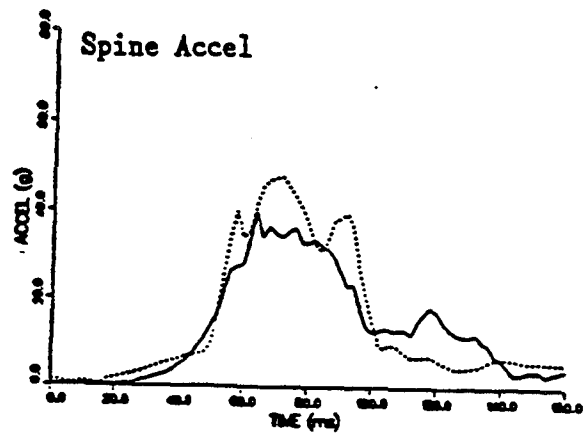
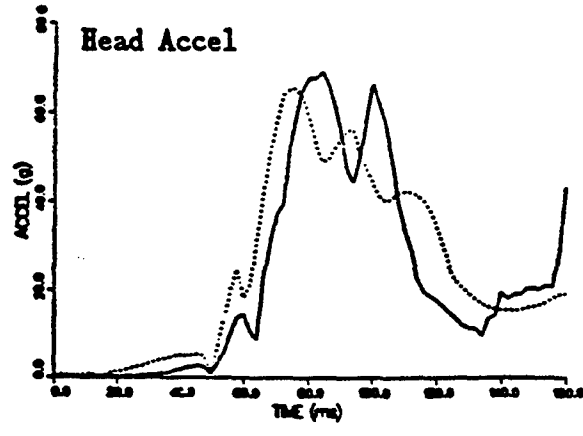


Fig. 13. Submarining simulation





**Solid : Test**  
**Dashed : Model**

**Fig. 14. Occupant impact response**

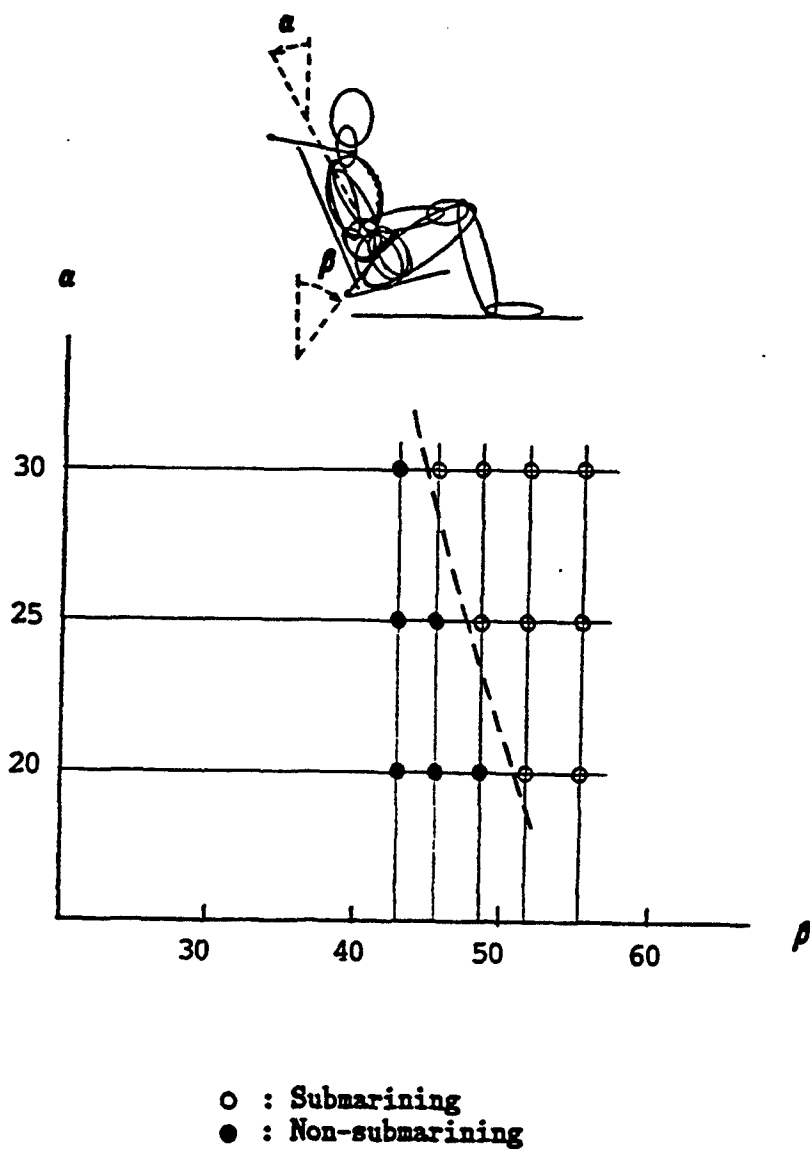


Fig. 15. Variation of seat back and lap belt angles

# **Summary of New Harness Features**

- **Automatic reference point generation**
- **New slip algorithms with numerical stability**
  - Webbing slip
  - Reference point slip
- **Anchor springs**
- **Satisfactory results for applications**

## References

1. Deng, Y.-C., "Analytical Study of the Interaction Between the Seat Belt and a Hybrid III Dummy in Sled Tests.", SAE International Congress & Exposition, Detroit, Michigan, Feb. 29 - Mar. 4, 1988, SAE Transaction 880648.
2. Deng, Y.-C., "An Improved Belt Model in CAL3D and Its Application", Vehicle Crashworthiness and Occupant Protection in Frontal Collisions, SAE Publication SP-807, pp. 155-164, 1990.
3. Deng, Y.-C., "Simulation of Belt-Restrained Occupant Response in 30 MPH Barrier Impact", International Journal of Vehicle Design, vol. 12, no. 2, pp. 160-174, 1991.
4. Deng, Y.-C., "Development of A Submarining Model in the CAL3D Program", The 36th Stapp CarCrash Conference, Seattle, Washington, Nov. 2-4, 1992.
5. Deng, Y.-C., "Development of A Mathematical Model for Predicting A Belt-Restrained Occupant Response in Automobile Crash", The ASME Winter Annual Meeting, New Orleans, Louisiana, Nov. 29 - Dec. 3, 1993.



# Aircraft Seat Development with DYNAMAN

Anne M. Curzon

1996 ATB Users' Group Conference  
February 8-9, 1996

## FAA Seat Certification

---

- Conduct dynamic tests with Hybrid-II
  - » 16g, 30 mph "forward" test
  - » 14g, 24 mph "down" test
  - » Helicopter seats, 30g "down" test
- Demonstrate structural integrity
  - » No failures in primary load path
  - » Permanent deformations don't impede egress

## FAA Certification , cont'd

---

- Demonstrate compliance with injury criteria
  - » HIC < 1000
  - » Lumbar load < 1500 lb
  - » Femur loads < 2250 lb
  - » Shoulder harness loads
  - » Belts stay in place

## DYNAMAN as a Tool

---

- Belt load prediction
- Head path and velocity prediction
- Seat attachment load prediction
- Effects of sled pulse shape
- Failure assessment
- Effects of restraint system mods

## Example - Partition-Mtd Seat

---

- **System description**
  - » Partition supported at top and bottom
  - » Seat mounted to partition
  - » Harness mounted to seat
- **DYNAMAN objectives**
  - » Validate model
  - » Evaluate restraint system mods
  - » Assess decel pulse effects

## Simulation Details

---

- **Model features**
  - » Seat as separate segment
  - » Spring dampers and slip joint
  - » Three-part harness
- **Initial input**
  - » System yawed 10 deg
  - » Occupant yawed about LT

## Validation Data from Test

---

- Instrumentation
  - » Partition attachment reaction loads
  - » Partition dynamic deflection
  - » Dummy head accelerations
  - » Belt loads
- Film analysis
  - » Dummy head and knee motion
  - » Partition target motion

## Simulation Results

---

- Validation
  - » Belt load comparison
  - » Partition deflection comparison
  - » Head motion comparison
- Harness mods
- Pulse effects



# Application of Ellipses, Ellipsoids and Hyperellipsoids in Computer Modeling of Human Body and Interior Surfaces

Mariusz Ziejewski, Ph.D., Xiaofeng Pan  
 Mechanical Engineering  
 North Dakota State University

## Introduction

Computer programs such as ATB and its derivatives (CVS, CAL3D, and DYNAMICS) use ellipsoids and hyperellipsoids in modeling the human body and frequently in modeling contact surfaces such as the dash boards of vehicles.

Understanding some of the mathematical concepts in regard to ellipses, ellipsoids, and hyperellipsoids is necessary to effectively use this modeling approach. Mathematical details have been addressed in a number of publications [1 through 5].

The objectives of this paper are:

1. To present some of the mathematical concepts behind ellipses, ellipsoids and hyperellipsoids.
2. To present a procedure for selecting the parameters necessary for modeling with ellipsoids and hyperellipsoids.

## Analysis

A generalized hyperellipsoid of type  $n$  is defined by

$$\frac{x_1^{2n}}{a_1^{2n}} + \frac{x_2^{2n}}{a_2^{2n}} + \dots + \frac{x_m^{2n}}{a_m^{2n}} = 1 \quad (1)$$

For  $m = 3$ , the equation represents a generalized ellipsoid. For  $m = 2$ , the equation represents a generalized ellipse. With the customary change in notation, the generalized ellipse of type  $n$  is defined by

$$\frac{x^n}{a^n} + \frac{y^n}{b^n} = 1; n = 2, 3, 4, \dots, a > b \quad (2)$$

The ordinary ellipse is obtained using a special case for,  $n = 2$

$$\frac{x^2}{a^2} + \frac{y^2}{b^2} = 1 \quad (3)$$

The eccentricity of (2) is defined by

$$b^n = a^n(1 - e^n) \quad (4)$$

A generalized ellipse with eccentricity equal to zero is called a generalized circle of type  $n$ . Its equation is

$$x^n + y^n = a^n; n = 2, 3, \dots \quad (5)$$

The line joining  $(-a, 0)$  and  $(a, 0)$  is called the major or semi-major axis. The line joining  $(0, -b)$  and  $(0, b)$  is called the minor or semi-minor axis. The two points,  $(ae, 0)$  and  $(-ae, 0)$  or  $(\sqrt[n]{a^n - b^n}, 0)$  and  $(-\sqrt[n]{a^n - b^n}, 0)$  are called the foci of the ellipse.

For a circle, the two foci coincide and the common point is called the center of the circle.

The ellipse (2) is symmetric about both axes. For all values of  $n$ , the ellipse passes through  $(\pm a, 0)$ , where the tangents have equations  $x = \pm a$  and the ellipse also passes through  $(0, \pm b)$  where the tangents have equations  $y = \pm b$ . This means that the ellipse lies within the rectangle formed by the tangents at the extremities of the major and minor axes. The first quadrant of ellipses of different types with the same lengths of major and minor axes are given in Figure 1.

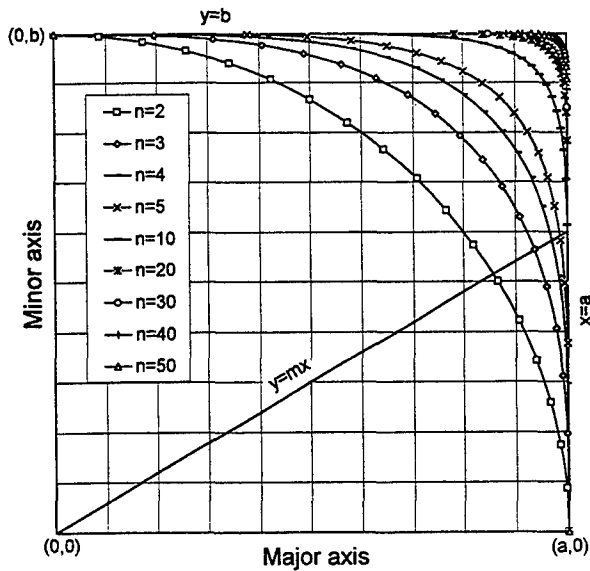


Figure 1 Ellipses of different types with the same lengths of major and minor axes.

Note as  $n$  increases from  $2 \rightarrow \infty$ , equation (2) represents a hierarchy of ellipses, all touching one another at  $(\pm a, 0)$  and  $(0, \pm b)$ . Moreover, each succeeding ellipse is outside of the preceding ellipse and is greater in area than the preceding ellipse. As  $n \rightarrow \infty$ , the ellipse tends to coincide with the boundaries of the rectangle with sides  $\pm a$ , and  $\pm b$ . All of the ellipses are inside this rectangle.

As an example, two 3-dimensional graphs for ellipsoids with  $n = 10$  and  $n = 50$  are given in Figure 2. In Figures 3 through 10

graphs for  $n = 2, 3, 4, 5, 10, 20, 40$  and  $50$  are given respectively. On each graph, ten curves are drawn for different ratios between the major and minor axes.

In a three-dimensional space as  $n \rightarrow \infty$  the graph represents a rectangular parallelepiped with vertices at points  $(\pm a, \pm b, \pm c)$ .

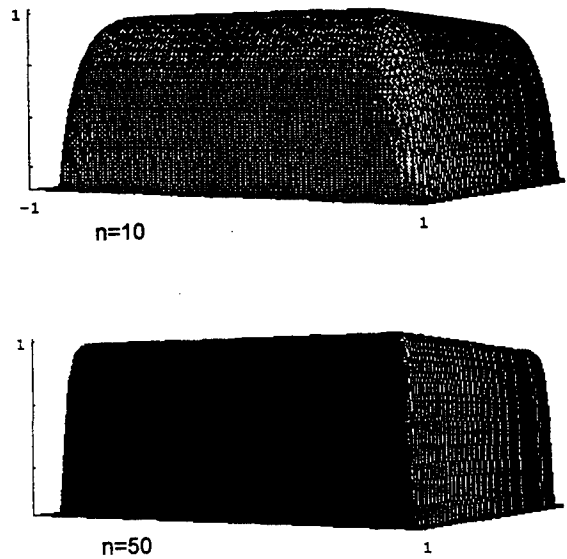


Figure 2 3-Dimensional graph for  $n=10$  and  $n=50$

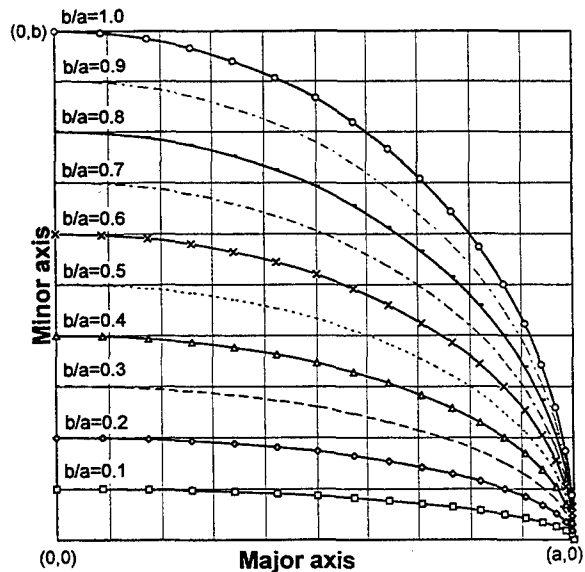


Figure 3 Family of curves for  $n=2$

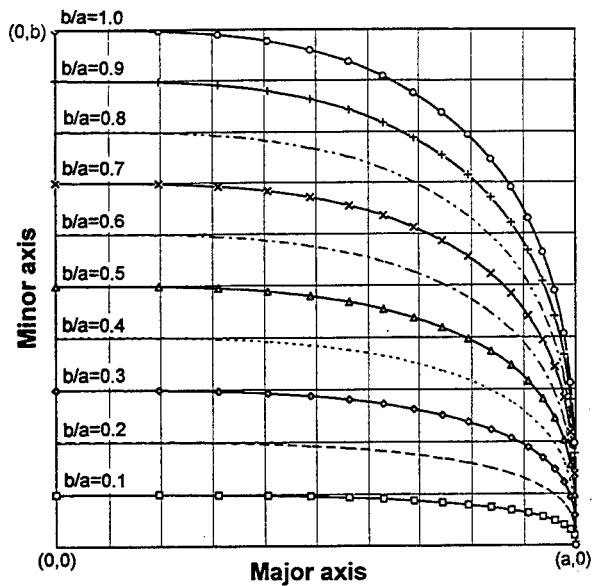


Figure 4 Family of curves for  $n=3$

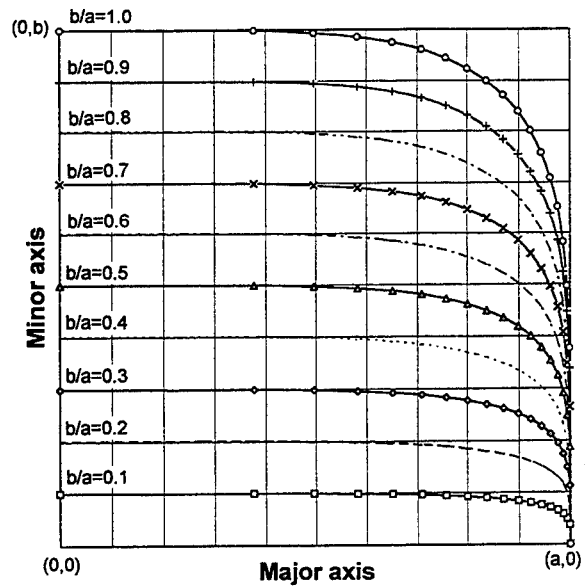


Figure 6 Family of curves for  $n=5$

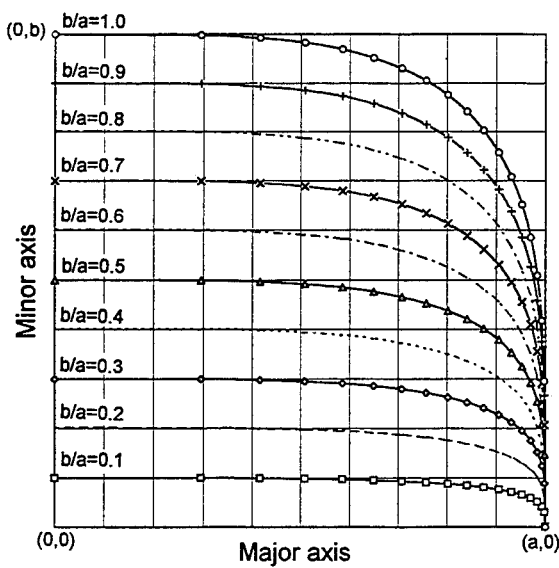


Figure 5 Family of curves for  $n=4$

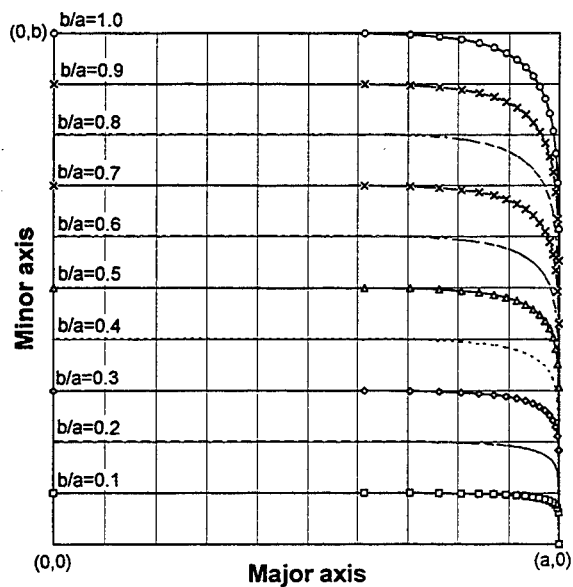


Figure 7 Family of curves for  $n=10$

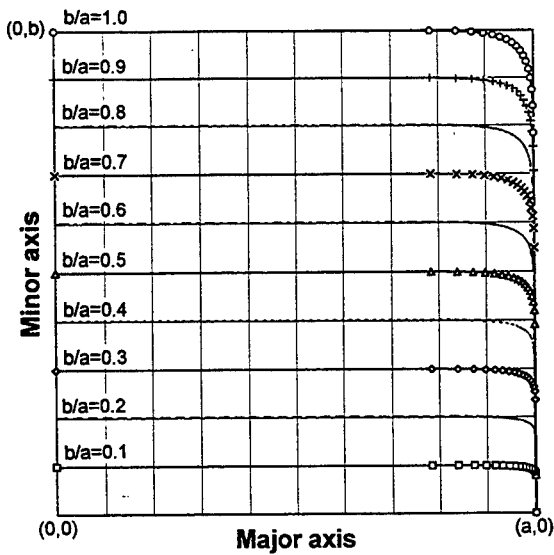


Figure 8 Family of curves for n=20

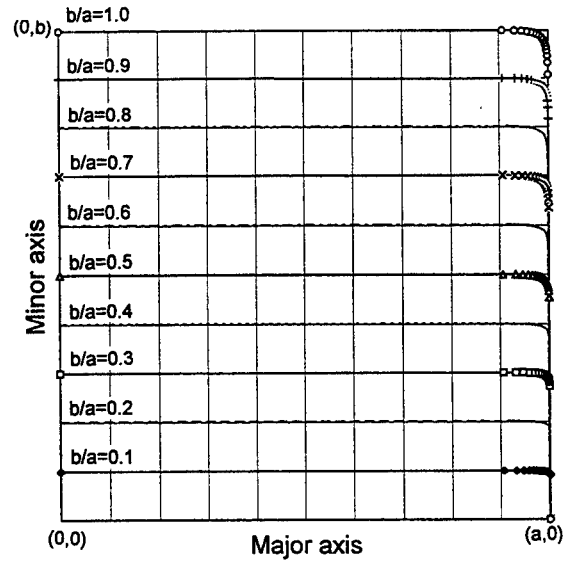


Figure 10 Family of curves for n=50

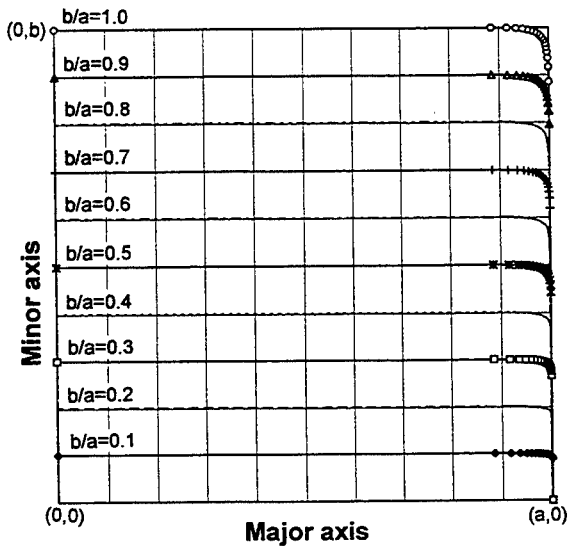


Figure 9 Family of curves for n=40

To establish the relation between the contact point of an ellipse and the center of the ellipse let's define the coordinates of the point of intersection of the ellipse with the line  $y = mx$  that lies in the first quadrant (Figure 1). The coordinate points are given by

$$x^n \left( \frac{1}{a^n} + \frac{m^n}{b^n} \right) = 1, y = mx, \quad (6)$$

$$x > 0, y > 0$$

With the knowledge of the intersection point (which can represent an impact point between a human body and the interior of the vehicle) and the parameters of the selected ellipse ( $a$ ,  $b$ , and  $n$ ) we can calculate the radius of curvature  $R$ . For example, the center of curvature for  $\theta = 45^\circ$  and  $n = 2$  through 50 is shown in Figure 11.

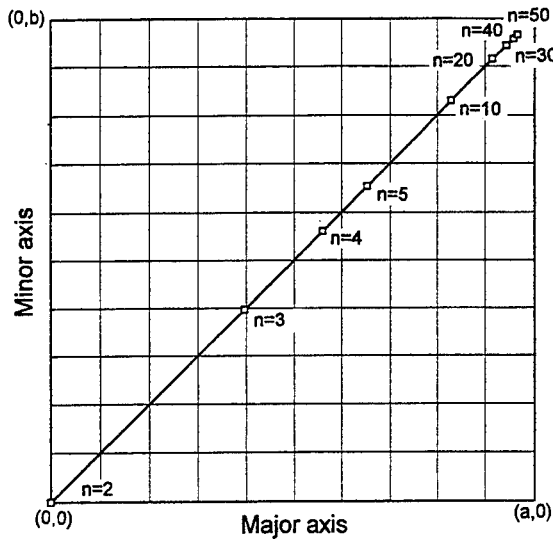


**Figure 11** Radius of curvature for  $\theta = 45^\circ$  and  $n = 2$  through 50

In the first quadrant,  $y$  is a concave function of  $x$  and if we join any two points on the curve, the curve lies above the straight line segment joining these points. Thus the region inside the ellipse equation (2) is a closed convex region in the sense that if we join any two points on it the line segment joining them lies entirely within the region.

For  $n = 1$  two dimensional graphs are given in Figure 12. In a three dimensional space, for  $n = 1$ , the graph represents an octahedron with its vertices at these six points.

For  $n < 1$  we get curves position below the line with  $n = 1$  (see Figure 12). For  $n < 1/2$ , we get four cusped curves (Figure 12) with cusps at the point  $(\pm a, 0)$  and  $(0, \pm b)$ . These however, do not bound convex regions.

For  $n=1/2$ , equation (2) gives four parabolic segments touching the  $x$  and  $y$  axes with coordinates of  $(\pm a, 0)$  and  $(0, \pm b)$ .

For  $n=1/3$ , equation (2) gives four line segments joining  $(\pm a, 0)$  and  $(0, \pm b)$  forming the sides of a rhombus.

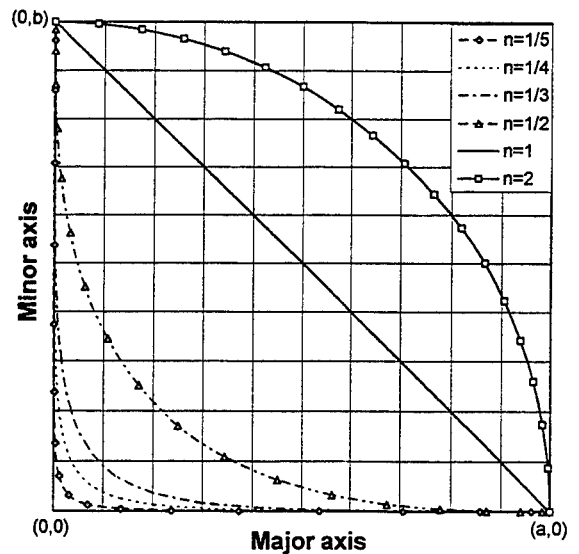


**Figure 12** Family of curves for  $n = 2, 1/2, 1/3, \text{ and } 1/4$

In a three-dimensional space, for  $0 < n < 1$  we get a surface which is the union of eight surfaces, each of which passes through each of the points  $(\pm a, 0, 0)$ ,  $(0, \pm b, 0)$ ,  $(0, 0, \pm c)$  and the coordinate planes of these six points.

When  $n \rightarrow 0$ , we get the segments joining  $(-a, 0)$  to  $(a, 0)$  and  $(0, -b)$  to  $(0, b)$ . As shown before for  $n \rightarrow \infty$ , we get the four sides of a rectangle with vertices at  $(\pm a, \pm b)$ .

For all combinations as  $n$  increases, each succeeding curve includes all the previous curves within it.

As  $n \rightarrow \infty$ , we get a rectangular parallelepiped with vertices at points  $(\pm a, \pm b, \pm c)$ .

The selection of ellipsoids representing the human body is based on the dimensions of the selected body parts. The shape of the

ellipsoids are only approximate the actual geometry of the modeled body parts.

For the selection of an ellipsoid, representing an area of impact, a number of steps have to be taken. First, a two dimensional scaled diagram representing the curvature of the area on impact has to be prepared. The scaled diagram can be used in conjunction with a family of curves given in Figures 2 through 10. By matching the shape of the scaled diagram to the shape of the provided curves, one can select a, b and c parameters. The c parameters can be selected based on the desired size or shape of the modeled object. The last final step is to position the ellipsoid with regards to the vehicle reference system. Using equation (6) with the knowledge of the impact presented between the human body and the interior of the vehicle, the point of impact on the ellipsoid can be calculated, and in turn the distance between the center of the selected ellipsoid and the vehicle reference system can be established.

### **Summary and Conclusion**

1. Selected mathematical concepts in regard to ellipses, ellipsoids, and hyperellipsoids as applied in computer modeling of the human body and contact surfaces is presented.
2. The following steps can be taken to complete the selection of parameters and to establish the location of the hyperellipsoid:
  - a) Prepare a scaled graph representing the curvature of the area of impact.
  - b) Match the prepared curve to the curves given in Figures 2 through 10.
  - c) Choose the best match and read

from the graph, the values for the major semi-axis, the minor semi-axis and the n value.

- d) Calculate the position of the center of the selected hyperellipsoid with respect to the vehicle reference system.

### **References**

1. Kulshrestha, D.K. (1985) 'A Note on Property of Weighted k Ellipses' *Mathematical Education, India I* (4), 33-34.
2. Z.A. Melzak (1975) *Companion to Concrete Mathematics*, John Wiley, New York.
3. Melzak, Z.A. and Foryth, J.S. (1977), 'Polyconics I: Polyellipses and Optimization' *Quart. App. Maths.* 35 (2), 235-255.
4. Phillips, E.G. (1948), *A Course of Analysis*, pages 155, 324, Camb. Univ. Press.
5. Whittakar, E.T. and Watson, G.N. (1980), *A Course of Modern Analysis*, page 237, Camb. Univ. Press.

# Three Dimensional Animation Generated From ATB Output

M. Ziejewski , Ph.D  
*North Dakota State University  
Mechanical Engineering Dept*

D. Grangaard  
*Insim, Inc.*

B. Anderson  
*North Dakota State University  
Mechanical Engineering Dept*

## Abstract

In the past few years computer animation has become used more widely in the efforts to present computer simulation results. This paper will provide a general overview of 3D Studio and Humanoid, and outline the procedure used to utilize ATB output and Humanoid models in 3D Studio to produce a three dimensional computer animation of a dynamic event which can be transferred to video tape.

## Introduction

Technical advances in personal computers along with the availability of affordable software programs that have the capabilities to create accurate graphical representations of dynamic events have prompted a wider use of computer animation as a means to present computer simulation results. These easy-to-use programs for personal computers have made computer animation, especially three dimensional animation a feasible choice for engineers, even those without access to super computers.

The computer program ATB generates the linear position and angular rotation data for body segments as a result of dynamic events [1]. The data generated can be used with an animation program like 3D Studio [2] and a human body modeler like Humanoid [3].

This paper will provide a general overview of 3D Studio and Humanoid, and outline the procedure used to utilize ATB output and Humanoid

models in 3D Studio to produce a three dimensional computer animation of a dynamic event which can be transferred to video tape.

For the purpose of this paper an automotive collision is used.

## Background

Three computer programs were used in this procedure . They are ATB, 3D Studio, and Humanoid.

ATB is a three dimensional model used to study human and/or dummy biomechanics in various dynamic events.

Autodesk 3D Studio is a three dimensional modeling and animation program designed for use on the personal computer. 3D Studio enables the user to build and create three-dimension models, assign properties and materials to the models, and animate the model to real time. 3D Studio is compatible with other software packages. For example, a complicated geometry created in AutoCad may be imported into 3D Studio via a DXF file. To enhance its performance, 3D Studio also has the ability to use external applications such as Liquid Speed and IPAS programs.

Humanoid : human animation designer is a library of three dimensional human models by Crestline Software.

## 3D Studio and Humanoid

The first step in the construction of most three dimensional models begins in the 2DSHAPER, one of the modules of 3D Studio. In 2DSHAPER the user creates the outline of an object in 2-dimensions with the desired complexity.

After the two dimensional geometry has been defined, the user brings the information into the 3DLOFTER, a module of 3D Studio. 3DLOFTER has the ability to take the 2DSHAPER information and an additional user supplied third dimension to loft the object to three-dimensions.

In the 3D EDITOR module of 3D Studio the user assigns materials, color and lighting to the object. At this point the objects are created and ready for animation.

The following steps are performed in the KEYFRAMER module of 3D Studio. KEYFRAMER is the module where the objects are animated. The user inputs all the necessary parameters to create the animation. Objects are positioned, rotated, and scaled by using the mouse, or for greater accuracy, the coordinates may be typed in.

Humanoid: *human animation designer* from Crestline Software is a library of three dimensional human models that can be used with 3D Studio.

Humanoid models are available for persons such as man, woman, and child (Figure 1) and can be scaled to proper sizes to represent the appearance of actual humans or ATB dummies. The models have proper positioning of pivots on the body to allow for proper anatomical range of motion.

An important quality about Humanoid is that, unlike other programs of the same nature, the designer has taken great care to make sure there

are no "holes" in the body that may appear when limbs are rotated about one another. However, one drawback of the program is that the Humanoid torso is divided into only 2 segments while the GEBOD torso is divided into 3 segments.

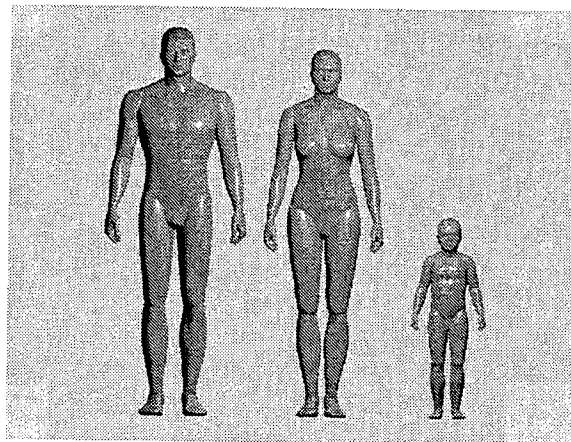


**Figure 1 Humanoid Models of Man, Woman and Child**

## Procedure for Utilizing ATB data and Humanoid in 3D Studio

In order to create a three dimensional animation that will accurately depict the results from an ATB simulation, necessary data has to be inputted into 3D Studio.

First, the vehicle, seat, and seatbelts are made two dimensionally in the 2DSHAPER, then lofted to three dimensions in the 3DLOFTER, and finally assigned materials in the 3D Editor.

Next, the proper human model is selected from Humanoid and scaled according to GEBOD data. The user can take dimensions from GEBOD data and use that to create an accurately matched Humanoid model. For example, the upper arm



may be scaled such that it is shorter or longer or a thigh may be scaled such that it is fuller.

The next step in the construction of the three dimensional animation is performed in the KEYFRAMER where the process of animation takes place.

The first thing to determine in the KEYFRAMER is how many frames are necessary for the animation. For a real time animation, you would use the ratio of 30 frames to 1 second. For example, if you wanted to create a real time animation that would last 10 seconds, the necessary number of frames is 300. However, for an animation based on ATB simulations that are representations of short duration impacts such as an automotive collision, real time animations are not useful. For animations of this type slow motion animation is utilized.

The next step is animation of the human model. This is done by taking certain important time intervals from the ATB output data, such as the beginning of body motion, body contact with a structure, and final resting position.

The user assigns the linear position and angular rotation to the human model for the initial state either by using the mouse, or for greater accuracy, by using the keyboard and typing in the numbers. It is recommended to manually type in data because it is more accurate than positioning by sight with the mouse.

At each important time interval the user assigns the human model its new linear position and angular rotation. Note that each individual body part can be assigned its respective position and rotation. Example output is given in Figures 2 through 5.

After completing the process of inputting the data from ATB into 3D Studio, rendering the

animation may be performed in the KEYFRAMER.

Before the actual rendering takes place, the user has the ability to preview their work. Because the actual rendering may take an extended period of time, depending on the complexity of the animation, the user may want to use the preview feature in the KEYFRAMER.

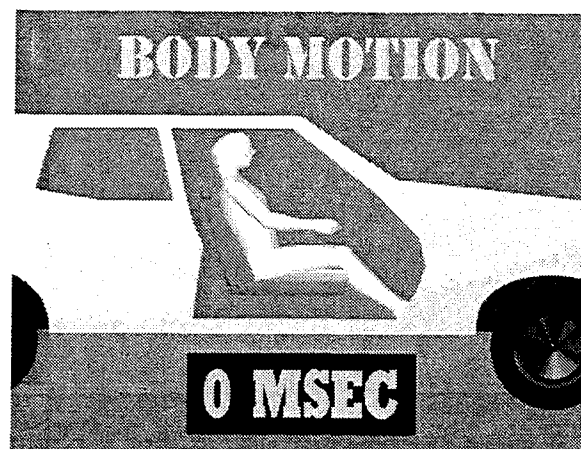


**Figure 2 Body Position at 0 msec**

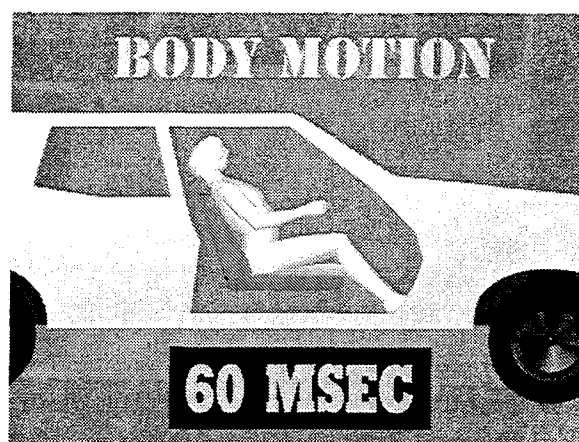


**Figure 3 Body Position at 60 msec**

The preview feature will render the animation regardless of size, usually in a matter of minutes.

This is because it only renders to shades of silver with a blue background, as opposed to the sometimes time consuming full color renderings. This is a very useful tool because the user can quickly check to make sure their work has been done correctly, or if changes need to be made.



Figure 4 Body Position at 102 msec

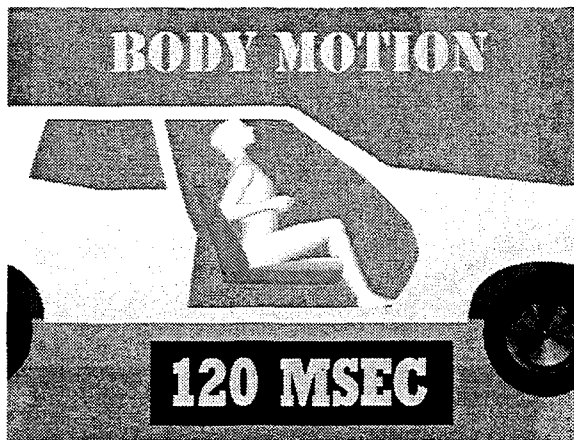


Figure 5 Body Position at 120 msec

Once the user is satisfied that their work is accurate and correct, they can run the full color rendering process that is also done in the KEYFRAMER.

## Summary and Conclusion

1. Procedure outline for the 3D Studio animation based on the ATB data is as follows:
  - a) Prepare the geometry of contact surfaces in 2DSHAPER, loft them to three dimensions in the 3DLOFTER, and assign materials to them in 3D EDITOR.
  - b) Select and scale the Humanoid model according to GEBOD data.
  - c) Input linear position and angular rotation from ATB into 3D Studio.
  - d) Render animation.
2. 3D Studio, and Humanoid can be effectively used in the preparation of precise graphical representation of an ATB simulation.

## References

1. Obergefell, L.A., Gardner, T.R., Kaleps, I., and Fleck, J.T., "Articulated Total Body Model Enhancements, Volume 2: User's Guide," AAMRL Report No. AAMRL-TR-88-043, January 1988 (NTIS No. A203 566)
2. Autodesk 3D Studio Reference Manual, 1990-1993
3. Humanoid : human animation designer, Reference Manual, Crestline Software Publishing

## **APPENDIX**

## LIST OF ATTENDEES

Dr Nabih Alem  
US Army Aeromedical Research Laboratory  
Commander  
SGRD-UAX-D/Alem  
Building 6901, P.O. Box 620577  
Fort Rucker, AL 36362  
Phone: 334-255-6892 Fax: 334-255-6937  
E-mail:

Dr Xavier J Avula  
University of Missouri-Rolla  
231 Mechanical Engineering Bldg  
Rolla, MO 65401  
Phone: 314-341-4585 Fax: 314-364-3351  
E-mail: avula@umr.edu

Mr Lindley Bark  
Simula Government Products  
10016 S. 51st Street  
Phoenix, AZ 85044  
Phone: 602-730-4447 Fax: 602-893-8643  
E-mail: lbark@enet.net

Mr David J Biss  
Automotive Safety Analysis, Inc.  
15506 Avery Road  
Suite Number One  
Rockville, MD 20855  
Phone: 301-294-7800 Fax: 301-294-0812  
E-mail: 71630.2432@compuserve.com

Mr Huaining Cheng  
Systems Research Laboratories  
2800 Indian Ripple Rd.  
WP 441  
Dayton, OH 45440-3696  
Phone: 513-255-3328 Fax: 513-255-3182  
E-mail: hcheng@falcon.al.wpafb.af.mil

Mr J. Robert Cromack  
Cromack Engineering Associates Inc  
P O Box 28243  
Tempe, AZ 85285-8243  
Phone: 602-831-7512 Fax: 602-831-2979  
E-mail:

Ms. Anne Curzon  
Failure Analysis Associates, Inc.  
1850 W. Pinnacle Peak Road  
Phoenix, AZ 58027  
Phone: 602-582-6949 Fax: 602-581-8814  
E-mail: acurzon@faamail.fail.com

Dr Yih-Chang Deng  
General Motors R & D Center  
Body Engineering Department  
Warren, MI 48090-9055  
Phone: 810-986-0450 Fax: 810-986-0446  
E-mail: ydeng@cmsa.gmr.com

Mr Charles Dickerson  
Arndt & Associates, Ltd  
2202 West Huntington Driver  
Tempe, AZ 85282  
Phone: 602-438-2004 Fax: 602-438-0898  
E-mail:

Mr. Richard M Downs  
National Transportation Safety Board  
490 L'Enfant Plaza, SW  
Washington, DC 20594  
Phone: 202-382-6890 Fax: 202-382-6715  
E-mail:

Dr John T Fleck  
J & J Technologies  
92 Henning Drive  
Orchard Park, NY 14127-2819  
Phone: 716-662-4294 Fax:  
E-mail:

Mr David Furey  
Simula Inc  
10016 South 51st Street  
Phoenix, AZ 85044  
Phone: 602-730-4445 Fax: 602-893-8643  
E-mail: dfurey@aztec.asu.edu

Mr Thomas Gardner  
Columbia University  
College of Physicians & Surgeons  
630 W 168th Street BB1412  
Orthopedic Research Laboratory  
New York, NY 10032  
Phone: 212-305-6618 Fax: 212-305-2741  
E-mail:  
GARDNER@CUORMA.ORL.COLUMBIA.EDU

Ms. Anita Grierson  
Simula, Inc.  
10016 S. 51st St.  
Phoenix, AZ 85044  
Phone: 602-756-4504 Fax: 602-893-8643  
E-mail: AGrierson@aol.com

Mr. Wesley Grimes  
Collision Engineering Associates  
P.O. Box 31900  
Mesa, AZ 85275  
Phone: 602-655-0399 Fax: 602-655-0693  
E-mail: wgrimes@host.yab.com

Dr Patrick Hannon  
Northern Arizona University  
School of Health Professions  
P O Box 15105  
Flagstaff, AZ 86011  
Phone: 520-779-9621 Fax: 520-779-9621  
E-mail:

Mr. Ray Jordan  
Jordan Consulting  
9402 S. 43rd Pl.  
Phoenix, AZ 85044  
Phone: 602-893-2595 Fax: 602-893-8360  
E-mail:

Dr Ints Kaleps  
AL/CFBV  
2610 Seventh St.  
Building 441  
Wright-Patterson AFB, OH 45433-7901  
Phone: 513-255-3665 Fax:  
E-mail: ikaleps@tweety.al.wpafb.af.mil

Mr Kerry Knapp  
3632 N. Schevene  
Flagstaff, AZ 86004  
Phone: 520-523-6771 Fax: 520-779-9621  
E-mail:

Mr. Richard Kozycki  
U.S. Army Research Laboratory  
AMSRL-HR-MB  
Bldg. 459  
Aberdeen Proving Ground, MD 21005  
Phone: 410-278-5880 Fax: 410-278-5032  
E-mail: rkozycki@hel4.arl.mil

Mr. Stewart Lilley  
Simula, Inc.  
10016 S. 51st St.  
Phoenix, AZ 85044  
Phone: 602-756-4523 Fax: 602-893-8643  
E-mail: lilley@primenet.com

Ms. Laura Liptai  
University of California - Davis  
Biomedical Engineering  
9 La Cresta  
Orinda, CA 94563  
Phone: 510-376-1240 Fax: 510-376-1245  
E-mail: liptai@venus.engr.ucdavis.edu

Mr Eugene Loverich  
Northern Arizona University  
College of Engineering  
NAU Box 15600  
Flagstaff, AZ 86011  
Phone: 520-523-4350 Fax: 520-523-8951  
E-mail: ebl@pine.cse.nau.edu

Dr Deren Ma  
Systems Research Laboratories  
2800 Indian Ripple Rd  
WP441  
Dayton, OH 45440-3696  
Phone: 513-255-3328 Fax: 513-255-3182  
E-mail: dma@falcon.al.wpafb.af.mil

Dr Donald Macko  
3521 Mission Avenue  
Carmichael, CA 95608-3610  
Phone: 916-482-4680 Fax: 916-482-4685  
E-mail:

Mr. Sean Mahoney  
Conax Florida Corp  
49A Centre Pointe Dr.  
St. Charles, MO 63304  
Phone: 314-936-1262 Fax: 314-936-2668  
E-mail:

Mr Joseph McCarthy  
BTS Consulting Engineers  
1725 North Talbot Rd.  
R.R. #1  
Windsor, Ontario  
Canada N9A 6J3  
Phone: 519-737-7233 Fax: 519-737-7203  
E-mail:

Mr Robert McConnell  
Naval Air Warfare Center  
Aircraft Division  
MS-15  
Warminster, PA 18974  
Phone: 215-441-1208 Fax: 215-441-2088  
E-mail: mcconnell@dfs.nadc.navy.mil



Mr Richard McMahon  
US Army Research Laboratory  
ARL-HRED-ERDEC Field Element  
AMSRL-HR-MM  
Chief  
Aberdeen Proving Gnd, MD 21005  
Phone: 410-278-5928 Fax: 410-278-9525  
E-mail: rcmahon@arl.mil

Mr Peter Mendoza  
MacNeal-Schwendler Corp.  
815 Colorado Blvd.  
Los Angeles, CA 90041  
Phone: 213-259-3860 Fax: 213-259-4992  
E-mail: peter.mendoza@macsch.com

Dr. Louise Obergefell  
AL/CFBV  
2610 Seventh St.  
Building 441  
Wright-Patterson AFB, OH 45433-7901  
Phone: 513-255-3665 Fax:  
E-mail: lobergef@tweety.al.wpafb.af.mil

Dr Gyung-Jin Park  
Hanyang University  
Mechanical Design and Production Engineering  
17 Haengdang-Dong  
Seongdong-Ku  
Seoul,  
Korea 133-791  
Phone: 82-345-400-5246 Fax: 82-345-407-0755  
E-mail:

Dr Amit L Patra  
University of Puerto Rico  
Department of General Engineering  
P O Box 5635 RUM  
Mayaguez, PR 00709  
Phone: 809-265-3816 Fax:  
E-mail:

Dr N Rangarajan  
GESAC Inc  
Route 2 Box 339A  
Kearneysville, WV 25430  
Phone: 304-267-6704 Fax: 304-267-6821  
E-mail: gesac@mountain.net

Ms. Annette Rizer  
Systems Research Laboratories  
2800 Indian Ripple Rd.  
WP 441  
Dayton, OH 45440-3696  
Phone: 513-255-3328 Fax: 513-255-3182  
E-mail: arizer@falcon.al.wpafb.af.mil

Mr. Joseph F Ruggieri  
ForDyn, Inc.  
1412 East Chicago Circle  
Chandler, AZ 85224-5440  
Phone: 602-917-2725 Fax: 602-917-2725  
E-mail: 72023.314@compuserve.com

Mr. Todd K Saczalski  
Environmental Research & Safety Technologists  
310 Lookout Dr.  
Laguna Beach, CA 92651  
Phone: 714-497-8446 Fax: 714-497-7013  
E-mail:

Dr. Kenneth J Saczalski  
Environmental Research & Safety Technologists  
310 Lookout Drive  
Laguna Beach, CA 92651  
Phone: 714-497-8446 Fax: 714-497-7013  
E-mail:

Mr. Michael Shanahan  
BTS Consulting Engineers  
1725 North Talbot Rd  
R.R. #1  
Windsor, Ontario  
Canada N9A 6J3  
Phone: 519-737-7233 Fax: 519-737-7203  
E-mail:

Mr. Mark Skidmore  
TNO-MADYMO North America  
21800 Haggerty Rd  
Suite 305  
Northville, MI 48167  
Phone: 810-449-1755 Fax: 810-449-7574  
E-mail: skidmore@madymo.com

Mr. Mark Skidmore  
Talley Defense Systems  
3500 N. Greenfield Rd.  
Mesa, AZ 85205  
Phone: 602-898-2271 Fax: 602-898-2358  
E-mail: mskidmore@talleyds.com

Ms Jeanne Smith  
Systems Research Laboratories  
2800 Indian Ripple Rd.  
WP 441  
Dayton, OH 45440-3696  
Phone: 513-255-3328 Fax: 513-255-3182  
E-mail: jas@osprey.al.wpafb.af.mil

Mr Stephen Soltis  
FAA Transport Airplane Directorate  
Aircraft Certification Service  
3960 Paramount Blvd  
LA Aircraft Certification Office  
Lakewood, CA 90712-4137  
Phone: 310-627-5207 Fax: 310-627-5210  
E-mail: Stephen\_Soltis@mail.hq.faa.gov

Mr Manohar Srinivasan  
General Motors Corp.  
Mail Code 482-109-251  
3031 W. Grand Blvd  
Detroit, MI 48232  
Phone: 313-556-2291 Fax: 313-556-2073  
E-mail:

Mr. Bill Torres  
MacNeal - Schwendler Corporation  
2975 Redhill Avenue  
Costa Mesa, CA 92626  
Phone: 714-444-5195 Fax: 714-540-8702  
E-mail: bill.torres@macsch.com

Mr Michael Varat  
JFK Engineering  
5636 La Cumbre Rd.  
Somis, CA 93066  
Phone: 805-386-3388 Fax: 805-386-4892  
E-mail:

Mr. Dan W Wall  
Cromack Engineering  
4500 E. Lakeshore Dr.  
#470  
Tempe, AZ 85282  
Phone: 602-831-7512 Fax:  
E-mail:

Mr Greg Weisenfeld  
Honda R&D  
1900 Harpers Way  
Torrance, CA 90501  
Phone: 310-781-5844 Fax:  
E-mail:

Dr Narayan Yoganandan  
Medical College of Wisconsin  
Department of Neurosurgery  
9200 West Wisconsin Avenue  
Milwaukee, WI 53226  
Phone: 414-384-3453 Fax: 414-382-5374  
E-mail: yoga@post.its.mcw.edu

Dr Mariusz Ziejewski  
North Dakota State University  
Dept of Mech Eng & Applied Mechanics  
Dolve Hall 111  
Fargo, ND 58105  
Phone: 701-232-9223 Fax: 701-231-8913  
E-mail: ziejewsk@plains.nodak.edu

Addendum

**Using ATB to Model Break-Away Head Supported Devices**

*Nabih Alem, Joe McEntire - US Army Aeromedical Research Laboratory*

*Hashem Ashrafiun - Villanova University*

**Using ATB on the SGI System**

*Wesley Grimes - Collision Engineering Associates, Inc.*

# **USING ATB TO MODEL BREAK-AWAY HEAD-SUPPORTED DEVICES**

**Nabih Alem  
Joe McEntire**

*US Army Aeromedical Research Laboratory*

and

**Hashem Ashrafiuon**

*Associate Professor  
Villanova University*

Presentation at the  
1996 ATB User's Group Conference  
Phoenix, AZ  
February 8-9, 1996

# BACKGROUND

---

## Concerns:

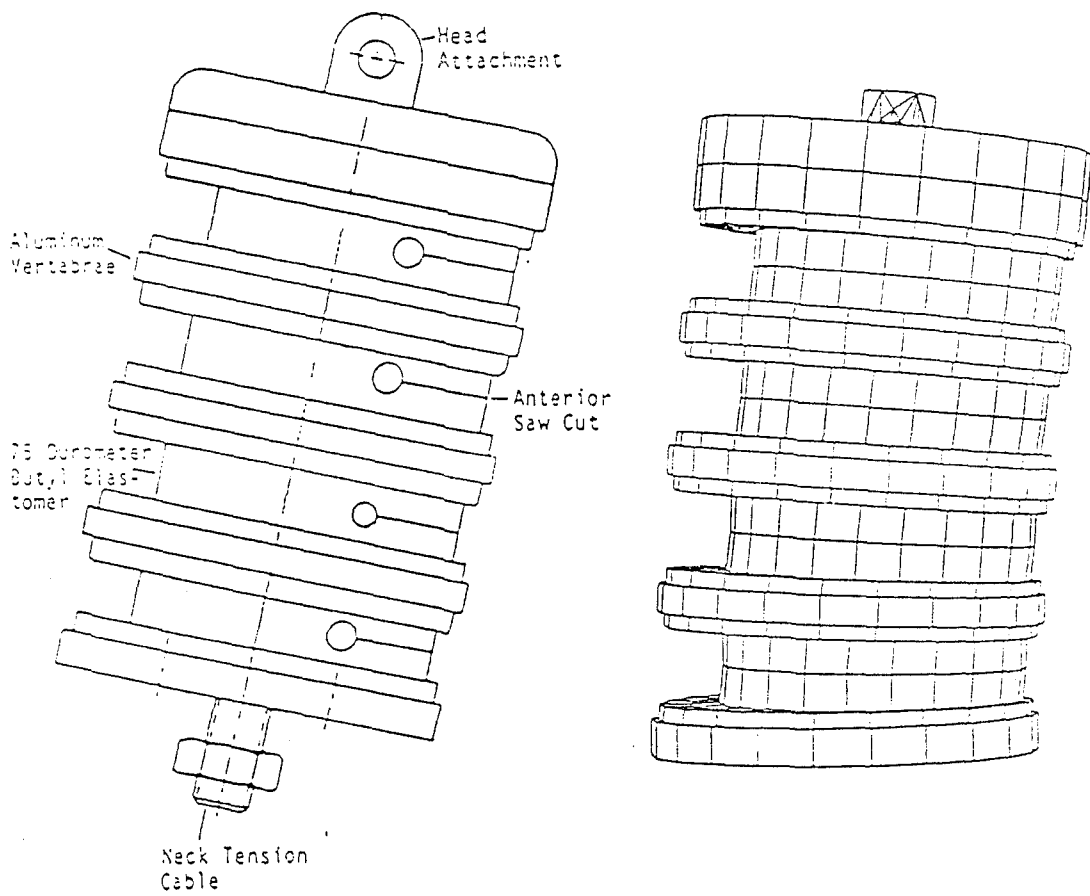
- Simplistic neck model, producing unrealistic neck forces and moments
- Difficulty of simulating head-supported devices (HSD)
- Unknown effects of HSD on neck forces when airbag is present

## Previous work:

- **INTRODUCTION OF DEFORMABLE SEGMENTS IN THE ATB MODEL**  
*Ashrafiuon & Colbert, Proceedings of the 1995 ATB User's meeting.*
- **MODIFICATION OF THE ATB MODEL TO INCORPORATE DEFORMABLE BODIES AND ITS VERIFICATION THROUGH DUMMY NECK MODELING AND SIMULATION**  
*Ashrafiuon, Colbert, Obergefell, and Kaleps. 1995 Armstrong Lab tech report (in press)*

# MECHANICAL & F.E. NECKS

---





# OBJECTIVES

---

- Study effects of head-supported devices on head and neck injury risk

*(incorporate realistic HSD models in ATB code)*

- Improve fidelity of head/neck response, and accuracy of injury risk assessment

*(incorporate better neck model in ATB code)*

- Study effects of helmet slippage on head & neck response

*(introduce friction into helmet-head interface)*

- Evaluate interaction between HSD and inflatable restraint and protection devices

*(merge ATB code with FEM of airbags)*

# STRATEGY

---

## Phase 1. (completed)

- ① Modify standard ATB-4 code to attach an extra segment to the head. (rearrange equations)
- ② Verify (debug) new code → [ATB+HSD]
- ③ Add deformable neck (DN) to [ATB+HSD]
- ④ Debug code → [ATB+HSD+DN] = ATB-Va

## Phase 2. (1996)

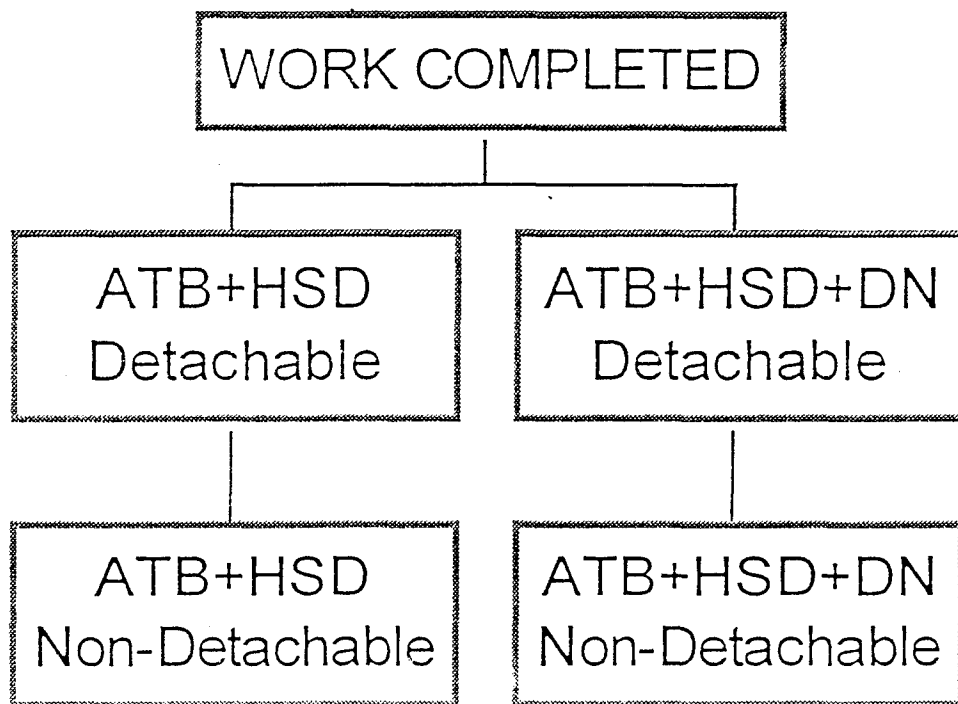
- ⑤ Validate **ATB-Va** (Minisled & pendulum manikin tests with break-away night vision goggles)
- ⑥ Introduce slippage between helmet and head

## Phase 3. (1996-97)

- ⑦ Merge **ATB-Va** with airbag software (with assistance from Armstrong Laboratory and/or Simula, Inc.)

# PHASE 1 WORK

---



ATB : Articulated Total Body  
HSD : Head Support Devices  
DN : Deformable Neck

# SIMULATIONS

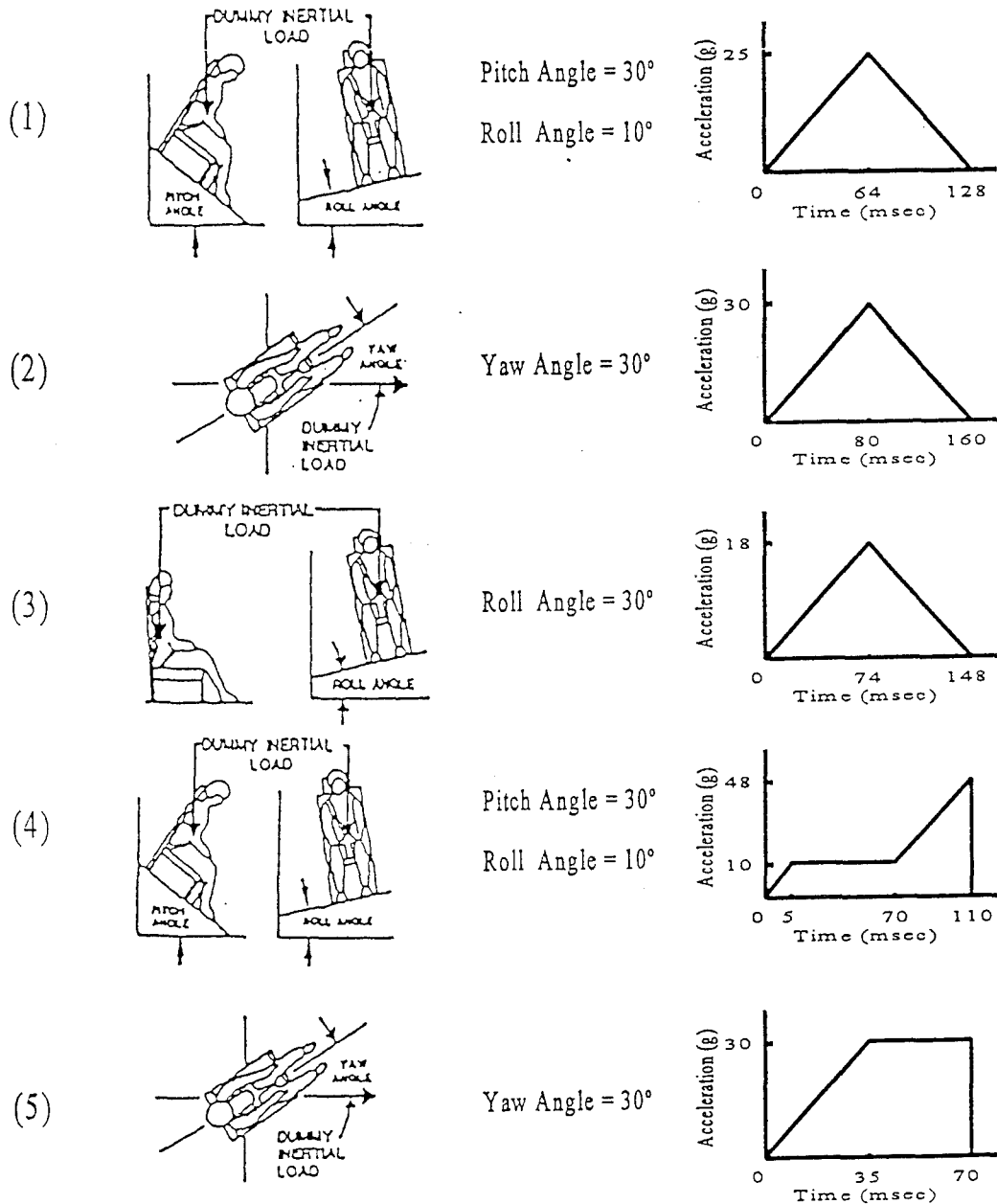
---

Seated helicopter pilot during mainly-vertical impact:

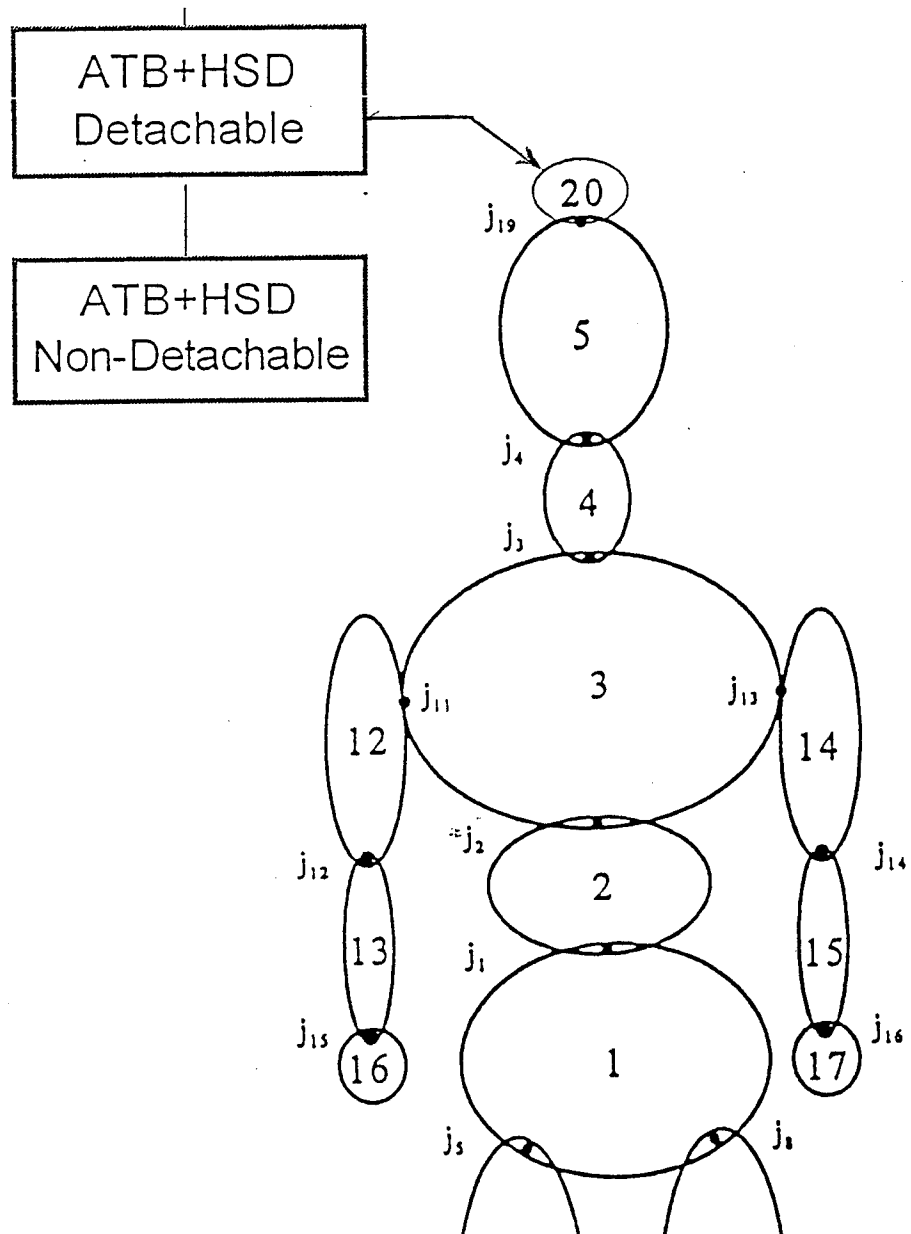
- 2 helmets:
  1. IHADSS with detachable HDU, and
  2. SPH-4B with detachable NVG
- 4 subjects (Hybrid III, and 3 sizes humans)
- 5 impact conditions (see next slide)
- Fixed and detachable HSD. Break-away criteria:
  1. Forward  $F_x > 13.0$  lb, or
  2. Twist  $M_z > 7.0$  lb-in, or
  3. Bending  $M_y > 10.5$  lb-in
- Simulations using **ATB+HSD** code were repeated using the latest **ATB+HSD+DN** code

*Note: Code modifications and finalized documentation will be sent to Armstrong Lab for re-distribution to other interested ATB users.*

# IMPACT CONDITIONS

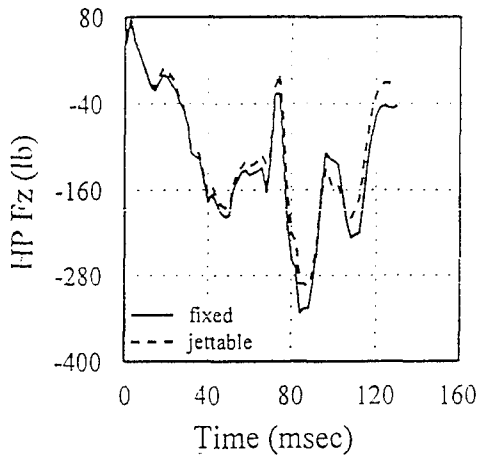


# STIFF NECK + HSD

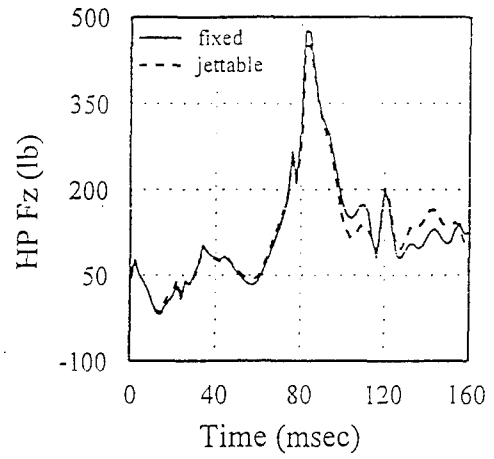


# AXIAL FORCE @ HEAD/NECK

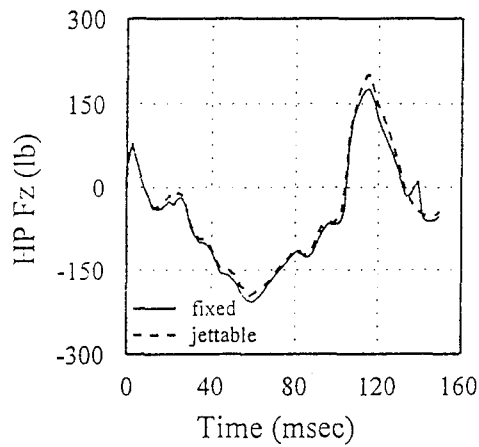
Hybrid III-Pulse 1



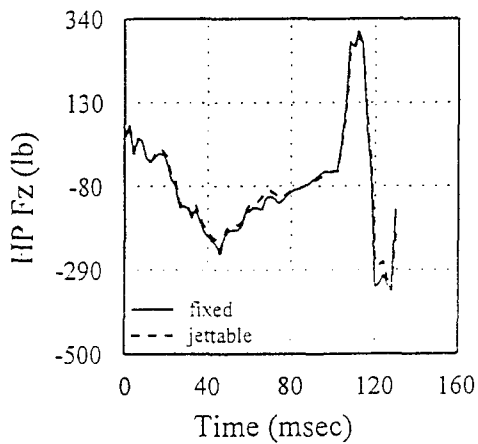
Hybrid III-Pulse 2



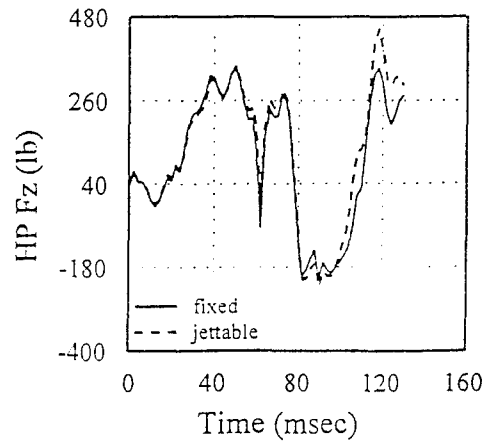
Hybrid III-Pulse 3



Hybrid III-Pulse 4

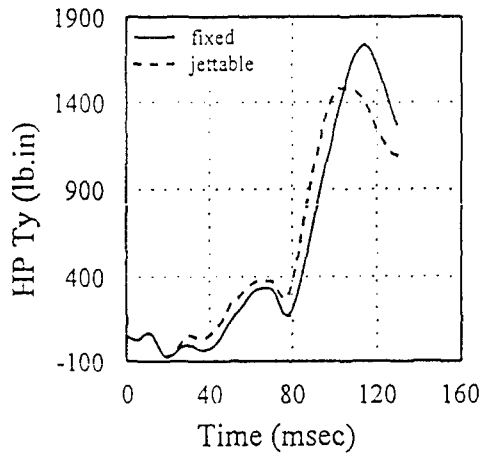


Hybrid III-Pulse 5

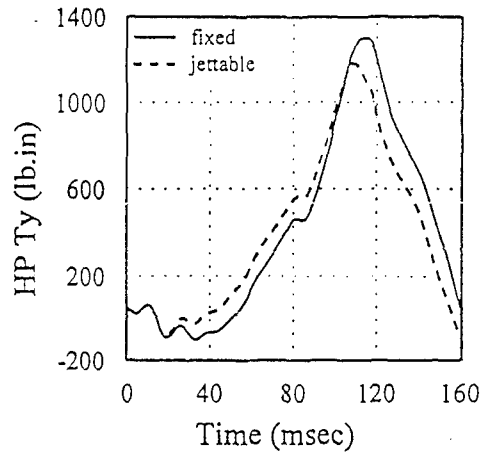


# PITCH MOMENT @ HEAD/NECK

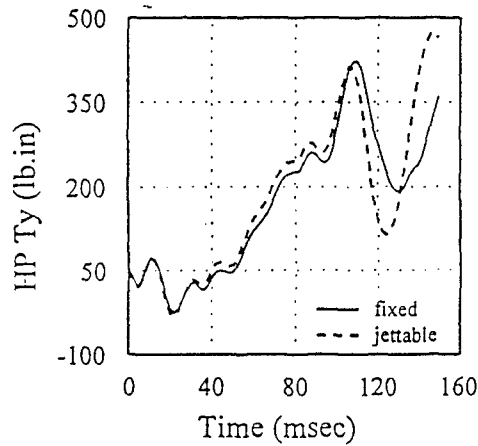
Hybrid III-Pulse 1



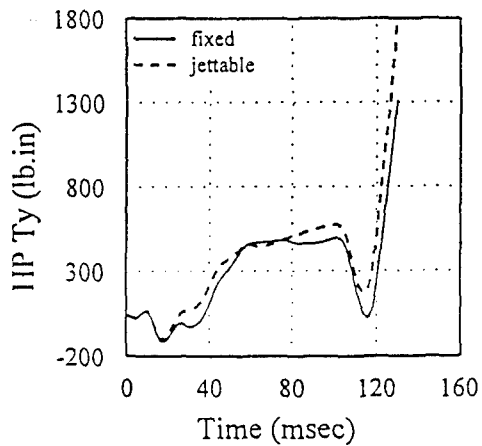
Hybrid III-Pulse 2



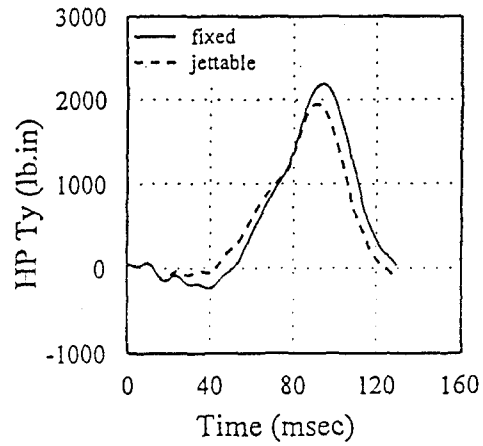
Hybrid III-Pulse 3



Hybrid III-Pulse 4

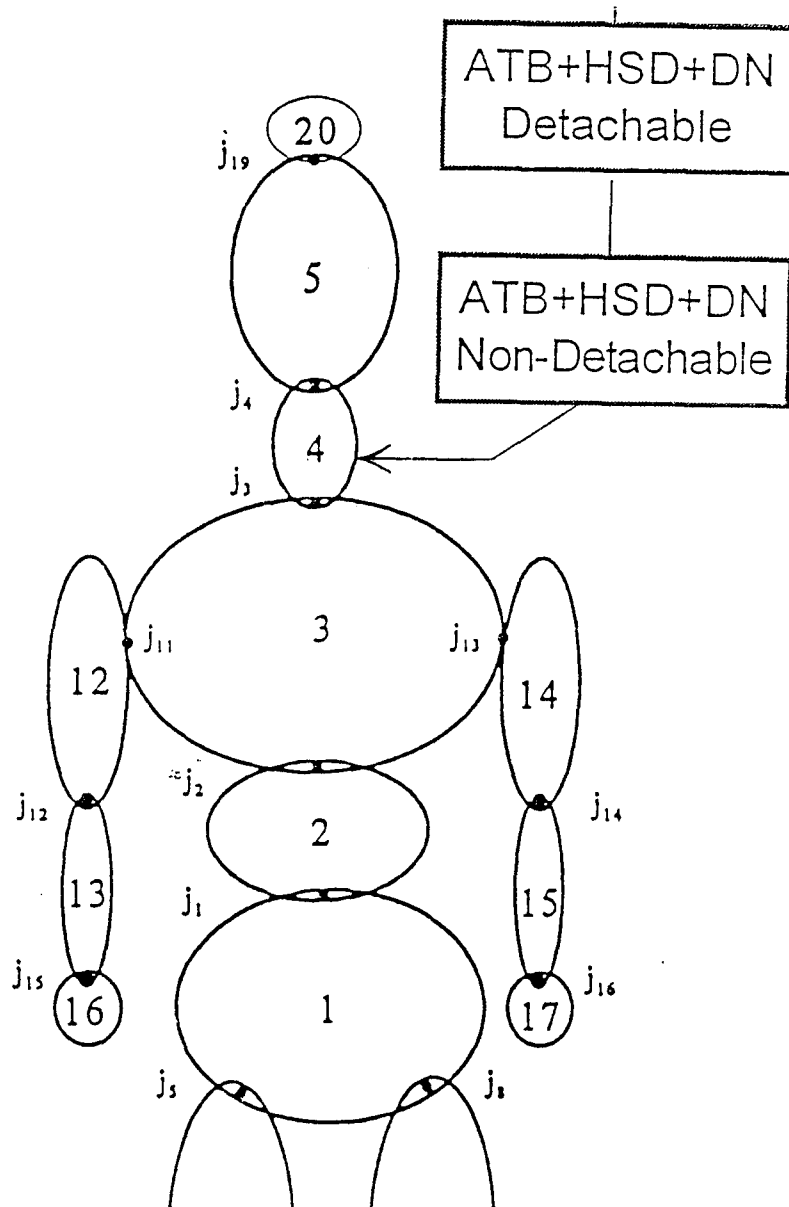


Hybrid III-Pulse 5



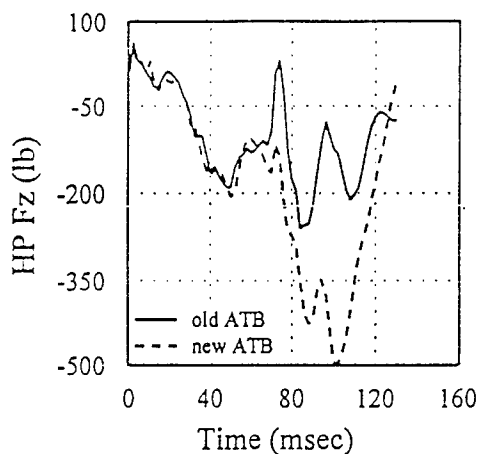


# DEFORMABLE NECK + HSD

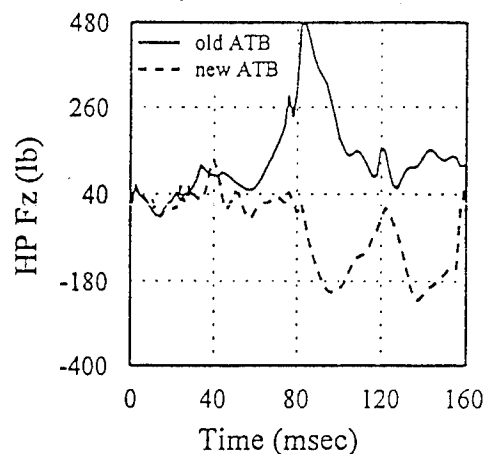


# AXIAL FORCE @ HEAD/NECK

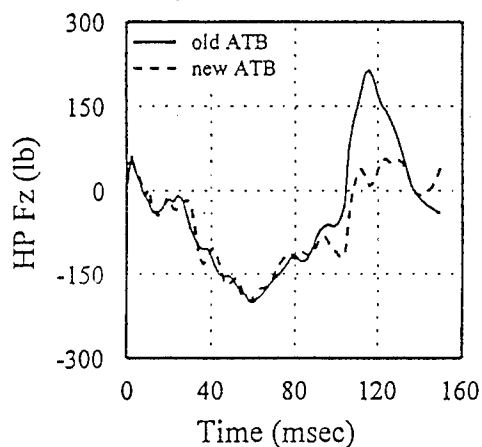
### Hybrid III-Pulse 1



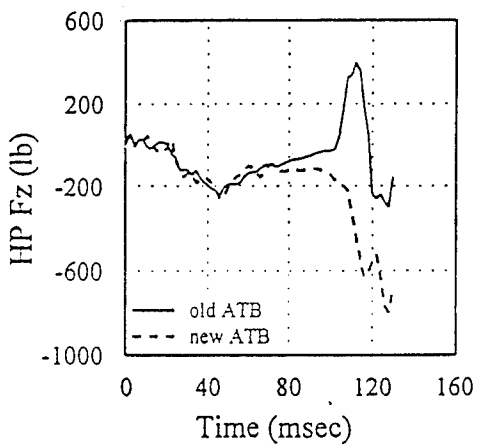
### Hybrid III-Pulse 2



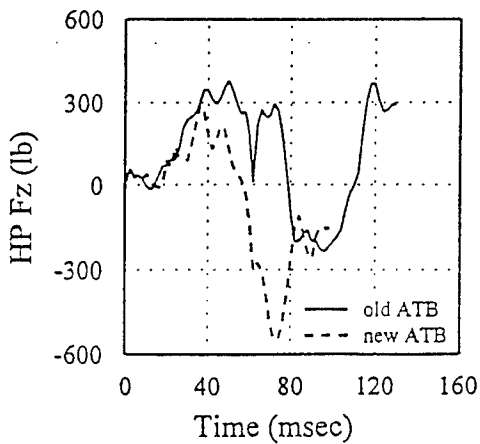
### Hybrid III-Pulse 3



### Hybrid III-Pulse 4

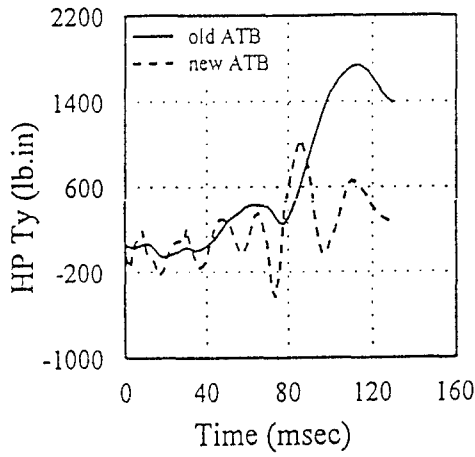


### Hybrid III-Pulse 5

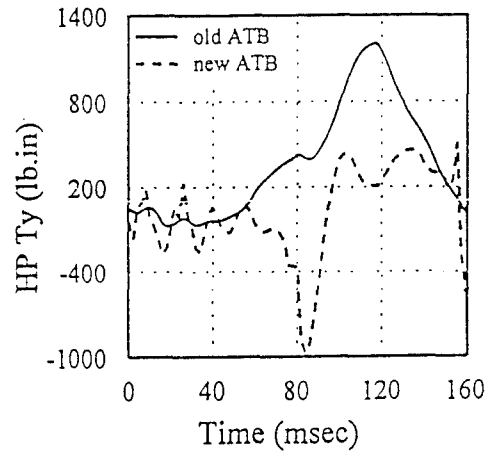


# PITCH MOMENT @ HEAD/NECK

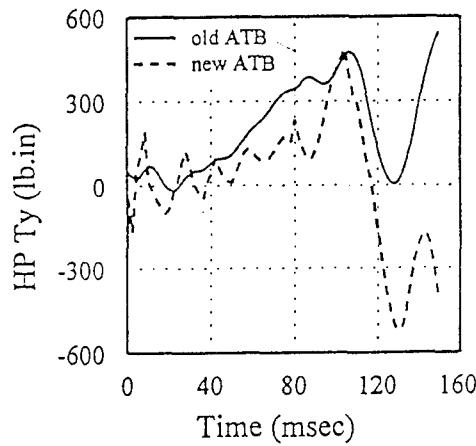
### Hybrid III-Pulse 1



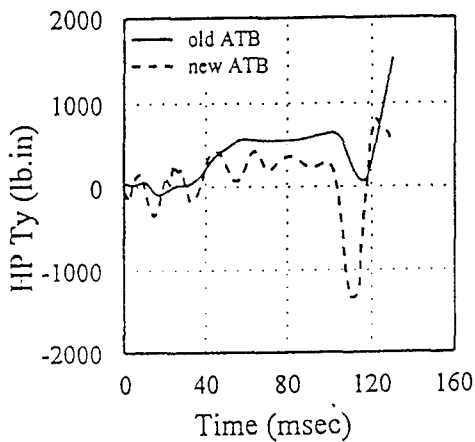
### Hybrid III-Pulse 2



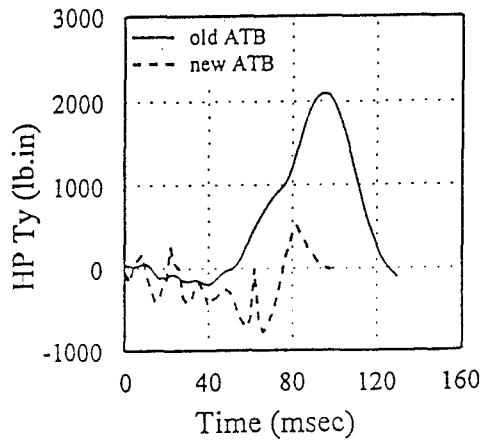
### Hybrid III-Pulse 3



### Hybrid III-Pulse 4

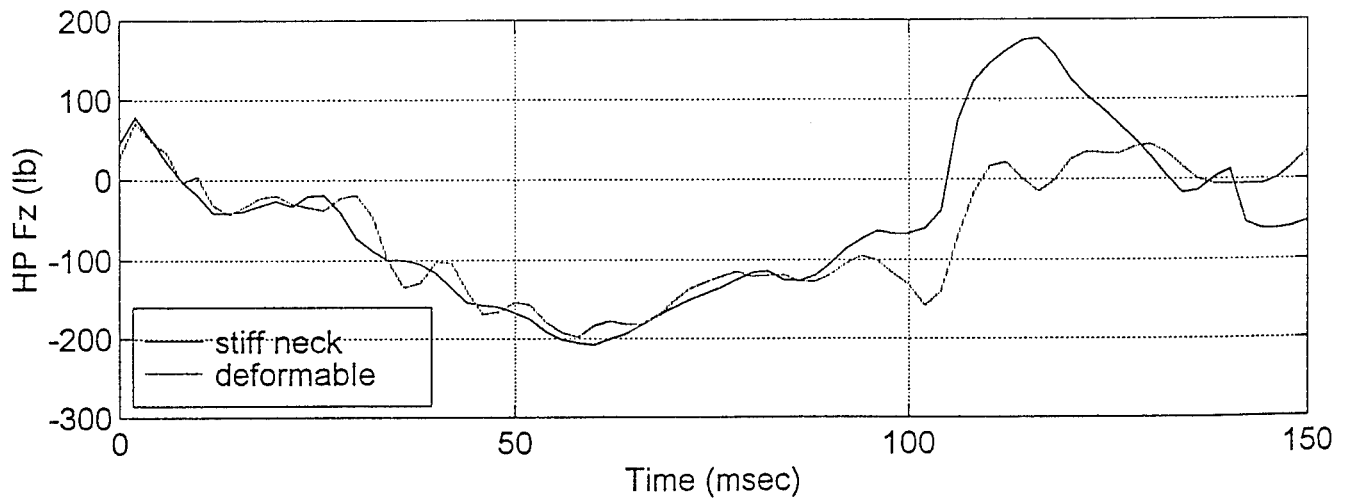
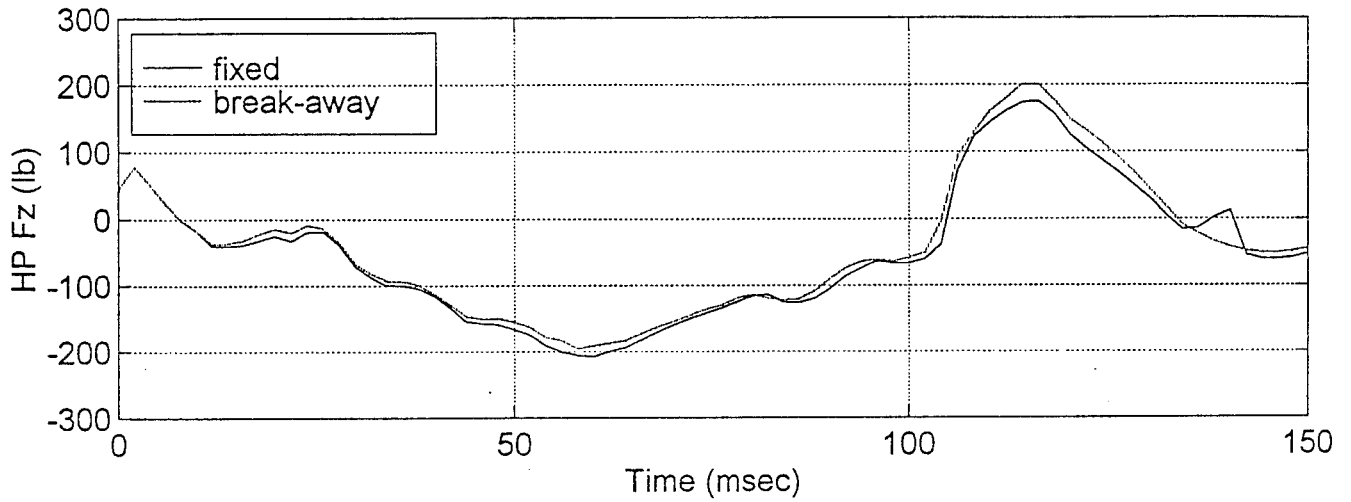


### Hybrid III-Pulse 5

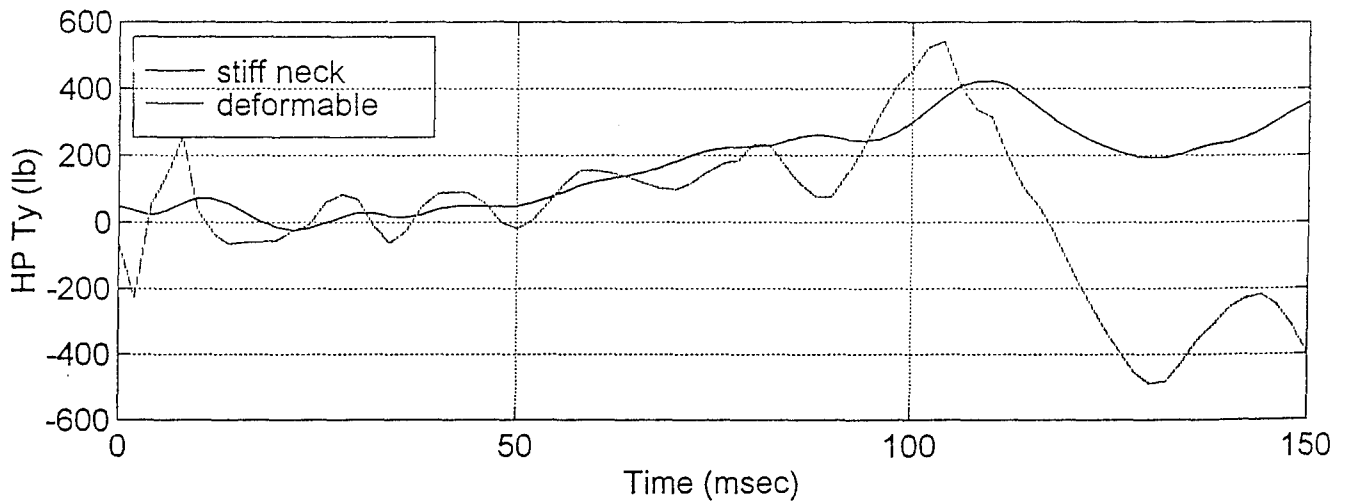
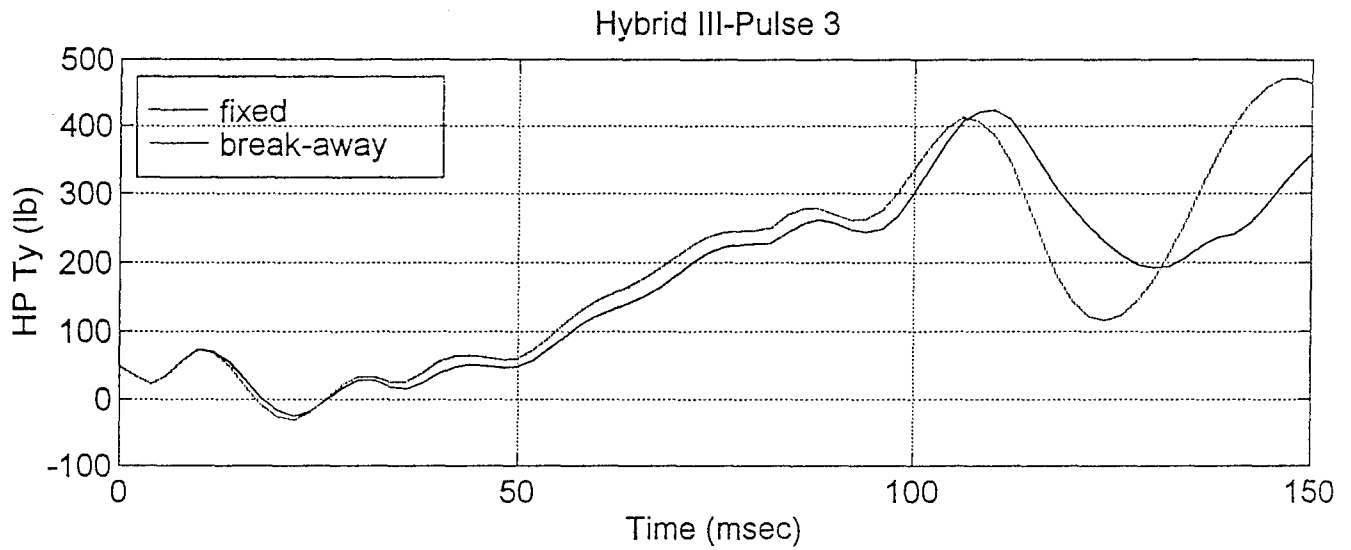


# COMPARISON OF AXIAL FORCE

Hybrid III-Pulse 3



# COMPARISON OF PITCH MOMENT



# SUMMARY

---

- **Early timing of breakway;**  
however, detachment criteria needs further tuning
- **Breakaway HSDs reduce neck forces by 15%:**  
however, further verification is needed
- **Modified ATB code to model detachable HSD:**  
appears to be bug-free; however, experimental validation is required.
- **Performed helicopter crash simulations:**  
produced 30% lower forces and moments at head/neck pivot.

# **FUTURE WORK**

---

- 1996:

Experimental validation (pendulum) of the deformable neck + detachable HSD model

- 1996:

Modify ATB-Va code to include slippage of helmet relative to pilot's head (*ATB-Vs?*)

- 1996-1997:

Merge ATB-V? with inflatable restraints and airbags

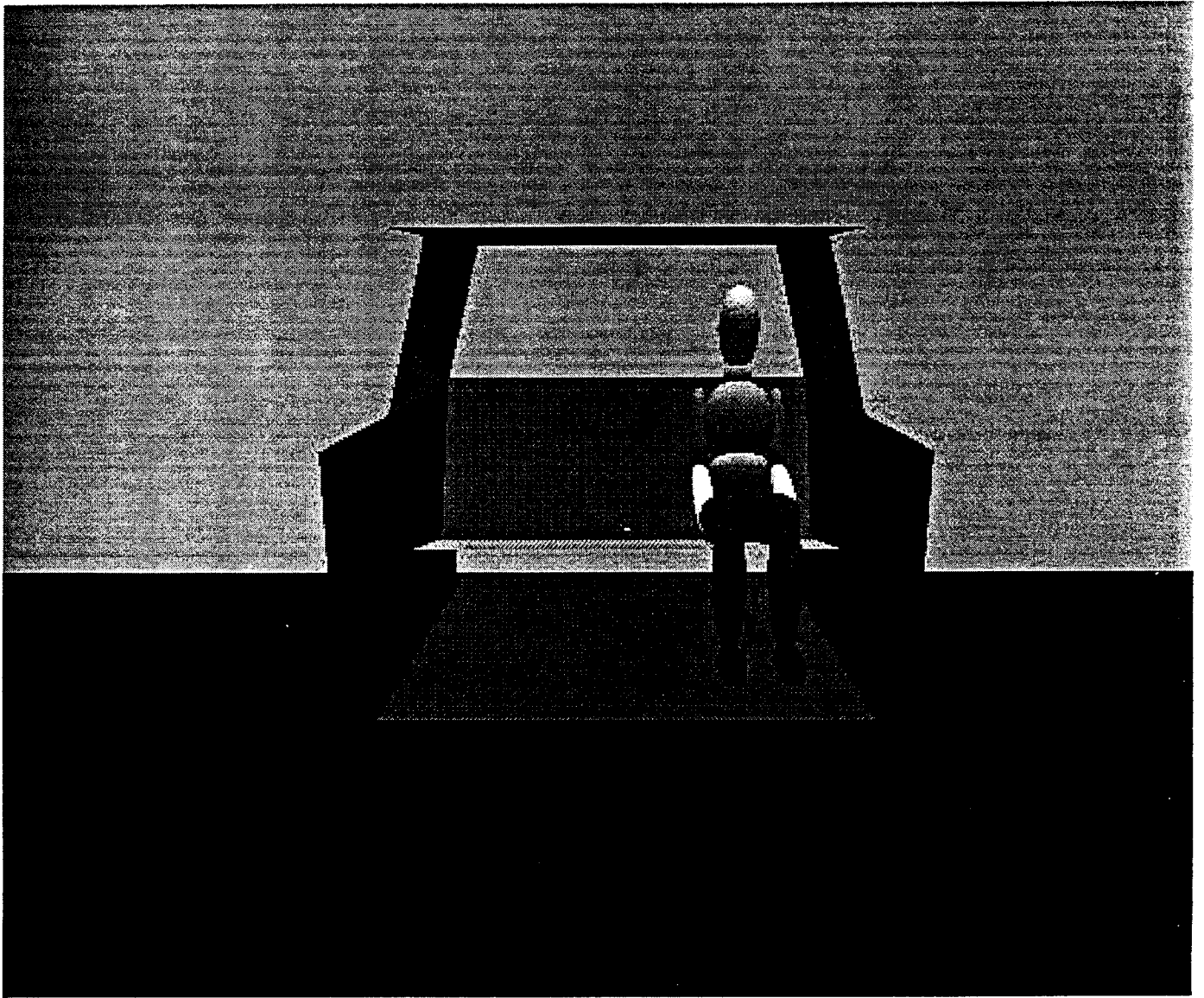
# **Using ATB on the SGI System**

**Presented by:**

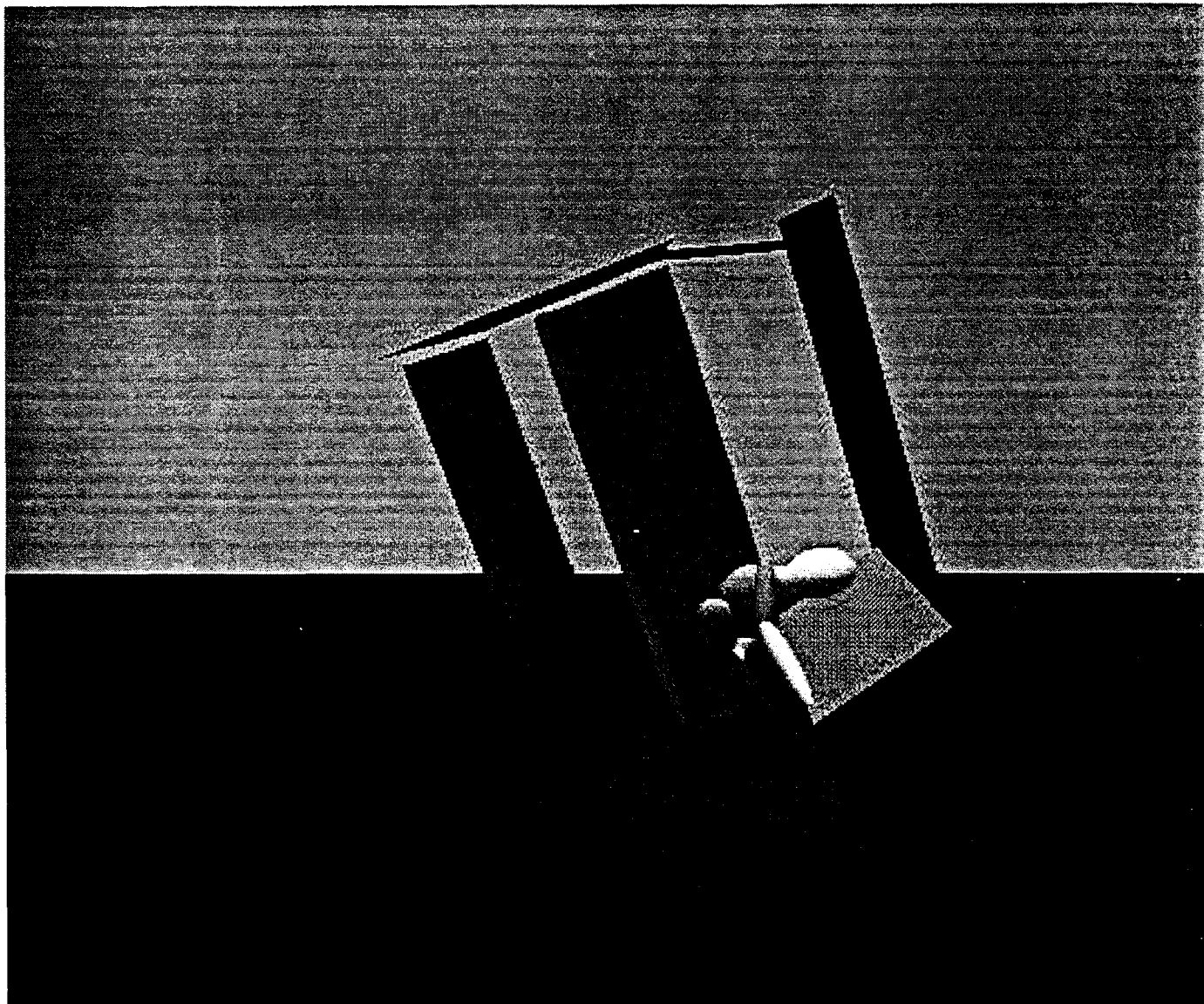
**Wesley Grimes**

**Collision Engineering Associates, Inc.  
Mesa, AZ  
(602) 655-0399**

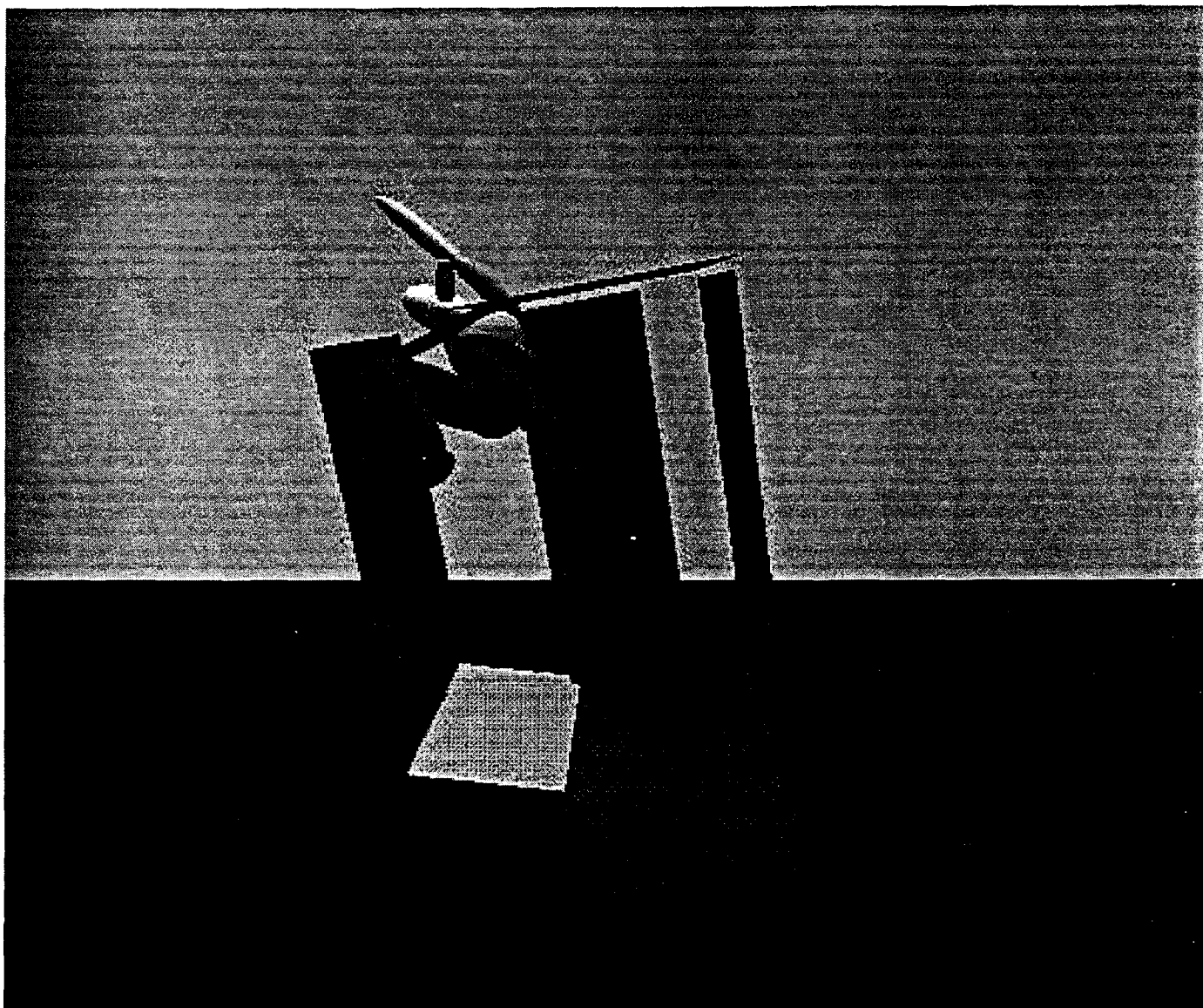




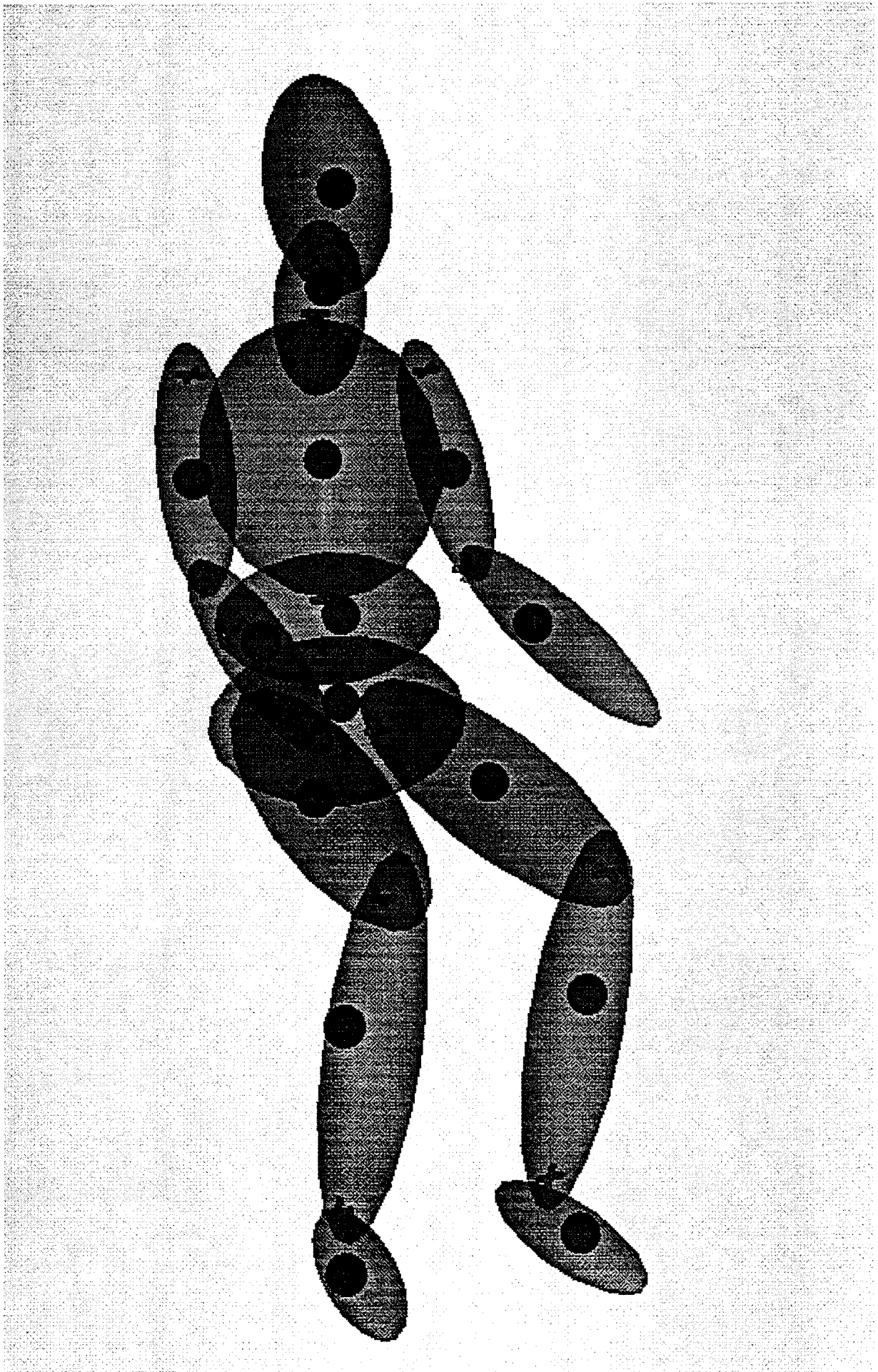
Sample output from IMAGE32  
- time 0 ms



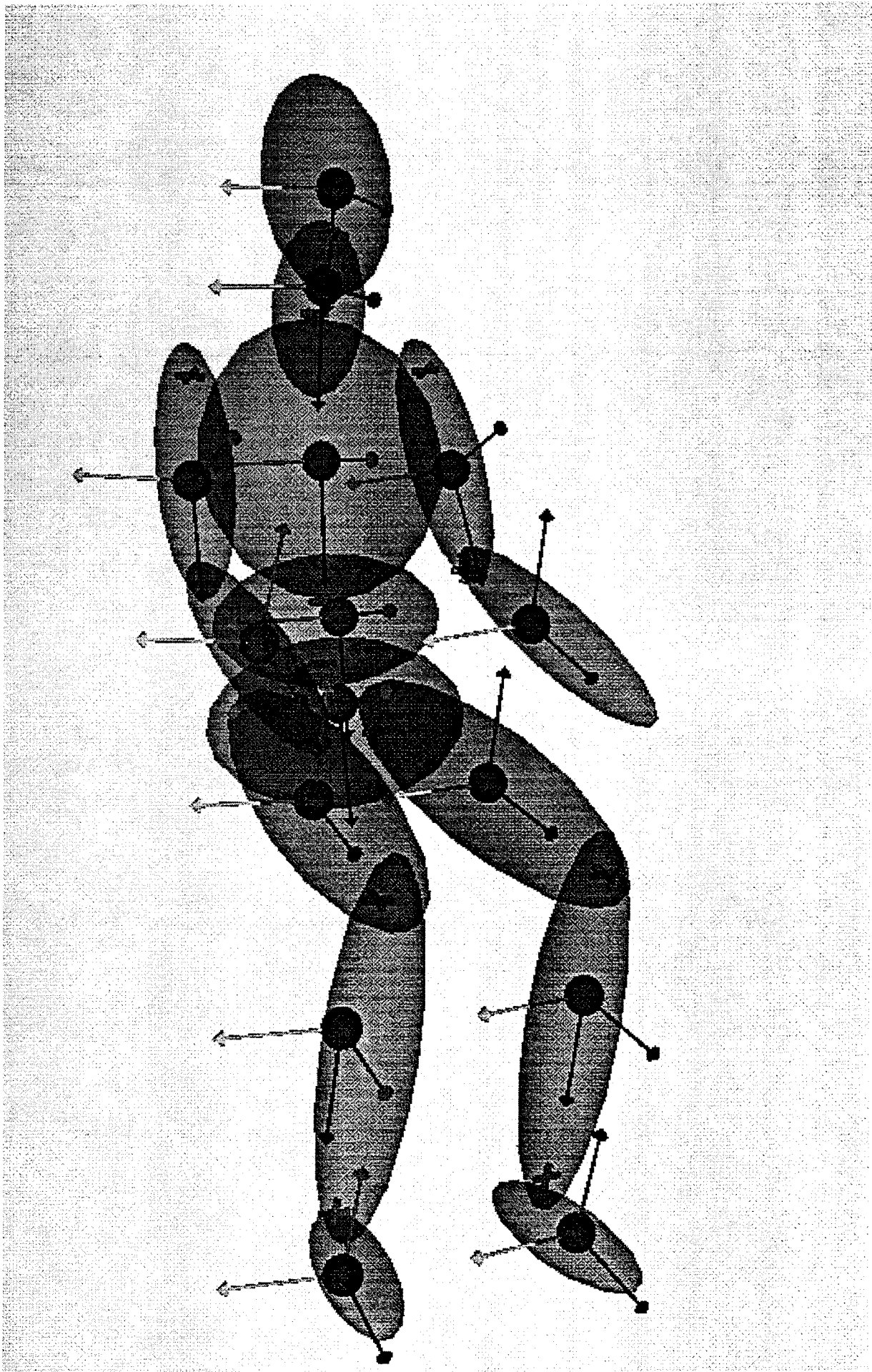
Sample output from IMAGE32  
- time 490 ms



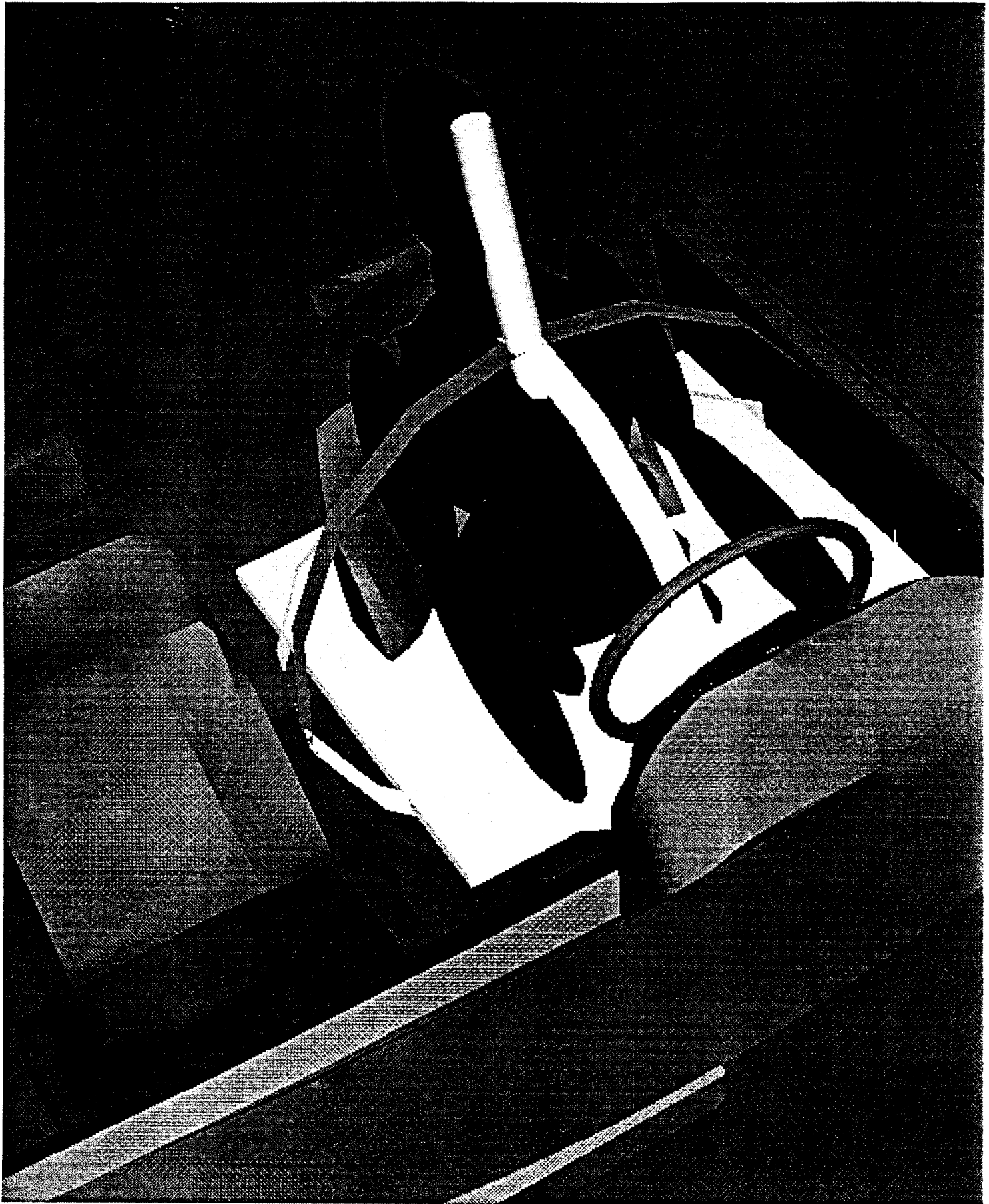
Sample output from IMAGE32  
- time 1020 ms



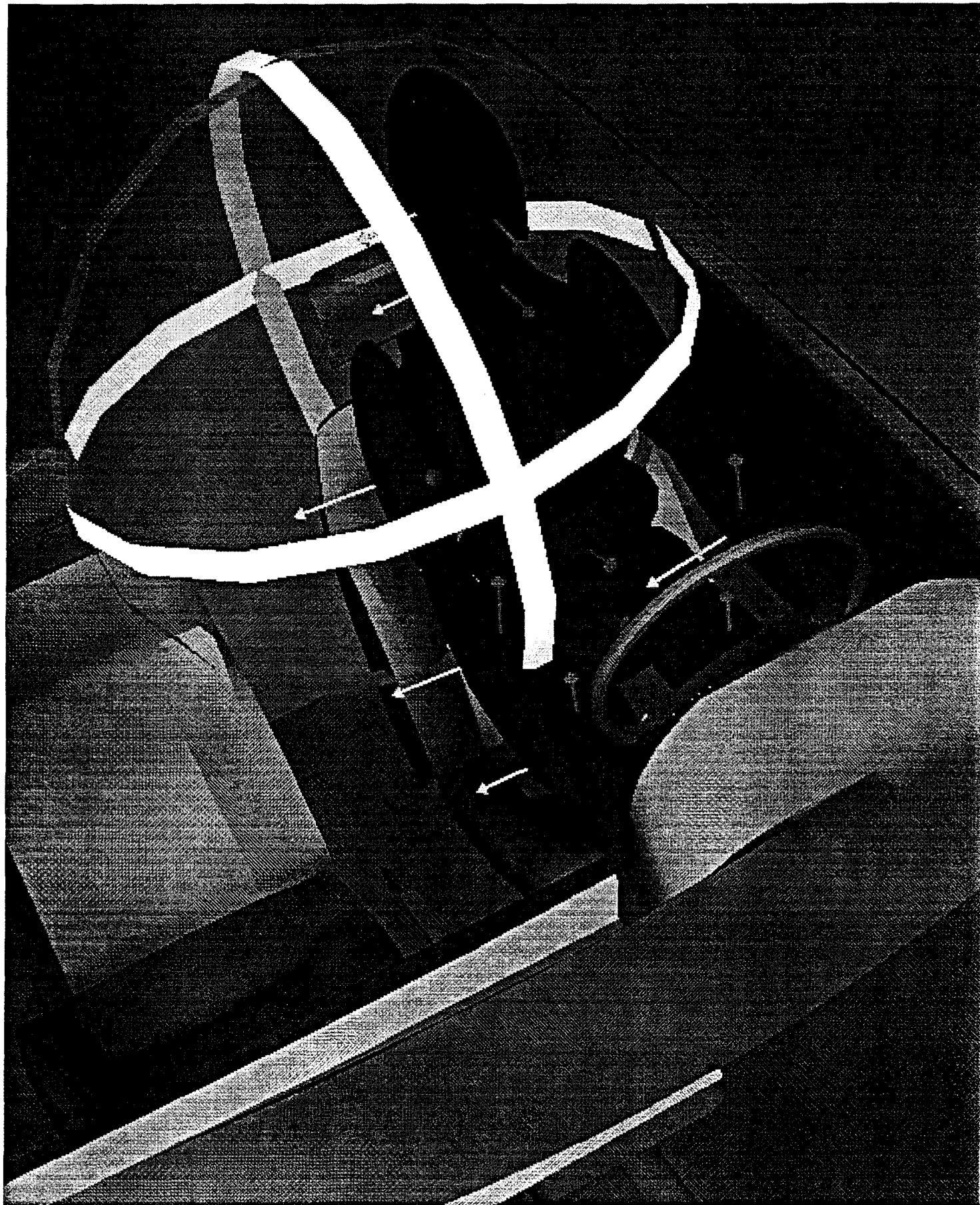
HVE Human model segments



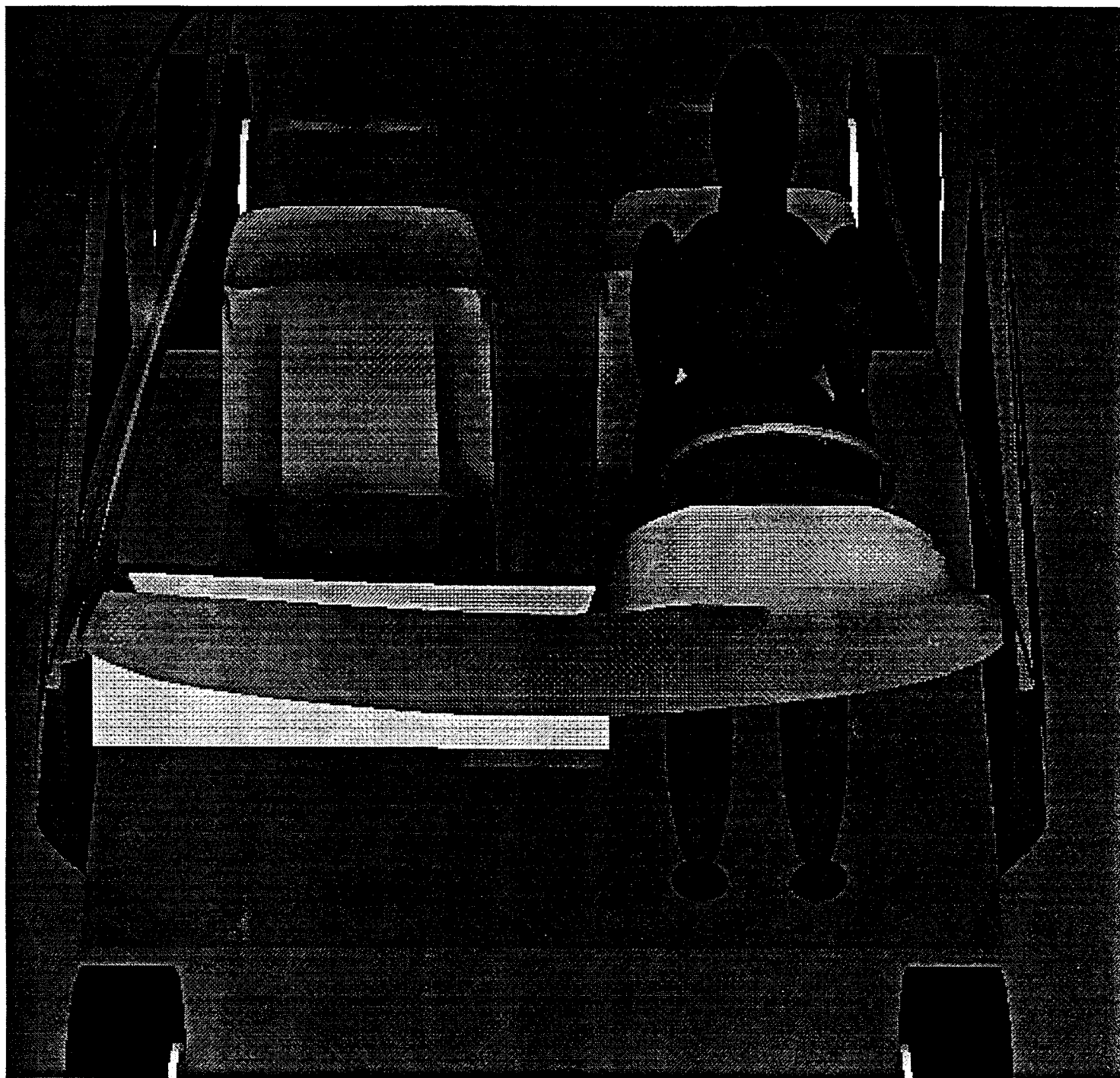
HVE Human - with segment axis shown



Positioning a human in HVE

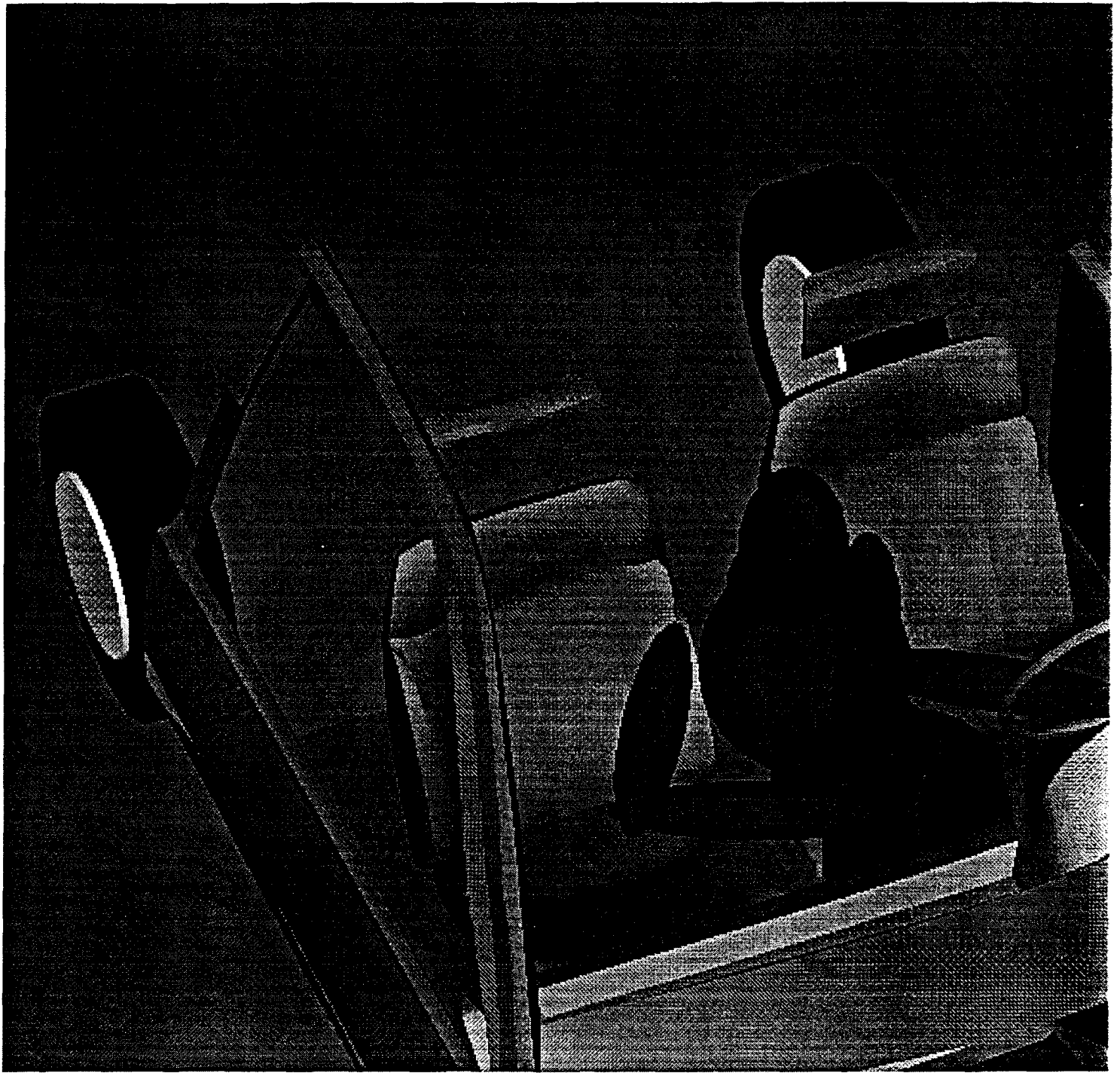


Positioning "ribbons" on right-upper arm segment



ATB run inside HVE  
- time 0 ms





ATB run inside HVE  
- time 150 ms

# An Overview of the HVE Human Model

Terry D. Day  
Engineering Dynamics Corp.

## ABSTRACT

Developers of human dynamics simulation software inherently use a mathematical/physical model to represent the human. This paper describes a pre-programmed, object-oriented human model for use in human dynamics simulations. This human model is included as part of an integrated simulation environment, called HVE (Human-Vehicle-Environment), described in previous research. The current paper first provides a general overview of the HVE user and development environments, and then provides detailed specifications for the HVE Human Model. These specifications include definitions for model parameters (supported human types and human properties, such as dimensions, inertias, joints and injury tolerances). The paper also provides detailed specifications for the HVE time-dependent human output group parameters (kinematics, joints, contacts, belts and airbags).

HUMAN DYNAMICS SIMULATION models are useful in several types of research. Vehicle manufacturers use occupant simulation to assist in the design and development of vehicle interiors and energy absorption characteristics; pedestrian simulation assists in the design of less aggressive vehicle frontal shapes. Biomechanical researchers use human simulation to model the human body in an effort to gain a better understanding of how injury occurs. The U.S. Air Force uses human simulation to help design cockpits and ejection systems. Accident reconstructionists use simulation to study injury causation.

Developers of human dynamics simulation software inherently use a mathematical/physical model (i.e., an object described by properties such as dimensions, inertias and mechanical constants) to represent the human. The required complexity of the human model is dependent upon

the complexity of the motion being simulated. For example, planar, two-dimensional (2-D) motion requires a relatively simple human model, while the simulation of three-dimensional (3-D) motion requires a model of significantly greater complexity. Historically, the use of occupant and pedestrian simulation has been limited because of the massive amounts of human and vehicle data required for execution.

This paper describes a 3-D human model available for use by developers of human dynamics simulation programs. The model, called the HVE Human Model, is included as part of an integrated simulation environment, called HVE (Human-Vehicle-Environment), described in previous research [1,2]. The purpose of this human model is to provide a standard, pre-programmed model available to researchers. It is hoped that by providing such a robust model in pre-programmed form, researchers will be inclined to produce more sophisticated simulators, thus, improving the state of the art in human occupant and pedestrian dynamics.

The purpose of this paper is to provide details of the HVE Human Model so that researchers may assess the applicability and suitability of the model to their human dynamics simulation programs.

## OVERVIEW OF HVE

HVE is a computer environment for executing human and vehicle dynamics simulations. It may be viewed as a computer abstraction of the nine-cell matrix for accident reconstruction originally proposed by the late Dr. William Haddon, first Director of the National Highway Traffic Safety Administration [3]. The nine-cell matrix describes the possible interactions between humans, vehicles and their environment during the pre-crash, crash and post-crash phases of an accident.

HVE is not itself an accident reconstruction program. Rather, HVE is an interface for *running* accident reconstruction and simulation programs, much like Microsoft Windows™ is an interface for running PC programs.

---

\* Numbers in brackets designate references found at the end of the paper.

The HVE interface is an integrated set of editors. The *Human Editor*, *Vehicle Editor* and *Environment Editor* are used for creating 3-D physical and visual models of humans, vehicles and environments. Once created, the interactions between these models may be simulated using any HVE-compatible human or vehicle simulation model in the *HVE Event Editor*. The simulation results may be displayed both numerically and *visually* by HVE. Using the *HVE Playback Editor*, simulations from several events may be edited into a single coherent sequence involving multiple humans and vehicles. The output may be routed to a display, printer, plotter or VCR. See reference 1 for further details.

### HVE Environment

A block diagram for the HVE simulation environment is shown in Figure 1. Note that, conceptually, the HVE interface *surrounds* the simulation model. The interface is comprised of five modes: Human Mode, Vehicle Mode, Environment Mode, Event Mode and Playback Mode.

The HVE Developer's Toolkit [2] is a library of functions and data structures that provide the developer of a human or vehicle dynamics model access to the HVE interface.

The HVE Human Model is the 3-D human created by the HVE Human Editor and used by HVE-compatible simulations. It is defined by the human data structure described in the HVE Developer's Toolkit.

The remainder of this document describes the details of the HVE Human Model which is created using the HVE

*Human Editor*. Although the information is provided in the form expected by the programmer/developer (refer to Appendix A for the actual data structures), it should also be useful to any technical person wishing to understand the basic parameters which define the human model.

### HUMAN MODEL

The HVE Human Model is created, viewed and edited in the Human Editor, one of the five editing modes which comprise HVE's graphical user interface (see figure 2). In general, the Human Editor allows the user to produce, from HVE's human database, one or more humans to be included in the *Active Humans List*. One or more of the humans in this list may then be selected for study in a human dynamics (or vehicle dynamics) simulator.

This section of the paper describes the following details of the HVE Human Model:

- Human Database (General Parameters)
- Human Properties (Model Inputs)
- Event-related Parameters (In-use Inputs)
- Output Parameters (Model Outputs)

### Human Database

The HVE Human Database is a user-extendable library of humans selectable according to the following keys:

- Sex (Male, Female)
- Age
- Weight Percentile
- Height Percentile

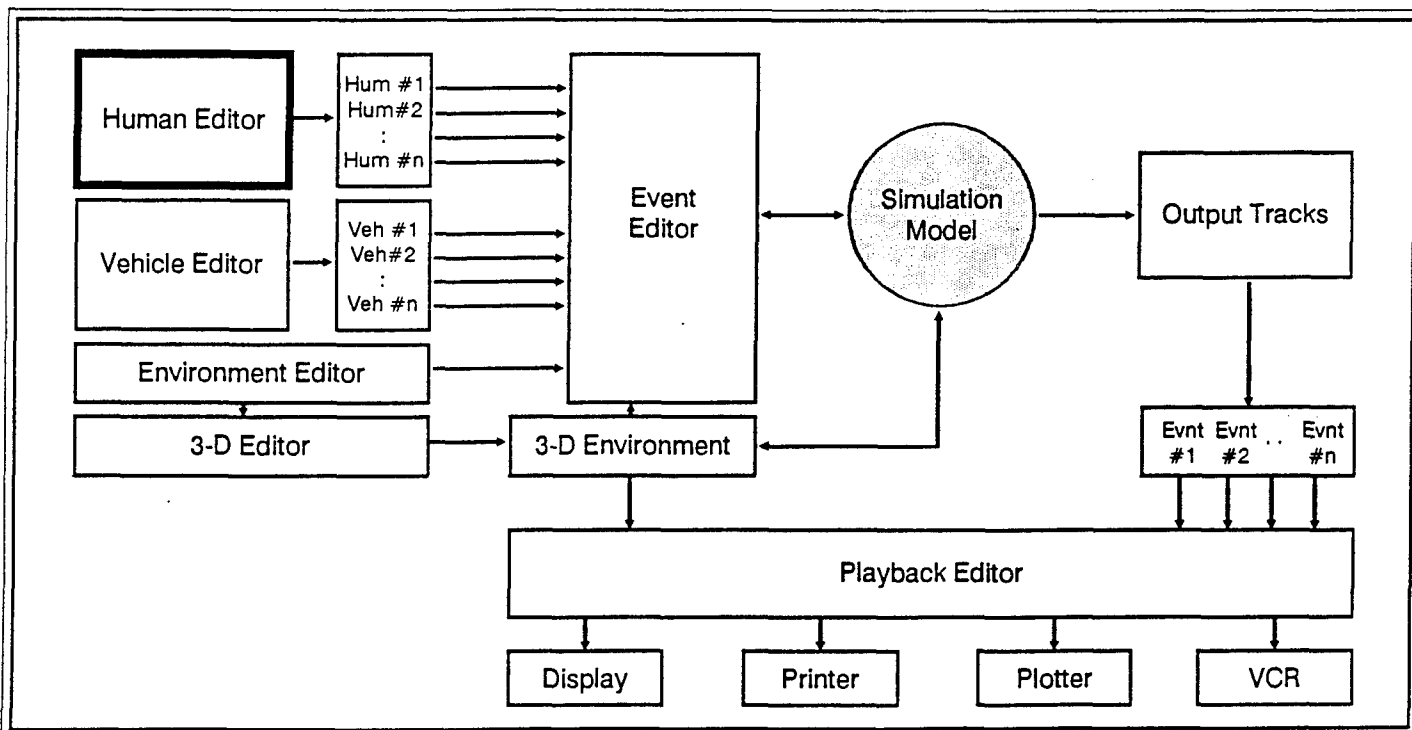


Figure 1 - Block Diagram for HVE application environment. The HVE Human Model is created and edited in the Human Editor (see heavy box). These humans may then be used in the Event Editor by any HVE-compatible simulation model.

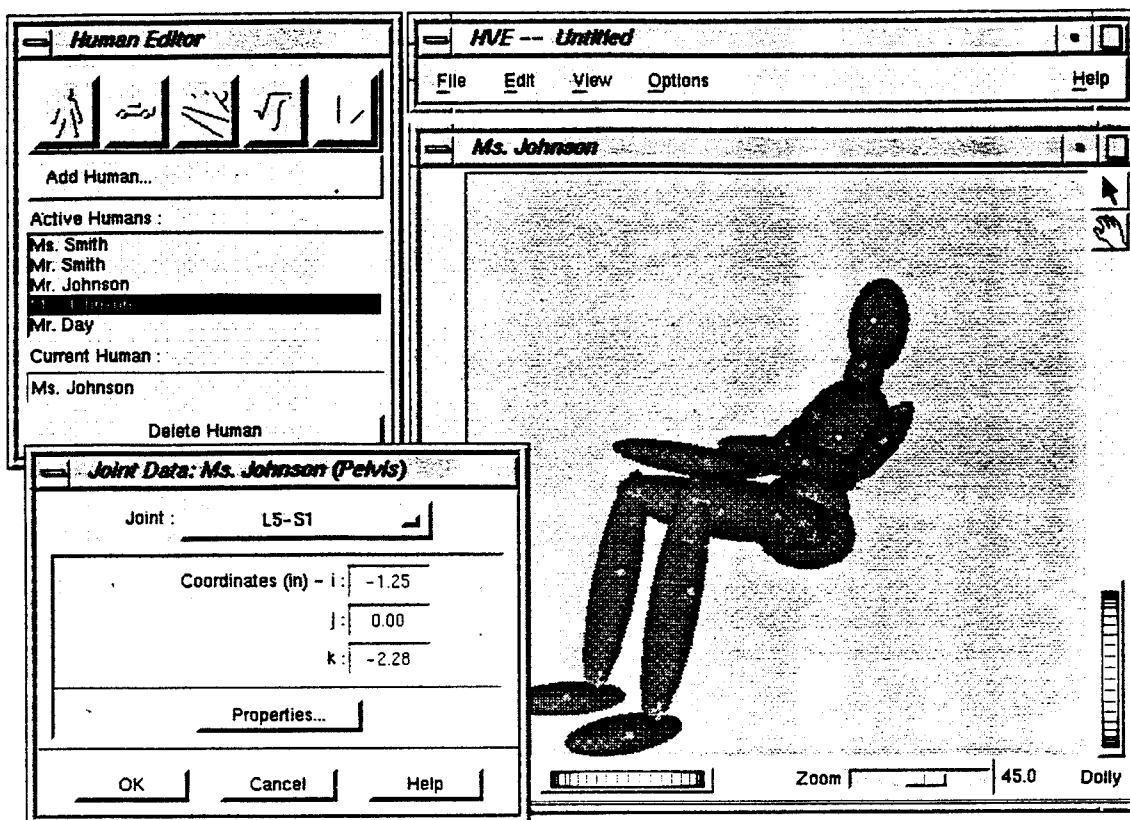


Figure 4 - Typical input dialog (in this case, the Joint Data dialog).

The event-related human parameters include the following:

- Position/Velocity
- Collision Pulse
- Contacts
- Restraint usage

The parameters for these three data groups are shown in Table 2.

### Position/Velocity

Human simulations require initial positions and velocities for each degree of freedom. Linear and angular positions are supplied during event editing, either by direct manipulation of the segments in the event viewer or by data entry into the position/velocity dialog. Velocities are assigned using the position/velocity dialog.

The simulation code is responsible for telling HVE which degrees of freedom to make available in the dialog. For example, a 2-D simulator such as MVMA-2D [7] would not request entries for roll, yaw and y positions, whereas 3-D simulators [8,9,10] would request entries for all fields.

Additional positions may be assigned as visual *targets*. Targets are humans which are displayed at user-selected positions along the vehicle path, and allow the researcher to assess how closely the simulation matches the desired

(actual) human path. The available human target positions are associated with vehicle positions, and are therefore named *Begin Perception*, *Begin Braking*, *Impact*, *Separation*, *Point-on-curve*, *End-of-rotation* and *Final/Rest*.

### Contacts

Human simulators predict motion by calculating the force between ellipsoids attached to the human model and surface planes attached to the vehicle model. If it is known ahead of time that certain ellipsoid/surface pairs will not interact (e.g., occupants will not normally interact with exterior surfaces), force calculations for the pair may be ignored. The Contacts information allows the user to deselect pairs of contacts from consideration during execution.

### Restraints

For each type of restraint device installed in the vehicle (availability of each device is determined by the vehicle), the Restraints parameters define how the restraint is being used (if at all) during a simulation.

### Collision Pulse

Occupant simulations require a collision pulse (actually, an acceleration vs time curve). This pulse defines the inertial environment. HVE knows if any collision pulses are available as a result of executing other events (e.g., EDSMAC [11]), and supplies the pulse automatically, if

Table 3. HVE Human Model Output Parameters

Variable Name	Pgm Units	Comments
SEGMENT KINEMATICS x,y,z or X,Y,Z coordinates Roll, Pitch, Yaw angles Total Velocity x, y, z linear velocity roll, pitch, yaw ang vel Total acceleration x, y, z linear accel roll, pitch, yaw ang accel	in rad in/sec in/sec rad/sec in/sec <sup>2</sup> in/sec <sup>2</sup> rad/sec <sup>2</sup>	occ or ped
JOINTS roll, pitch yaw articulation Mx, My, Mz (joint elasticity) Mx, My, Mz (joint damping) M <sub>x</sub> , M <sub>y</sub> , M <sub>z</sub> (joint stop) ΣM <sub>x</sub> , ΣM <sub>y</sub> , ΣM <sub>z</sub> (total)	rad in-lb in-lb in-lb in-lb	segment-fixed
CONTACTS i,j,k ellipsoid location contact deflection contact total force contact normal force contact friction force	in in lb lb lb	for each contact vs ellipsoid pair segment-fixed
BELTS x,y,z anchor point belt stretch belt tension	in in lb	segment-fixed
AIRBAGS bag pressure bag radius contact force	psi in lb	for each bag posn

desired. The pulse factors may be used to vary the amplitude of the individual pulses.

### Output Parameters

Output parameters related to the HVE Human Model are called *human output tracks*. Note that a human's output tracks are also event-related, because it is the responsibility of the simulation to calculate them and send them back to HVE as output.

Output tracks contain time-dependent results calculated by the simulation code (the code tells HVE which parameters it calculates; HVE then makes these available as output).

The output tracks for the HVE Human Model are divided into five categories:

- Kinematics
- Joints
- Contacts
- Belts
- Airbags

Each of these output categories is described in detail below.

#### Kinematics

The Kinematics output group contains position, velocity and acceleration results for each segment.

The results are presented in the vehicle-fixed reference frame for occupants and the earth-fixed reference frame for pedestrians.

#### Joints

The Joints output group contains joint articulation angles (segment-fixed) and torques for each of the 14 joints.

#### Contacts

The Contacts output group contains the parameters associated with interactions between occupant ellipsoids and vehicle contact surfaces. Segment-fixed contact locations, force and deflection results are included.

#### Belts

The Belts output group contains the parameters associated with interactions between the occupant and vehicle belt restraint systems, and includes belt stretch and tension.

#### Airbags

The Airbags output group contains the parameters associated with interactions between the occupant and the vehicle airbag system, and includes current levels of airbag pressure and force

#### Static Reports

In addition to the time-dependent output track parameters described above, additional output information related to the HVE human is monitored. These results are displayed in the form of static reports and include:

- **Messages** - Textual information relevant to the simulation (e.g., execution warnings and diagnostics)
- **Accident History** - Time, simulated position and velocity for each segment for each of the specified positions (impact, separation, etc.)
- **Human Data** - A report containing a list of the HVE Human Model parameters which were actually *used* by the simulation (Note that, although the HVE Human Model may contain several hundred parameters, the simulation might *use* only ten or 20.)
- **Injury Data** - A report containing information about those forces and accelerations which exceeded the user-defined tolerance levels

Whereas the output track groups produce results at each simulation output interval, the above static reports are produced only once; this occurs at the end of the run.

### DISCUSSION

The HVE Human Model may be used by relatively simple, 2-D simulators as well as sophisticated, 3-D simulators. Although the HVE Human Model contains literally hundreds of parameters per human, the programmer may select as many or as few of these parameters as are necessary to meet the needs of the simulation model.

The HVE Human Model is included as part of the HVE interface specification [1]. As an evolving standard, the

The above keys provide inputs to the HVE human database which calculates the parameters for a 15 segment human using GEBOD [4]. In addition to these database keys, the user may specify the Location (the options are Pedestrian or one of nine seat positions in the HVE Vehicle Model [5]), and an image filename (the name of an editable, 3-D geometry file for the human; if none is supplied, the 15 segment ellipsoids are used to visualize the human).

The Human Editor creates a *copy* of the selected human for use in the current simulation. Therefore, changes to an individual human do not affect the human database. Any modified human may be added to the human database after modification.

### Human Properties

The HVE Human Editor displays the current human in the *Human Viewer* (see Figure 2). The HVE Human Model has 15 segments and 14 joints, as provided by GEBOD. A schematic diagram is shown in figure 3.

Input data categories for the current human are selected by clicking the mouse on one of the 15 segment CGs to display the following input data categories:

- Inertias
- Contact Ellipsoids
- Injury Tolerance
- Joints

These input categories, and their associated parameters, are defined in the following sections.

### Inertias

Inertial parameters are defined for each of the 15 segments. The individual parameters are shown in Table 1. Mass is actually entered as weight and divided by the current acceleration of gravity. For reference, the human's total weight is displayed. Product of inertia,  $I_{ij}$ , is not included in the parameters.

### Contact Ellipsoids

Contact ellipsoids are the physical surfaces the simulation uses to determine the force on a human segment. The default ellipsoids for the selected segment are the same as the segment ellipsoids defined by GEBOD. Up to two additional ellipsoids may be created for each segment. Their location and orientation are defined relative to the segment's  $i,j,k$  coordinate axis system.

### Injury Tolerance

Injury tolerance parameters may be specified for the entire human (regardless of which segment is selected, the same injury tolerance dialog is displayed). Human tolerance levels for motor vehicle impacts are defined in SAE J885 [6]. The simulation code may compare these user-entered

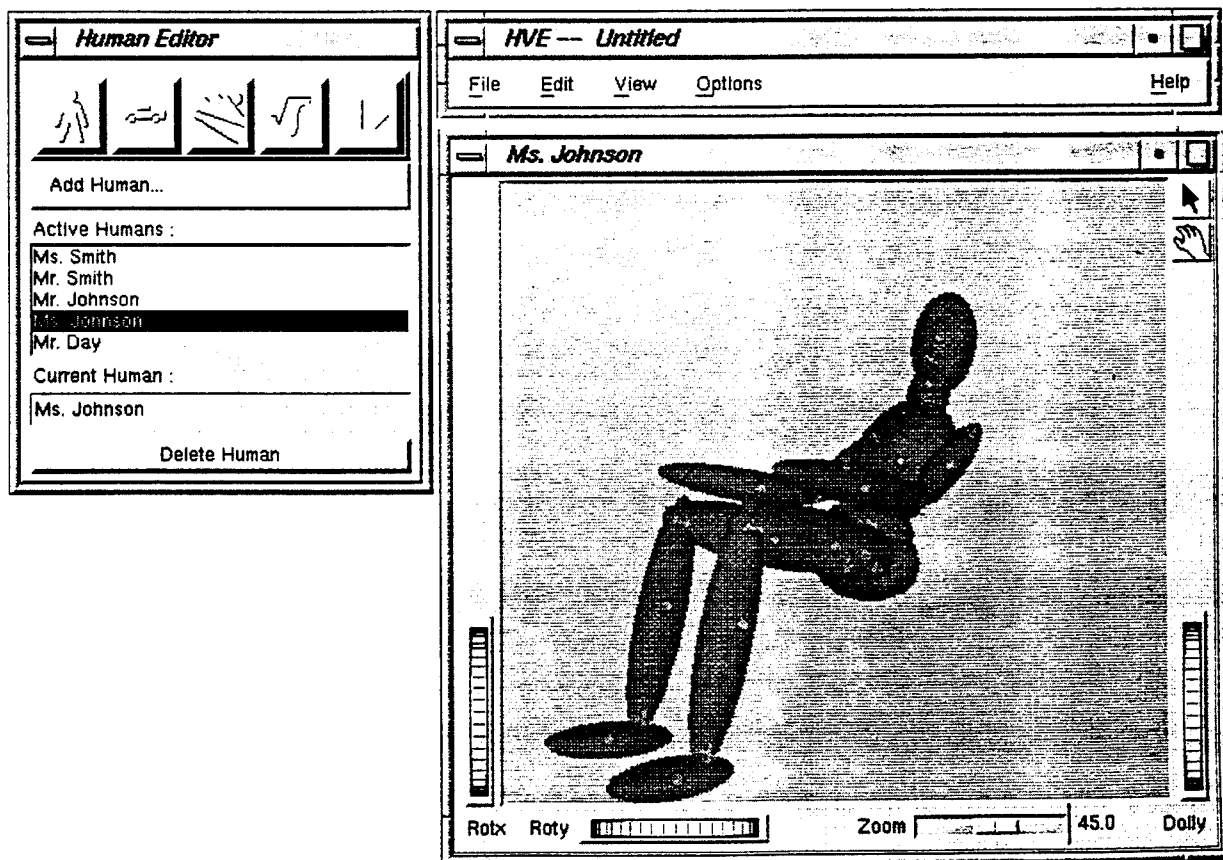


Figure 2 - HVE Human Editor and Viewer. The Human Editor is used for selecting and editing HVE Human Models.

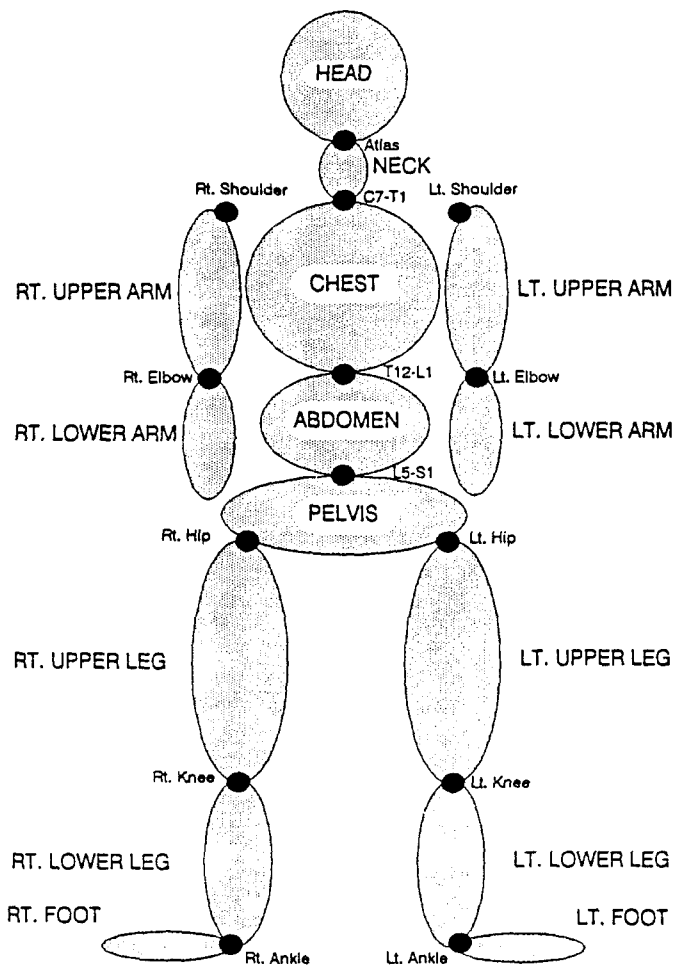


Figure 3 - 15 Segment, 14 Joint HVE Human Model based on GEBOD [4].

tolerance levels with the current levels of simulated force and acceleration to predict injury. This, in turn, may be used by the simulation code to produce a message alerting the researcher that the specified tolerance levels have been exceeded. The individual tolerance parameters are shown in Table 1.

### Joints

Each of the 14 joints is shown in the Human Viewer, and is selectable by clicking the mouse on the segment CG, and then selecting the desired joint from the joint list. Joint locations are editable and are defined relative to the segment's i,j,k coordinate axis system (see Figure 4).

HVE provides for *ball-and-socket* and *hinge* joint types. The individual parameters which define the joint properties are shown in Table 1.

### Event-related Parameters

Event-related parameters are *in-use factors* which affect the human model during execution of the simulation. Because these parameters are not related to the human, but, rather to the event, they are assigned to the human during *event editing*. Event editing is the process of setting up the simulation for execution.

Table 1. Human Model Parameters for 15 Segment Humans

Variable Name	Pgm Units	Comments
<b>INERTIAS</b>		
mass	lb-sec <sup>2</sup> /in	
Roll, Pitch, Yaw Inertia	lb-sec <sup>2</sup> -in	
<b>CONTACT ELLIPSOIDS</b>		
Ellipsoid Name		
Center Coords	in	i,j,k relative to segment
Length	in	i,j,k relative to segment
Principal Axes	rad	roll, pitch, yaw
<b>INJURY TOLERANCE</b>		see reference 6
HIC		Head Injury Criterion
Head Pitch Concussion	rad/sec <sup>2</sup>	
Head Side Accel	in/sec <sup>2</sup>	
Chest SI	in/sec <sup>2</sup>	
Chest Force	lb	
Chest Fwd Accel	in/sec <sup>2</sup>	
Max Axial Femur Load	lb	
Max Lap Belt Force	lb	left and right belts
Max Torso Belt Force	lb	left and right belts
<b>JOINTS</b>		
Joint Name		see figure 3
Joint Coordinates	in	i,j,k relative to segment
Joint Properties:		
Joint Type		Ball/Socket or Hinge
Stop Angle, + Rotation	rad	about i,j,k
Stop Angle, - Rotation	rad	about i,j,k
Stop Elasticity, + Rotn	in-lb/rad	about i,j,k
Stop Elasticity, - Rotn	in-lb/rad	about i,j,k
Stop Energy Dissipation	dimensionless	
Elastic Const, Linear	in-lb/rad	about i,j,k
Elastic Const, Quadratic	in-lb/rad <sup>2</sup>	about i,j,k
Elastic Const, Cubic	in-lb/rad <sup>3</sup>	about i,j,k
Damping Constant	in-lb-sec/rad	about i,j,k
Full Damping Ang Vel	rad/sec	about i,j,k
Max Angle, + Axis Rotn	rad	about i,j,k
Max Angle, - Axis Rotn	rad	about i,j,k

Table 2. Event-related Parameters

Variable Name	Pgm Units	Comments
PositionName		Initial, Begin Perception, Begin Braking, Impact, Separation, Point-on-curve, End-of-rotation, Final/Rest
x,y,z or X,Y,Z	in	occ or ped
Roll, Pitch, Yaw	rad	
<b>COLLISION PULSE</b>		
fwd, lat, vert lin accel	in/sec <sup>2</sup>	table vs time
roll, pitch, yaw ang accel	rad/sec <sup>2</sup>	table vs time
pulse factors	dimensionless	table multipliers
<b>CONTACTS</b>		
Selected Contacts	boolean switch	Allow Interaction?
<b>RESTRAINTS</b>		
Selected Restraint System	switch	Belts or Airbag
In Use	boolean switch	TRUE or FALSE
BeltAttachedTo		segment name
AttactCoords	in	i,j,k segment coords
BeltSlack	in	right, left sections
AirbagBeginFillTime	sec	
AirbagFillDuration	sec	

model and its associated database could be incorporated into any simulator using a relatively simple data translator.

Because it is an evolving standard, simulation developers are likely to develop simulations which require a few parameters not included in the HVE Human Model. For parameters not included in the model, the developer may hard-code the values (this is only reasonable for parameters which seldom change) or put the values in a separate file called by the simulation code. However, the developers of HVE are encouraging these simulation developers to participate and make suggestions for new human model parameters consistent with the needs of researchers.

A typical occupant or pedestrian simulation program using the HVE Human Model is built using the HVE Developer's Toolkit [2,12] and, thus, takes advantage of the HVE 3-dimensional interface for setting up, executing and viewing simulations.

The HVE Developer's Toolkit is written in C and assumes the simulation will be programmed in C or C++. FORTRAN programs have not yet been included. It is, however, possible that FORTRAN programs could be incorporated using C or C++ "wrappers" around the FORTRAN program. This requires further research.

The HVE interface has been developed for use on Silicon Graphics (SGI) workstations. It is written in C++, and leverages off the SGI Open GL and video libraries. Open Inventor [13] is used to visualize all HVE objects (humans, vehicle and environments). HVE requires a level of graphics processing power not yet available on personal computers (see reference 1 for performance comparisons). The HVE executable program is approximately 10 megabytes, requires a minimum of 32 megabytes of random access memory, and at least 1 gigabyte of hard disk space. An individual human binary file is 6,852 bytes (without 3-D image geometry data).

## SUMMARY

This paper has presented a detailed overview of the features of the HVE Human Model. Individual input and output parameters were presented and discussed.

The main purpose of the HVE Human Model is to provide a standard model available for use by the simulation community. The model may be used directly from within the HVE simulation environment or included as a standard for use in other simulation environments.

As a result of the availability of the HVE Human Model, it is hoped that researchers will consider enhancing their current simulations as well as developing new and more advanced occupant and pedestrian simulation applications.

## TRADEMARKS

HVE and EDSMAC are trademarks of Engineering Dynamics Corporation. Windows is a trademark of Microsoft Corp. Open GL and Open Inventor are trademarks of Silicon Graphics, Inc.

## REFERENCES

1. Day, T.D., "A Computer Graphics Interface Specification for Studying Humans, Vehicles and Their Environment," SAE Paper No. 930903, Society of Automotive Engineers, Warrendale, PA, 1993.
2. Day, T.D., "An Overview of the HVE Developer's Toolkit," SAE Paper No. 940923, Society of Automotive Engineers, Warrendale, PA, 1994.
3. Gross, M.E., "The GEBOD III Program User's Guide and Description," AL-TR-1991-0102, Beacher Research Co., Dayton, OH, 1991.
4. Lee, S.N., Fell, J.C., "An Historical Review of the National Highway Safety Administration's Field Accident Investigation Studies," NHTSA, Washington, DC, 1988.
5. Day, T.D., "An Overview of the HVE Vehicle Model," SAE Paper No 950308, Society of Automotive Engineers, Warrendale, PA, (to be presented at 1995 SAE International Congress, February, 1995).
6. *Human Tolerance to Impact Conditions as Related to Motor Vehicle Design*, SAE Technical Report No. J885 JUL86, Society of Automotive Engineers, Warrendale, PA, 1986.
7. Bowman, B.M., Robbins, D.H., Bennett, R.O., "MVMA Two-Dimensional Crash Victim Simulation, Version 4, Vol. III," UM-HSRI-79-5-3, University of Michigan, Ann Arbor, 1979.
8. Fleck, J.T., Butler, F.E., "Validation of the Crash Victim Simulator, Volume I, Engineering Manual - Part 1: Analytical Formulation," DOT-HS-6-01300, Calspan Corp., Buffalo, 1981.
9. Robbins, D.H., Bennett, R.O., Roberts, V.L., "HSRI Three-Dimensional Crash Victim Simulator: Analysis, Verification and User's Manual and Pictorial Section," DOT-HS-800 551, University of Michigan, Ann Arbor, 1971.
10. Bennett, R.O., Bowmar, D.H., Robbins, D.H., "Supplement to the HSRI Three-Dimensional Crash Victim Simulation Report," HSRI Report No. UM-HSRI-77-20, University of Michigan, Ann Arbor, MI, 1977.
11. *EDSMAC User's Manual*, Fifth Edition, Engineering Dynamics Corporation, Beaverton OR, 1994.
12. *HVE Developer's Toolkit*, Engineering Dynamics Corporation, Beaverton, OR, 1994 (currently under development).
13. *The Inventor Mentor*, Wernecke, J., Addison-Wesley Publishing Co., Menlo Park, CA, December, 1993.



## Appendix A - HVE Human Model Data Structures

Review of this structure provides an overview of the HVE Human Model. Simulation programmers familiar with the C programming language may use this information to design human simulations; it is also useful for providing a basic understanding of the model's parameters.

```
/* human.h
Human Data Structure (7-5-94)
*/
struct HumanData {
    long Id;
    char Name[MAXNAMELENGTH];
    INT Location;
    INT Sex;
    INT Age;
    INT BodyType;
    INT Percentile;

    struct HumanSegment {

        struct HumanColor {
            FLOAT r;
            FLOAT g;
            FLOAT b;
        } Color;

        struct SegmentInertia {
            FLOAT Mass;
            FLOAT Inertia[3];
        } Inertia;

        INT NumEllipsoids; /* on this segment */
        INT CurrentEllipsoid; /* on this segment */

        struct SegmentEllipsoid {
            char EllipsoidName[MAXNAMELENGTH];
            FLOAT Coord[3];
            FLOAT Length[3];
            FLOAT PrincipalAxes[3];
        } Ellipsoid[MAXELLIPSOIDSPERSEGMENT]; /* #define 3 */

        INT NumJoints; /* on this segment */
        INT CurrentJoint; /* on this segment */

        struct SegmentJoint {
            INT Id; /* Index of joint (up to MAXHVEJOINTS) */
            FLOAT Coord[3]; /* rel to selected seg CG */
        } Joint[MAXJOINTSPERSEGMENT]; /* #define 4 */
    } Segment[MAXHVESEGMENTS]; /* #define 15 */

    struct HumanJoint {

        struct JointProperties {
            INT Type; /* BALL_JOINT = 0, HINGE_JOINT = 1 */
            FLOAT StopAngPlus[3];
            FLOAT StopAngMinus[3];
            FLOAT StopElasticityPlus[3];
            FLOAT StopElasticityMinus[3];
            FLOAT EnergyDissipation[3];
            FLOAT ElasticLinear[3];
            FLOAT ElasticQuadratic[3];
            FLOAT ElasticCubic[3];
            FLOAT DampingConst[3];
            FLOAT DampingVelocity[3];
            FLOAT ToleranceAnglePlus[3];
            FLOAT ToleranceAngleMinus[3];
        } Property;

    } Joint[MAXHVEJOINTS]; /* #define 14 */

    struct HumanTolerance {
        FLOAT HIC;
        FLOAT HeadPitch;
        FLOAT HeadSideAccel;
        FLOAT ChestSI;
        FLOAT ChestForce;
        FLOAT ChestAccel;
        FLOAT KneeForce;
        FLOAT LeftLap;
        FLOAT LeftTorso;
        FLOAT RightLap;
        FLOAT RightTorso;
    } Tolerance;
};
/* end of human.h */
```